COMPUTER SIMULATION OF RADIO FREQUENCY (RF) HEATING IN DRY FOOD MATERIALS AND QUALITY EVALUATION OF RF TREATED PERSIMMONS

By

GOPAL TIWARI

A dissertation submitted in partial fulfillment of
the requirements for the degree of

DOCTOR OF PHILOSOPHY

WASHINGTON STATE UNIVERSITY
Department of Biological Systems Engineering

MAY 2010

To the Faculty of Washington State University:

The members of the Committee appointed to examine the dissertation of GOPAL TIWARI find it satisfactory and recommend that it be accepted.

_____
Dr. Juming Tang, Chair

_____
Dr. Barbara Rasco

_____
Dr. John K. Fellman

_____
Dr. Shyam Sablani

_____
Dr. Shaojin Wang

ACKNOWLEDGEMENT

I express my greatest gratitude to my advisor Dr. Juming Tang for his guidance, support, consistent encouragement, and great patience throughout my studies and research. Because of his insightful advices, understanding and moral support, I could stay focused on my PhD research. I also express my sincere thanks to my doctoral committee members: Drs. Barbara Rasco, John K. Fellman, Shyam Sablani and Shaojin Wang for their valuable time, suggestions and comments whenever I approached them with problems. Dr. Shaojin Wang also helped me in designing experiments and developing manuscripts during my research work.

I acknowledge Dr. Sohan Birla with whom I received valuable research inputs from time to time. I thank to Galina Mikhaylenko, Wayne Dewitt, Frank Younce, and Vince Himsl for providing technical assistance. I extend my thanks to my friends and fellow students Balunkeswar Nayak, Kanah Kereilemang Mokwena, Derick Jiwan, Shunshan Jiao, Sumeet Dhawan, Roopesh Shayamaldevi, Prabhakar Singh and Fermin Resurrection for the support throughout my research.

Last but not the least, I express my deepest gratitude to my parents, brothers and their families who have sacrificed a lot towards my education. Without their moral support, it was not possible to accomplish this research.

COMPUTER SIMULATION OF RADIO FREQUENCY (RF) HEATING IN DRY FOOD MATERIALS AND QUALITY EVALUATION OF RF TREATED PERSIMMONS

Abstract

by Gopal Tiwari, Ph.D.

Washington State University

May 2010

Chair: Juming Tang

Radio frequency (RF) heating is a novel heat treatment that has been explored for control of pests and pathogens in several agricultural commodities such as fresh fruits, dry nuts, food grains, legumes and flours. A major problem for the technology to be commercially applicable is its non uniform heating in different food materials. It is important to understand, investigate and analyze the complex behavior of RF heating. The present research was aimed to study RF heating uniformity in food materials.

As a preliminary step of the research, RF heating was experimentally evaluated in '*Fuyu*' persimmon, a selected specialty crop fruit. The objective was to develop a RF based heat treatment protocol to control Mexican fruit fly in persimmon. Quality parameters, including weight loss, firmness, soluble solids, titratable acidity, peel and pulp color, and calyx browning of persimmons were evaluated after 7 days of RF heat treatments. Results showed that RF heat treatment provided potential for disinfestations of persimmons with acceptable quality.

As a next step, a computer model was developed to simulate RF heating in dry food materials using finite element software FEMLAB. The aim of this part of the study was to

understand the complex behavior of RF heating in the dry food materials. Whole wheat flour was selected as a representative material for dry food materials. Simulated and experimental results showed that temperature values were higher at the corners and lower sections of flour in a rectangular container after RF heating.

The computer model was further used to investigate the effect of different influencing parameters on heating uniformity in dry food materials placed between two parallel electrodes. Results showed that smaller values of dielectric properties resulted in better RF power uniformities in the samples. RF power uniformity in cuboid shaped samples, placed on the bottom electrode, first decreased and then increased with the increase in sample size. Reducing electrode gap improved RF power uniformity. This research is useful to understanding the RF heating mechanism, to improve heating uniformity in agricultural commodities, and to design and scale up efficient RF systems.

TABLE OF CONTENTS

ACKNOWLEDGEMENT

ABSTRACT

LIST OF TABLES

LIST OF FIGURES

OUTLINE OF DISSERTATION

CHAPTER 1……..1

RADIO FREQUENCY (RF) HEATING IN FRESH FRUITS AND DRY

AGRICULTURAL COMMODITIES: A REVIEW

1. Introduction……...……2

2. RF heating mechanism…….....3

3. RF heating applications…….....4

3.1. Fresh fruits……..……4

3.2. Dry agricultural commodities….....6

3.2.1. Pest-insects control……..……6

3.2.2. Fungi control…….……..7

3.2.3. Pathogen control……..……8

3.2.4. Enzymatic deactivation…….……..8

4. Mathematical models used for RF heating in dry agricultural commodities……....9

5. Current research directions…….....10

References…….…..11

CHAPTER 2…….…...18

EFFECT OF WATER ASSISTED RADIO FREQUENCY HEAT TREATMENT ON THE QUALITY OF 'FUYU' PERSIMMONS

1. Introduction……..……20

2. Materials and methods……..……...22

2.1. Sample preparations and thermal treatment designs…….…...22

2.2. Treatment parameter determinations……..……..23

2.3. Treatment procedures……..……..…24

2.4. Quality evaluation…….…….……..25

3. Results and discussions……..…….26

3.1. Comparison of thermal imaging and thermocouple methods……..…26

3.2. Preheating time determination…….……26

3.3. Temperature time profile of persimmon…….…….27

3.4. Quality……..……27

3.4.1. Weight loss……..……..27

3.4.2. Firmness…….……...28

3.4.3. Peel and pulp color……..……..29

3.4.4. Total soluble solids and titratable acidity……..……29

3.4.5. Visual observations……..…….30

4. Conclusions……..…30

References……...40

CHAPTER 3…….....45

COMPUTER SIMULATION OF RADIO FREQUENCY HEATING OF DRY FOOD MATERIALS, PART I: MODEL DEVELOPMENT AND VALIDATION…….……46

1. Introduction…….47

2. Materials and methods……..……..49

2.1. Material selection…….…50

2.2. Dielectric and thermal properties measurement…….……..50

2.3. Development of computer model…….…50

2.3.1. Physical model……..50

2.3.2. Governing equations…….……51

2.3.3. Initial and boundary conditions…….....52

2.3.4. Solution procedure…….....53

2.4. Model validation……...54

2.4.1. Material selection……..54

2.4.2. Experimental procedure…….....55

3. Results and discussions……...55

3.1. Dielectric and thermal properties of wheat flour…….55

3.2. Simulated thermal propertied of wheat flour……...56

3.3. Comparison of simulated and experimental thermal profiles of wheat flour…….…….57

3.4. Sensitivity analysis…….…..58

4. Conclusions…….…58

References…….……..71

CHAPTER 4

COMPUTER SIMULATION OF RADIO FREQUENCY HEATING OF DRY FOOD MATERIALS, PART II: MODEL PREDICTIONS…….……..75

1. Introduction……..……...77

2. Materials and methods……..…….....79

2.1. Governing equations……..…….....79

2.1.1. RF power density and Laplace equations……..……79

2.1.2. Average RF power density and RF power uniformity index (PUI) of the sample……...…….……80

2.2. Physical and simulation model……..……...80

2.3. DPs of sample and surrounding medium…….……81

2.4. Boundary conditions…….……....81

2.5. Simulation methodology…….……81

2.6. Simulation sequence…….……82

2.6.1. Simulation with varying sample size, position, and shape…….....82

2.6.2. Simulation with varying sample DPs of the sample and surrounding medium…….……..……...83

2.6.3. Simulation with varying electrode gap and top electrode configuration…….....83

3. Results and discussions…….……..84

3.1. Distribution of RF power density in different sample sizes…….....85

3.2. Distribution of RF power density in different sample shapes at different positions between the RF electrodes…….……..…85

3.3. Effect of sample size on sample PUI…….……...86

3.4. Effect of sample vertical position on sample PUI…….……...86

3.5. Effect of DPs of sample and surrounding medium on sample PUI….…….88

3.6. Effect of electrode gap on PUI……..…88

3.7. Effect of top electrode bending/configuration……..…89

4. Conclusions…….....89

References…….105

CONCLUSIONS AND RECOMMENDAIONS……..……109

LIST OF TABLES

Chapter 2

Table 1. Experimental design of radio frequency heat treatment……..……31

Table 2. Comparisons of measured surface and core temperatures of 'Fuyu' persimmon between thermal imaging (TI) and thermocouple (TC) methods during preheating and hydro-cooling……32

Table 3. Preheating time determinations at 40°C water baths based on heating uniformity after RF treatment of 'Fuyu' persimmon at three different target temperatures……...……...33

Table 4. Quality parameters of control and RF treated 'Fuyu' persimmons after 7 days storage at room temperature (22°C, 35% RH)……...……..34

Table 5. Quality parameters of control and RF treated 'Fuyu' persimmons after 7 days at cold storage (4 °C, 80% RH)……...35

Table 6. ANOVA P values ($\alpha = 0.05$) for the effect of treatment, storage and treatment × storage interaction for persimmon quality parameters……...…..36

Chapter 3

Table 1. Dielectric and thermal properties of hard red spring wheat flour at a bulk density of 800 kg m^{-3} and moisture content of 8.8 % w.b……...……59

Table 2. Dielectric and thermo-physical properties of wheat flour, polypropylene and air used in computer simulation as a function of temperature (T ,°C)…….60

Table 3. Relative sensitivity of simulated temperature uniformity (STU) of sample with respect to model input parameters……..……61

Table 4. Experimented and simulated average temperature ± standard deviation (° C)

at four different horizontal layers of wheat flour in a plastic container ($300 \times 220 \times 60$ mm^3) after 3 min RF heating with an electrode gap of 155 mm and initial temperature of 23 ° C……..……..62

Chapter 4

Table 1. Simulated PUIs of wheat flour sample in three different shapes (a cuboid, an ellipsoid and a cylinder), placed at three different vertical positions between RF electrodes with a fixed gap of 155 mm……91

LIST OF FIGURES

Chapter 2

Fig. 1. Experimentally determined preheating and radio frequency (RF) heating times for the surface and core temperature of 'Fuyu' persimmon to each of the three selected temperatures……37

Fig. 2. Heating and cooling profiles for surface and core of 'Fuyu' persimmon (diameter of 7 cm), subjected to preheating in hot water at 40 °C followed by RF heating to raise temperature up to 48 °C, holding at 48 °C for 6 min and hydro-cooling for 30 min at 4 °C water……38

Fig. 3. Temperature distributions of persimmons obtained by thermal imaging after: (a) water preheating at 40 °C for 20 min, (b) RF heating from 40°C to 48°C, (c) holding in hot water at 48 °C for 6 min, and (d) cooling in cold water at 4 °C for 30 min…….39

Chapter 3

Fig. 1. Schematic diagram of a 12 kW, 27.12 MHz radio frequency system……..…63

Fig. 2. Geometrical and boundary conditions of one quadrant of 12 kW, 27.12 MHz RFsystem (dimensions are in mm)……...64

Fig. 3. Flow chart of modeling using FEMLAB 3.4……....65

Fig. 4. Simulated temperature (°C) profiles of one quadrant wheat flour sample ($150 \times 110 \times 60$ mm^3) at (a) four different horizontal layers (0, 20, 40, and 60 mm) from the bottom (b) four different vertical layers (0, 36, 72, and 110 mm) from the vertical center plane of sample after 3 min RF heating with an electrode gap 155 mm and initial temperature 23 °C…….66

Fig. 5. Simulated electric field distribution (a) and RF power density distribution (W m^{-3}) of one quadrant wheat flour sample (150× 110 × 60 mm^3) after 3 min RF heating with an electrode gap 155 mm……..67

Fig. 6. Experimental (a) and simulated (b) temperature distributions (°C) of hard red spring wheat flour in top and first mid layers (60 and 40 mm from the bottom of sample) placed in a polypropylene container (300×220×60 mm^3) on the top of the bottom electrode with the comparison of the temperature profiles (c) along the line LL', after 3 min RF heating with an initial temperature of 23 °C and a fixed electrode gap of 155 mm…….68

Fig. 7. Experimental (a) and simulated (b) temperature distributions (° C) of hard red spring wheat flour in second mid and bottom layers (20 and 0 mm from the bottom of sample) placed in a polypropylene container (300×220×60 mm^3) on the bottom electrode with the comparison of the temperature profiles (c) along the line LL' after 3 min RF heating with an initial temperature of 23 °C and a fixed electrode gap of 155 mm…….....69

Fig. 8. Experimental and simulated temperature-time histories of hard red spring wheat flour at the center of first mid layer (40 mm) from the bottom of sample (300×220×60 mm^3), placed in a polypropylene container on the top of grounded electrode during 3 min RF heating with an electrode gap of 155 mm…….70

Chapter 4

Fig. 1. Geometrical and boundary condition of one quadrant of 12 kW, 27.12 MHz RF system (dimensions are in mm)……92

Fig. 2. Schematic diagram of radio frequency cavity showing change in top electrode configuration by bending it upward from its both ends at different lengths and angles……93

Fig. 3. Simulated RF power density contours (W m^{-3}) of wheat flour sample in three different sizes, placed on the bottom electrode with a fixed electrode gap of 155 mm. Top electrode size was 525 × 400 mm^2……94

Fig. 4. Simulated RF power density contours (W m^{-3}) of wheat flour sample in three different shapes (a cuboid, an ellipsoid and a cylinder) placed at three different vertical positions between the RF electrodes of fixed gap of 155 mm…….....95

Fig. 5. Simulated RF power uniformity indexes (PUIs) of cuboid shaped wheat flour mass with varying sample lengths and widths. Cuboids were placed on the bottom electrode with top electrode size (525 × 400 mm^2) and a fixed electrode gap of 155 mm. Sample heights were set as 60 mm…….....96

Fig. 6. Simulated RF power uniformity indexes (PUIs) of cuboid shaped wheat flour with varying sample heights. Samples were kept on the bottom electrode with a fixed electrode gap of 155 mm. Top electrode size was 525 × 400 mm^2 and samples length and width both were set as 150 mm…….....97

Fig. 7. Simulated power uniformity indexes (PUIs) of cuboid shaped wheat flour in three different sizes, kept at seven different vertical positions (in mm) under the fixed electrode gap of 155 mm…….....98

Fig. 8. Simulated power uniformity indexes (PUIs) in cuboid shaped sample (150×150×60 mm^3) with varying DPs. Samples were placed on the bottom electrode with an electrode gap of 155 mm……..99

Fig. 9. Trends of simulated power uniformity indexes (PUIs) of samples with varying dielectric constants in five different sizes. Loss factor value fixed as 10……..100

Fig. 10. Simulated power uniformity indexes (PUIs) in sample (150×150×60 mm^3) in different surrounding medium dielectric constant. Sample DPs was fixed as $(8-10*j)$ and it was kept on the bottom electrode with an electrode gap of 155 mm……...101

Fig. 11. Simulated power uniformity indexes (PUIs) of cuboid shaped wheat flour (150×150×60 mm^3) with varying electrode gaps. Sample was kept on the bottom electrode with an electrode gap of 155 mm……...102

Fig. 12. Simulated power uniformity indexes (PUIs) in a cuboid shaped wheat flour (300 ×210 × 60 mm^3) sample, placed on the bottom electrode when top electrode (525×400 mm^2) was bent (A) at six different positions (0, 100, 200, 300, 400 and 500 mm) along the length of electrode, keeping bending angle fixed as 15°. (B) at different angles (in degrees), keeping bending position fixed as 200 mm……..103

Fig. 13. Simulated power density contours (W m^{-3}) in a cuboid shaped wheat flour sample (300 ×210 × 60 mm^2) placed on the bottom electrode when top electrode (525×400 mm^2) was (A) bent 100 and 300 mm along the length of electrode, keeping bending angle fixed as 15° (B) bent upwards 5° and 45°, keeping bending position fixed as 200 mm……104

OUTLINE OF DISSERTATION

The dissertation is organized into four self-contained chapters. The first chapter provides an overview of radio frequency (RF) heating, its various applications in dry food materials and fresh fruits, and the motivation for developing a computer model to help understand RF heating behavior in dry food materials. Chapter 2 evaluates the potential of RF heating in a selected fresh fruit persimmon (*Diospyros kaki*) as a quarantine heat treatment to control Mexican fruit fly (*Anastrepha ludens*). Chapter 3 describes a mathematical model for RF heating of dry food products for a parallel plate RF system. Chapter 4 investigates the effect of different influencing parameters on the RF heating behavior of dry food products.

Since the dissertation is composed of individually published and prepared manuscripts, the chapter formats vary according to submitted journals. A list of articles published or manuscripts prepared from this research are shown below:

Tiwari, G., Wang, S., & Tang, J. (2010). Radio frequency (RF) heating in fresh fruits and dry agricultural commodities: A review. *Journal of Food Engineering* (Chapter 1)

Tiwari, G., Wang, S., Birla, S.L., & Tang, J. (2008). Effect of water-assisted radio frequency heat treatment on the quality of 'Fuyu' persimmons. *Biosystems Engineering*, 100(2), 227-234. (Chapter 2)

Tiwari, G., Wang, S., Tang, J., & Birla, S.L. (2010). Computer simulation of radio frequency heating of dry food materials, Part I: model development and validation. *Journal of Food Engineering* (Chapter 3)

Tiwari, G., Wang, S., Tang, J., & Birla, S.L. (2010). Computer simulation of radio frequency heating of dry food materials, Part II: model predictions. *Journal of Food Engineering* (Chapter 4)

CHAPTER 1

RADIO FREQUENCY HEATING IN FRESH FRUITS AND DRY AGRICULTURAL COMMODITIES: A REVIEW

G. Tiwari, S. Wang, J. Tang

Prepared manuscript for the Journal of Food Engineering

Department of Biological Systems Engineering,

Washington State University, Pullman, WA 99164-6120, USA

Corresponding author:

Juming Tang, 213 LJ Smith Hall, Pullman, WA 99164-6120, USA;

Phone: 509-335-2140; fax: 509-335-2722; e-mail: jtang@wsu.edu.

Abstract

The literature review focuses on the radio frequency (RF) heating application on fresh fruits and dry agricultural commodities. RF heating mechanism and different available mathematical models for RF heating in dry agricultural commodities are also discussed in detail. It was identified that complex nature of RF heating needs to be investigated experimentally as well as mathematically.

1. Introduction

Conventional heating methods use steam or hot water or hot air or a combination of any of them to heat food materials for food safety against pathogens, insects and pests. These methods are relatively slow as they rely on slow heat transfer from outer to inner sections of samples. The larger the sample sizes, the slower the heat transfer (Wang et al., 2001b). Slow heating in food materials often result in inferior food quality in terms of texture, color, flavor, and nutritional values. The desire to eliminate these problems and achieve fast and effective heating for food materials has increased interest in using novel thermal technologies such radio frequency (RF) and microwave (MW) energy.

RF and MW heating involve interaction of electromagnetic (EM) field with food materials. When food materials are placed in an alternating EM field, charges (free ions and electric dipoles) present in foods get displaced and attempt to follow changes in external alternating EM field. The EM energy absorbed by the material to carry out these displacements is dissipated as heat. Since nature of heat is volumetric, these methods are rapid compared to other conventional heating methods. In an EM spectrum, RF (3-300 MHz) and MW (300 MHz-300 GHz) bands occupy adjacent sections, with RF waves having lower frequencies. The major

advantage of RF heating over MW heating is its ability to penetrate deeper in food materials as RF wave length is much longer (e.g., ~ 11 m at 27.12 MHz) than MW wavelength (e.g., ~ 12 cm at 2450 MHz). The only concern with the RF heating technology is its non uniform heating (Tang et al., 2000). Different factors such as sample dielectric and thermo-physical properties, size, shape, its position between the RF electrodes, and electrode configuration may affect temperature uniformity in a RF treated food product. Therefore, it is essential to understand complex behavior of RF heating mathematically as well as experimentally.

2. RF heating mechanism

An accurate calculation of RF power density (Q, W m^{-3}) is essential to determining temperature rise in food materials during RF heating. RF power density in the material is given by (Rowley, 2001):

$$Q = 2\pi f \varepsilon_o \varepsilon'' \left|\boldsymbol{E}\right|^2 \qquad (1)$$

where f is the frequency (Hz), ε_o and ε'' are the permittivity of the free space (8.86 × 10^{-12} F m^{-1}), and the loss factor of the material, respectively. $\left|\boldsymbol{E}\right|$ is the modulus of electric field (V m^{-1}). Temperature rise in the food materials can be calculated by the unsteady heat transfer equation given by **(**Birla et al., 2008**):**

$$\frac{\partial T}{\partial t} = \nabla \alpha \nabla T + \frac{Q}{\rho C_p} \qquad (2)$$

where T is the local temperature (°C) inside the material, t is the time (s) of heating, ρ, α, and C_p are the density (kg m^{-3}), thermal diffusivity (m s^{-2}) and specific heat (J kg^{-1} $°C^{-1}$) of the food material, respectively.

It is clear from the Eq. (1) that determination of electric field is necessary to calculate the RF power density inside the dielectric material. Electric field inside the RF applicator can

be determined by solving a set of partially differential equations (Eqs. 3-6), known as Maxwell equations (Balanis, 1989).

$$\nabla \times \boldsymbol{E} = -\mu \frac{\partial \boldsymbol{H}}{\partial t} \tag{3}$$

$$\nabla \times \boldsymbol{H} = \sigma_c \boldsymbol{E} + \varepsilon_0 (\varepsilon' - j\varepsilon'') \frac{\partial \boldsymbol{E}}{\partial t} \tag{4}$$

$$\nabla \cdot \boldsymbol{D} = \rho_v \tag{5}$$

$$\nabla \cdot \boldsymbol{H} = 0 \tag{6}$$

where $\boldsymbol{E}$, $\boldsymbol{H}$ and $\boldsymbol{D}$ are electric field (V m^{-1}), magnetic field (A m^{-2}), and electric flux density (C m^{-2}) of the dielectric material, respectively. ε', μ, ρ_v, σ_c are the dielectric constant, magnetic permeability (H m^{-1}), free volume charge density (C m^{-3}) and electrical conductivity (S m^{-1}) of the material, respectively. A general solution of Maxwell equations leads to wave nature of RF electric field. Since, RF wave lengths are substantially longer (e.g., ~ 11 m at 27.12 MHz) compared to practically available RF applicator sizes, Maxwell equations can be simplified into a single Laplace equation by neglecting the effect of magnetic field. The assumption results in the static RF electric field approximation inside the RF applicator. Laplace equation is used by (Birla et al., 2008):

$$\nabla(\sigma + j2\pi f \varepsilon_o (\varepsilon' - j\varepsilon'')\nabla V) = 0 \tag{7}$$

where $j = \sqrt{-1}$, V is the voltage between the two electrodes (V) and related to the electric field ($\boldsymbol{E} = -\nabla V$).

3. RF heating applications

3.1. Fresh fruits

RF heating has been explored as an potential alternative quarantine treatment to control insect pests such as codling moth, Mexican fruit fly, and Mediterranean fruit fly in fresh fruits.

Quarantine security against insect and pests in fresh fruits is required before exporting them to countries such as Japan and South Korea. Currently, methyl bromide fumigation is used to control pests in fresh fruits (Aegerter & Folwell, 2000) but its future use is uncertain as it has been recognized as an ozone depleting substance under Montreal Protocol (USEPA, 1998). Increased international pressure to limit the use of methyl bromide due to environmental issues, continual increase in price and reduced production result in urgent needs for developing non-chemical alternative quarantine treatments. Ikediala et al. (2002) evaluated the feasibility of RF heating as a potential postharvest treatment against codling moth in cherries. Cherries immersed in water were RF heated in a 6 kW RF system. The dielectric and ionic conductivity properties of the water and that of the fruit were matched by adding salt in the water to improve temperature uniformity in RF treated cherries. Birla et al. (2004) developed a fruit mover to improve the RF heating uniformity in large fruits such as apples and oranges. Rotation and movement to fruits subjected to RF heating improved temperature uniformity in treated fruits. Birla et al. (2005) applied RF energy on oranges to control Mediterranean fruit fly. Oranges immersed in saline water were rotated in the fruit mover and their temperatures were raised from 19 to 48 °C using RF heating. These authors reported temperature non uniformity in oranges and recommended conventional hot water heating prior to RF heat treatment in fresh fruits to improve temperature uniformity in fresh fruits. Based on the recommendations, Wang et al. (2006b) combined hot water surface preheating with RF core heating to develop RF based heat treatment protocol for apples. Treatment parameters were selected based on the minimum time-temperature conditions required for 100% mortality of fifth-instar codling moth. Results showed that hot water assisted RF heating improved temperature uniformity in apples. Monzon et al. (2007) applied RF heating in persimmon, a specialty fruit crop as a quarantine heat

treatment against Mexican fruit fly. In that study, persimmons were immersed in salt water to reduce non-uniform heating during RF treatments. The dielectric properties of water were adjusted to match that of persimmon by adding appropriate amount of salt. RF non-uniform heating was still found in the treated persimmons, resulting in loss of firmness and calyx browning in some treatments. Recently, the water assisted RF treatments for disinfesting mangoes were also conducted (Sosa-Morales et al., 2009). Quality parameters such as firmness, soluble solids and acidity of treated mangoes were measured and compared with controls after 12 days of storage at 21°C. No significant difference in quality parameters between RF treated and control mangoes were reported in this study.

3.2. Dry agricultural commodities

Advancements of RF heating in dry products started in 1940s, when RF heating was first used to control molds in breads (Cathcart et al., 1947). RF heating technology in dry agricultural commodities was mainly used to control pest insects, fungi, pathogens and enzymatic activity. A brief history of research activities related to RF heating applications in dry agricultural commodities is provided in subsequent sections

3.2.1. Pest- insects control

Wheat, infested with seven different pests, was heated inside a 39 MHz RF system (Nelson & Kantack, 1966). It was reported that complete elimination of pests varied with RF heating intensity, and duration. Nelson (1972, 1973) applied RF energy to control insects in several stored food grains. RF heat treatment was also used to eradicate pinewood nematode in loblolly and eastern white pine boards (Dwinell et al., 1994). Results showed that nematode mortality was a function of RF heating intensity and wood moisture content. Walnuts were heated in a 27.12 MHz RF system to control codling moth (*Cydia pomonella*), navel

orangeworm (*Amyelois transitella*), and Indian meal moth (*Plodia interpunctella*) (Wang et al., 2001a, 2002, 2003, 2005). It was reported that RF heating eliminated pests without affecting walnut quality. Langua- Solar et al (2005) used RF heating to control Angoumois grain moths in dried storage rough rice. It was reported that RF heating between 55 °C to 60 °C for 5 min resulted in 99% control of all biological stages of Angoumois grain moth. RF heating of walnuts was again examined to investigate the effect of different influencing factors such as walnut orientation, walnut type (open and closed shell), and intermittent mixing during RF heating (Wang et al., 2006a). Results showed that vertically oriented walnuts received higher temperature values than those of horizontally oriented. Open shell walnuts were heated faster than closed shell walnuts after washing. Mixing walnuts twice during 3 min RF heating, improved heating uniformity in walnuts. Temperature uniformities of RF treated walnuts were assessed and compared under different conditions such as mixing of walnuts and hot air circulation in a large scale RF experiment using an industrial scale 27.12 MHz, 25 kW RF system (Wang et al., 2007a, b). These authors reported that single mixing optimized the heating uniformity of walnuts. Recently, RF heating combined with hot air was used to control cowpea weevil (*Callosbruchus maculatus*) and Indian meal moth (*Plodia interpunctella*) in chickpea, lentil and green pea (Wang et al., 2010). It was reported that quality parameters including moisture loss, germination rate and color of treated legumes were the same as controls.

3.2.2. Fungi control

In the past, RF heating was also explored to control fungi in different dry agricultural products. Two different varieties of wheat were RF heat treated to eradicate *Fusarium graminearum,* a harmful fungi accountable for 'head blight' disease (Cwiklinski & von Hoersten, 2001). Germination of wheat seeds after RF heat treatment increased from 40% to

88%. Corn (Vassanacharoen et al., 2006) and Barley (Akaranuchat et al., 2007) seeds were RF heated to control seed-borne fungi such as *Aspergillus flavus, Alternaria* sp., *Penicillium* sp. and *Rhizopus* sp., and *Fusarium semitectum*. Three varieties of seasame seeds (white, black and red), infected with fungi *Macrophomina phaseolina,* were RF treated using five different selected temperatures (60, 70, 80, 85, and 90 °C) for 3 min (Vasanachalorn et al., 2004). RF heating eliminated fungi without affecting the quality of seasame seeds. The efficacy of RF heat treatment has been evaluated in oak, poplar and southern yellow pine wood to control wood decay fungi (*Gloeophyllum trabeum, Ganoderma lucidum and Irpex lacteus*) using an industrial 40-kW RF oven (Tubajika et al., 2007). Authors reported that RF treatment successfully eliminated fungi in treated wood samples.

3.2.3. Pathogen control

RF heating was also explored to inactivate pathogenic micro-organisms in dry agricultural commodities. Alfalfa seeds were RF treated to control pathogenic microorganisms *Solmonella*, *Escherichia coli O157:H7*, and *Listeria monocytogenes* (Nelson et al., 2002). RF heat treatment caused significant reduction in all three pathogens without affecting seed quality. Langua- Solar et al. (2007) used RF heating to inactivate *Solomonella* spp and *Escherichia coli O157:H7* in fishmeal. It was reported that RF energy caused five log reductions of these micro-organisms, without affecting fishmeal quality.

3.3.4. Enzyme deactivation

Lyman et al. (1948) studied RF treatment of cottonseeds. They reported that RF heating reduced the formation of free fatty acids, accountable for bad odor in cottonseeds. Growth inhibitor enzymes in soybeans were inactivated using RF heating (Borchers & Manage, 1972). Quality of RF treated soybeans was better than controls. Oberndorfer and Lucke (1999)

preheated rapeseeds at different temperatures inside a RF applicator, before pressing them against a laboratory screw press, in order to evaluate the effect of RF heating on oil yield. It was reported that RF preheat treatment increased oil yield. Irfan and Pawelzil (1999) evaluated the quality of RF preheated rapeseed oil and reported that RF preheat treatment did not affect the oil quality. Pungency of yellow mustard seeds were reduced by RF heating (Cserhalmi et al., 2001). RF heating inactivated *myrosinase* enzyme, accountable for seeds pungency. Schuster-Gajzago et al. (2006) also inactivated *myrosianse* enzyme in mustard seeds using RF energy. RF treated mustard seeds had the similar chemical composition and colloid-chemical properties as controls.

4. Mathematical models used for RF heating of dry agricultural commodities

Ptasznik et al. (1990) developed a semi-empirical mathematical model for RF assisted convective drying of hygroscopic materials based on the experimental data. The model was used to simulate RF drying of broad bean. Neophytou and Metaxas (1998) simulated RF heating of paper block in three different size (0.80×0.35× 0.40 m^3, 1.50×0.50×0.80 m^3, 2.00×0.60×1.00 m^3) applicators, using finite element method. They solved Maxwell and Laplace equations and compared the solutions to establish the validity of quasi static assumption of electric field using blocks of paper as a dielectric material. It was reported that assumption of quasi-static electric field was true only for small size applicator (0.80×0.35× 0.40 m^3) with the lowest RF frequency (13.56 MHz). Marshall and Metaxas (1998) simulated the RF electric field strength developed during the RF assisted heat pump drying of particulate materials. Experimental results showed that RF heating increased the drying rate as well as the performance of heat pump.

Yang et al. (2003) simulated RF heating of alfalfa and radish seeds packed inside rectangular polypropylene boxes in a 1 kW RF system. They solved wave equations using a transmission line method. A commercially available finite difference time domain based software TLM-FOOD HEATING was used to solve heat transfer in the model. Model was experimentally validated by comparing the simulated and experimented temperatures profiles of seeds at four different locations. They reported disagreements in the model. A model on RF assisted fluidized bed drying was developed for the corn (Jumah, 2005). Effect of electric field strength, frequency, inlet temperature and intermittency on RF drying was analyzed. Wang et al. (2005) developed a mathematical model to predict the required temperature time combination for insect thermal mortality and product quality as a function of number of intermittent mixing in RF treatment of walnuts. The model was based on the normal distribution of product final and initial temperatures. It was shown that increased number of mixing could increase the effective temperature time combinations for effective insect control without affecting the product quality. The model was also validated using soybean, lentil, and wheat.

5. Current research direction

It is clear from the literature review that the complex behavior of RF heating requires further studies for fresh fruits and dry agricultural commodities. In the current research, persimmon, a fresh fruit and whole wheat flour are selected as representative materials to investigate the potential of RF heating in fresh fruits and dry agricultural commodities. Following are the general objectives of this research:

1. Develop a RF based quarantine heat treatment for persimmon
2. Investigate the efficacy of RF heat treatments on the quality of persimmon

3. Develop a computer model to simulate RF heating in dry food materials
4. Experimentally validate the developed computer model
5. Analyze the effects of influencing parameters on temperature uniformity of RF treated dry food materials, using the validated computer model
6. Study options to improve temperature uniformity in the treated dry food materials

References

Aegerter, A.F. & Folwell, R. J. (2000). Economic aspects of alternatives to methyl bromide in the postharvest and quarantine treatment of selected fresh fruits. *Crop protection,* 19(3), 161–168.

Akaranuchat, P., Noimanee, P., Krittigamms, N., Von Hoersten, D., & Vearaslip, S. (2007). Control seed-borne fungi by radio frequency heat treatment as alternative seed treatment in barley (*Hordeum vulgare*). *Conference on International Agricultural Research for Development*, Witzenhausen, Germany.

Balanis, C.A. (1989). *Advanced engineering electromagnetics*. John Wiley & Sons, New York

Banerjee, M., & Sarkar, P.K. (2003). Inhibitory effect of garlic on bacterial pathogens from spices. *World Journal of Microbiology and Biotechnology,* 19 (6), 565-569.

Birla, S.L., Wang, S., & Tang, J. (2008). Computer simulation of radio frequency heating of model fruit immersed in water. *Journal of Food Engineering*, 84(2), 270-280.

Birla, S.L., Wang, S., Tang, J., Fellman, J.K., Mattinson, D.S., & Lurie, S. (2005). Quality of oranges as influenced by potential radio frequency heat treatments against Mediterranean fruit flies. *Postharvest Biology and Technology,* 38(1), 66-79.

Birla, S.L., Wang, S., Tang, J., & Hallman, G. (2004). Improving heating uniformity of fresh fruit in radio frequency treatments for pest control. *Postharvest Biology and Technology,* 33(2), 205-217.

Borchers, R., & Manage, L.A. (1972). Rapid improvement in nutritional quality of soybeans by dielectric heating. *Journal of Food Science*, 37, 333-334.

Cserhalmi, Zs., Markus, Zs., Czukor, B., Barath, A., & Toth, M. (2001). Physico-chemical properties and food utilization possibilities of RF-treated mustard seed. *Innovative Food Science and Emerging Technologies*, 1, 251-254.

Cwiklinski, M., & von Hoersten, D. (2001). Effect of exposure to radio-frequency electric fields on *fusarium graminearum* in wheat seed. *Annual International Meeting of the American Society of Agricultural Engineers*, Sacramento, California, USA.

Dwinell, L.D., Avramidis, S., & Clark, J.E. (1994). Evaluation of a radiofrequency vacuum dryer for eradicating the pinewood nematode in green sawn wood. *Forest Products Journal,* 44(4), 19-24.

Ikediala, J.N., Tang, J., Hansen, J., Drake, S.R., & Wang, S. (2002) Quarantine treatment of fruits using radio frequency energy and an ionic-water-immersion technique. *Postharvest Biology and Technology*. 24, 25-37.

Irfan, I., & Pawelzil, E. (1999). The effect of rapeseed treatment by microwave and radio-frequency application on oil extraction and oil quality. Part II: Influence on oil quality. *Fat Science Technology,* 101(5), 168–171.

Jumah, R. (2005). Modelling and simulation of continuous and intermittent radio frequency-assisted fluidized bed drying of grains. *Food and Bioproducts Processing*, 83(C3), 203-210.

Lagunas-Solar, M.C., Pan, Z., Zeng, N.X., Truong, T.D., Khir, R., & Amaratunga, K.S.P. (2007). Application of radio frequency power for non-chemical disinfestation of rough rice with full retention of quality attributes. *Applied Engineering in Agriculture*, 23(5), 647-654.

Lagunas-Solar, M. C., Zeng, N. X., Essert, T. K., Truong, T. D., Pina, C., Cullor, J. S., Smith, W. L., & Larrain, R. (2005). Disinfection of fishmeal with radiofrequency heating for improved quality and energy efficiency. *Journal of the Science of Food and Agriculture*, 85(13), 2273-2280.

Lyman, C.M., Burda, E.J., & Olschner, P.Q. (1948). The effect of dielectric heating on storage quality of cottonseed. *Journal of the American Oil Chemists' Society*, 25(7), 246-249.

Marra, F., Lyng, J., Romano, V., & McKenna, B. (2007). Radio-frequency heating of foodstuff: solution and validation of a mathematical model. J*ournal of Food Engineering*, 79(3), 998-1006.

Marra, F., Zhang, L., & Lying, J. (2009). Radio frequency treatment of foods: Review of recent advances. *Journal of Food Engineering,* 91(4), 497-508.

Marshall, M.G. & Metaxas, A.C. (1998). Modeling of the radio frequency electric field strength developed during the RF assisted heat pump drying of particulates. *Journal of Microwave Power and Electromagnetic Energy,* 33(3), 167-177.

Monzon, M.E., Biasi, B., Mitcham, E.J., Wang, S., Tang, J.M., & Hallman, G.J. (2007). Effect of radiofrequency heating on the quality of 'Fuyu' persimmon fruit as a treatment for control of the Mexican fruit fly. *HortScience*, 42(1), 125–129.

Nelson, S.O. (1972). Possibilities for controlling stored grain insects with radio frequency energy. *Journal of Microwave Power and Electromagnetic Energy*, 7(3), 231-239.

Nelson, S.O. (1973). Insect-control studies with microwaves and other radio frequency energy. *Bulletin of the Entomological Society of America*, 19(3), 157-163.

Nelson, S.O., & Kantack, B.H. (1966). Stored-grain insect control studies with radio-frequency energy. *Journal of Economic Entomology*, 59(3), 588-594.

Nelson, S.O., Lu, C.Y., Beuchat, L.R., & Harrison, M.A. (2002). Radio-frequency heating of alfalfa seed for reducing human pathogens. *Transactions of the ASAE*, 45(6), 1937-1942.

Neophytou, R.I., & Metaxas, A.C. (1998). Combined 3D FE and circuit modeling of radio frequency heating systems. *Journal of Microwave Power and Electromagnetic Energy*, 33(4), 243-262.

Oberndorfer, C., & Lucke, W. (1999). The effect of rapeseed treatment by microwave and radio-frequency application on oil extraction and oil quality. Part I: Influence on mechanical oil extraction. *Fat Science Technology*, 101(5), 164–167.

Ptasznik W, Zygmunt S, & Kudra T. (1990). Simulation of RF-assisted convective drying for seed quality broad bean. *Drying Technology,* 8(5), 977-992.

Rowley, A.T. (2001). Radio frequency heating. In P. Richardson (Ed.), *Thermal technologies in food processing* (pp 163-177). Woodhead Publishing Limited, Abington

Schuster-Gajzago, I., Kiszter, A.K., Toth-Markus, M., Bardth, A., Markus-Bednarik, A., & Czukor, B. (2006). The effect of radio frequency heat treatment on nutritional and colloid-chemical properties of different white mustard (Sinapis alba L.) varieties. *Innovative Food Science & Emerging Technologies*, 7(1-2), 74-79.

Sosa-Morales M.E., Tiwari, G., Wang, S., Tang, J., Lopez-Malo A., & Garcia, H.S. (2009). Dielectric heating as a potential post-harvest treatment of disinfesting mangoes, II: development of RF based protocols and quality evaluation of treated fruits. *Biosystems Engineering,* 103(3), 287-296.

Tang, J., Ikediala, J.N., Wang, S., Hansen, J., & Cavalieri, R. (2000). High temperature short time thermal quarantine methods. *Postharvest Biology and Technology,* 21, 129-145.

Tubajika, K.M, Jonawiak, J.J., Mack, R., & Hoover, K. (2007). Efficacy of radio frequency treatment and its potential for control of sapstain and wood decay fungi on red oak, poplar, and southern yellow pine wood species. *Journal of Wood Science,* 53(3), 258-263.

[USEPA] United States Environmental Protection Agency (1998). Reregistration Eligibility Decision. Aluminum and Magnesium Phosphide. Case s0025 and 0645. Office of Pesticide Programs, Special Review and Reregistration Division. Agricultural Statistics. Washington, DC.

Vassanacharoen, P., Janhang, P., Krittigamas, N., von Hörsten, D., & Lücke, W. (2006). Radio frequency heat treatment to eradicate *Fusarium semitectum* in corn grain (Zea Mays). *Agricultural Science Journal*, 37(5), 180-182.

Vasanachalorn, P., Kritigamas, N., Thanapornpoonpomg. (2004).Radio frequency heat treatment to control seed-borne *Macrophomina phaseolina* in sesame seed (*Ses amum indicum* L.). *Deutcher Tropentag*. Berlin, Germany.

Wang, S., Birla, S.L., Tang, J., & Hansen, J.D. (2006a). Postharvest treatment to control codling moth in fresh apples using water assisted radio frequency heating. *Postharvest Biology and Technology*, 40(1), 89-96.

Wang, S., Ikediala, J.N., Tang, J., Hansen, J.D., Mitcham, E., Mao, R., & Swanson, B. (2001a). Radio frequency treatments to control codling moth in in-shell walnuts. *Postharvest Biology and Technology*, 22(1), 29-38.

Wang, S., Monzon, M., Johnson, J.A., Mitcham, E.J., & Tang, J. (2007a). Industrial-scale radio frequency treatments for insect control in walnuts: I. Heating uniformity and energy efficiency. *Postharvest Biology and Technology*, 45(2), 240-246.

Wang, S., Monzon, M., Johnson, J.A., Mitcham, E.J., & Tang J. (2007b). Industrial-scale radio frequency treatments for insect control in walnuts: II. Insect mortality and product quality. *Postharvest Biology and. Technology*, 45(2), 247-253.

Wang, S., Tang, J., & Cavalieri, R.P. (2001b). Modeling fruit internal heating rates for hot air and hot water treatments. *Postharvest Biology and Technology,* 22, 257-270.

Wang, S., Tang, J., Cavalieri, R.P., & Davies, D.C. (2003). Differential heating of insects in dried nuts and fruits associated with radio frequency and microwave treatments. *Transactions of the ASAE*, 46(4), 1175-1182.

Wang, S., Tang, J., Johnson, J.A., Mitcham, E., Hansen, J.D., Cavalieri, R.P., Bower, J., & Biasi, B. (2002). Process protocols based on radio frequency energy to control field and storage pests in in-shell walnuts. *Postharvest Biology and Technology*, 26(3), 265-273.

Wang, S., Tang, J., Sun, T., Mitcham, E.J., Koral, T., & Birla, S.L. (2006b). Considerations in design of commercial radio frequency treatments for postharvest pest control in inshell walnuts. *Journal of Food Engineering,* 77(2), 525-534.

Wang, S., Tiwari, G., Jiao, S., Johnson J.A., & Tang, J. (2010). Developing postharvest disinfestation treatments for legumes using radio frequency energy. *Biosystems Engineering,* 105(3), 341-349.

Wang, S., Yue, J., Tang, J., & Chen, B. (2005). Mathematical modelling of heating uniformity for in-shell walnuts subjected to radio frequency treatments with intermittent stirrings. *Postharvest Biology and Technology*, 35(1), 97-107.

Yang, J., Zhao, Y., & Wells, J.H. (2003). Computer simulation of capacitive radio frequency (RF) dielectric heating on vegetable sprout seeds. *Journal of Food Process Engineering,* 26(3), 239-263.

CHAPTER 2

EFFECT OF WATER ASSISTED RADIO FREQUENCY HEAT TREATMENT ON THE QUALITY OF 'FUYU' PERSIMMONS

G. Tiwari[1], S. Wang[1], S.L. Birla[2], J. Tang[1]

Published manuscript in Biosystems Engineering

[1]Department of Biological Systems Engineering,

Washington State University, Pullman, WA 99164-6120, USA

2 Department of Biological Systems Engineering,

University of Nebraska, Lincoln, NE 68583, USA.

Corresponding author:
Juming Tang, 213 LJ Smith Hall, Pullman, WA 99164-6120, USA;

Phone: 509-335-2140; fax: 509-335-2722; e-mail: jtang@wsu.edu.

Abstract

Water assisted radio frequency (RF) heat treatment was evaluated as a potential alternative to chemical fumigation for providing quarantine security against Mexican fruit fly (*Anastrepha ludens*) in 'Fuyu' persimmon. Three holding times were chosen for each of the three treatment temperatures (46, 48 and 50 °C), one time at, one above and another below 100% mortality. Heat treatment protocols included preheating the fruit in 40°C water, followed by RF heating in 12 kW, 27.12 MHz RF system, holding at the target temperature for the required time and then hydro cooling at 4°C for 30 min. The preheating time at 40°C was determined based on the final RF heating uniformity over the fruit cross-section. Quality parameters, including weight loss, firmness, soluble solids, titratable acidity, peel and pulp color, and calyx browning of persimmons, were evaluated after 7 days of room (22°C) and cold storage (4°C). All treatments except for one condition (48°C + 8 min holding) had no significantly adverse effects on quality attributes. Slight calyx browning was observed in the treated samples and the degree of browning increased with treatment time for each treatment temperature. Results suggested that water assisted RF heat treatments provided potential for disinfestation of persimmons with acceptable product quality in terms of firmness, soluble solids and peel and pulp color.

1. Introduction

China, Japan and Korea are traditionally major producers of persimmon (*Diospyros kaki)* fruit, contributing 95 % of world production (Soriano *et al*., 2006). In the United States, the Human Nutrition Information Service (HNIS) in the Department of Agriculture has placed it into the category of specialty fruit of increasing popularity to the US consumers (Homnava *et al*., 1991). California is a major producer of 'Fuyu' persimmons in the US (Forbus *et al*., 1991; Clark & MacFall, 2003). The Mexican fruit fly, *Anastrepha ludens* (Loew), though originated in Mexico, is found in tropical fruit such as persimmons in California (Monzon *et al*., 2007), posing major threat for international and inter-state persimmon fruit trade, which requires quarantine security before exporting.

Currently, methyl bromide fumigation is used for pest control in fresh fruits (Aegerter & Folwell, 2000; Hansen *et al*., 2000) but its use in future is uncertain as it has been recognized as ozone depleting substance under Montreal Protocol (USEPA, 1998). Increased international pressure to limit the methyl bromide use due to environmental issues, continual increase in price and reduced production result in urgent needs for developing non-chemical alternative quarantine treatments.

Hot air and hot water treatments have been studied as alternatives to disinfest codling moth (*Cydia pomonella*) in cherries (Feng *et al*., 2004), Caribbean fruit fly (*Anastrepha suspense*) in oranges (Sharp & McGuire, 1996), Mexican (*Anastrepha ludens*) and West Indian fruit fly (*Anastrepha obliqua*) in mangoes (Sharp *et al*., 1989) and other insects in apples (Smith & Lay-Yee, 2000), and persimmons (Dentener *et al*., 1996; 1997; LayYee *et al*., 1997). These conventional heating methods require lengthy treatment times (in hours) for 100% disinfestations of fruit flies as heat transfers slowly from surface to core of the fruit. Exposure

to heat for prolong time results in adverse effects on overall quality of fruits, such as weight and firmness loss, skin browning and other quality losses.

Radio frequency (RF) heating has been investigated as a quarantine treatment in dry products such as walnuts (Wang *et al*., 2001; 2002) and in fresh fruits such as apples (Wang *et al*., 2006), cherries (Monzon *et al*., 2006), oranges (Birla *et al*., 2005) and more recently in persimmons (Monzon *et al*., 2007). The main advantages of RF heating over other conventional heating methods are its rapid heating, potential differential heating between pest and commodity (Wang *et al*., 2003), and ability to penetrate deep into the target material (Tang *et al*., 2000; Hansen & Johnson, 2007).

Monzon *et al*. (2007) evaluated potential for RF heating as a quarantine heat treatment in persimmon fruit using saline water immersion technique. In that study, fruit samples were immersed in salt water to reduce non-uniform heating during RF treatments. The dielectric properties of water were adjusted to match that of persimmon by adding appropriate amount of salt. RF non-uniform heating was still found in the treated persimmons, resulting in loss of firmness and calyx browning in some treatments. Similar studies on RF treatments of apples and oranges showed that even matching dielectric properties of fruit with surrounding water did not provide adequate heating uniformity among the fruit (Birla *et al*., 2004; 2005). By combining RF core heating with water surface pretreatment, RF treatments have been successfully explored for disinfesting apples (Wang *et al*., 2006) with acceptable product quality. It is desirable to develop the water assisted RF treatments for controlling the insect pests in persimmons without quality damage.

The objectives of this study were to: (1) determine the preheating times at each target temperature based on the required RF heating uniformity, (2) develop a treatment protocol of

water assisted RF heating for 'Fuyu' persimmon control of Mexican fruit fly, and (3) evaluate product quality of RF treated persimmons under ambient and cold storage conditions.

2. Material and methods

2.1. *Sample preparations and thermal treatment designs*

'Fuyu' persimmons (average weight of 137 ± 9.6 g and diameter of 6.9 ± 0.4 cm) were purchased from a commercial orchard in Visalia, CA and shipped overnight to Washington State University, Pullman, WA, USA. Persimmons were kept in cold storage (4 °C) until used for next day treatments. The samples were left at ambient temperature (~22 °C) for at least 12 hours to achieve uniform fruit temperature before RF treatments and avoid the enhanced thermal tolerance of insects (Wang *et al.*, 2005). Fruits had initial average firmness 40.3 ± 5.3 N, total soluble solids 11.3 ± 0.5 %, and peel color 60.8 ± 3.0, 31.3 ± 3.8 and 53.9 ± 5.6 in L, a*, b* scale.

Thermal death kinetic studies of third instars (most heat tolerant stage) of Mexican fruit fly indicated that 100% mortality can be achieved by exposing to 46 °C for 25 min, or 48 °C for 6 min, or 50 °C for 2 min (Hallman *et al*., 2005). In this study, three target temperatures of 46, 48, and 50 °C and three holding times corresponding to a level at, above and below 100% mortality were selected for RF heat treatment and quality analysis (Table 1).

2.2. *Treatment parameter determinations*

We selected 40 °C as the preheating temperature for all thermal treatments. Liu (1978) reported that heat exposure to 40 °C for 4 days had no adverse effects on the quality of '*Golden Delicious*' apples in terms of firmness and peel and pulp color. In preliminary tests, we also observed no quality change in persimmons after treating in 40 °C water for 60 min. Prior to RF treatments, eight fruits were placed in a circulating water bath (Model ZD, Grant, Cambridge,

UK) at 40 °C for 30 min. Two thermocouples (Type-T, THQSS-020U-6, Omega Engineering Inc., Stamford, CT) were inserted in one fruit to measure the fruit surface and core temperatures, the data were recorded every 5 s using a data logger (DL2e, Delta-T Devices Ltd., Cambridge, UK). At the heating times of 5, 10, 15, 20, 25 and 30 min, one randomly selected fruit was removed from the water bath and cut into halves along the surface perpendicular to calyx. One half fruit facing upward was immediately placed into a water filled container with 90 percent fruit volume immersed in water. Water temperature was maintained equal to fruit surface temperature (40 °C) to reduce heat loss from the exposed fruit surface. A thermal image of the exposed fruit surface was taken immediately using an infra-red imaging camera with accuracy ± 2°C (ThermaCAM ^{TM} Researcher 2001, FL-IR Systems, Portland, OR). The subsurface and core temperatures of the preheated fruits were measured at 2 mm below the peel and the fruit center, respectively, by thermocouple, which were compared with those measured by thermal imaging methods for the mentioned specific times. The fruit surface and core temperatures after RF treatments with a target temperature of 48 °C were also recorded during 30 min of cooling using 4 °C water.

To determine the best preheating time for each target temperature, a preliminary experiment was conducted to compare the heating uniformity of the fruit samples after RF treatments for different preheating times at 40°C. After preheating for the given times, eight fruits as a group were immediately transferred into a fruit mover filled with 40°C water. Water inside the fruit mover was circulated using a 0.745 kW, single phase centrifugal pump (TEEL Model # 2PC27, Dayton Electrical Mfg. Co., Niles, IL). The description and operation procedures of the fruit mover can be found in Birla *et al*. (2004). The fruit mover was placed between the two parallel electrodes of a 12 kW, 27 MHz batch type RF heating system (E-200,

Strayfield International Limited, Workingham, UK). RF heating was conducted using 8 kW power with an electrode gap of 210 mm. Circulating water temperature was monitored by thermocouples, placed in the circulation pipe outside the RF system. RF power was switched off once the circulating water temperature reached the target temperature (46 or 48 or 50 48 °C). Two fruit samples were immediately taken out from the fruit mover and cut into halves to map the temperature distribution by the infra-red imaging camera. The mean temperature and standard deviation of RF treated samples were estimated for each thermal image. The best heating uniformity around the target temperature was used to determine the preheating time for final RF treatments.

2.3. *Treatment procedures*

Based on those preliminary tests, three preheating times of 25, 30 and 35 min, 15, 20 and 25 min, and 5, 10 and 15 min were chosen for the target fruit temperatures of 46, 48 and 50 °C, respectively. Longer preheating times at 40 °C and shorter RF heating were used to achieve the desired heating uniformity for lower final target temperature.

In experiment for quality studies, eight persimmons were heated in the water bath at 40°C with the optimized preheating time for each final temperature. Preheated fruits were transferred into the fruit mover filled with 40 °C water inside the RF system. RF power (8 kW) was applied till the circulating water reached the target temperatures (46 or 48 or 50 °C). Fruits were immediately removed from the fruit mover and kept in the water bath maintained at the selected target temperature for different holding times (Table 1). Fruits were then hydro-cooled in 4 °C water for 30 min and stored in open space at room (22°C and 35% relative humidity) and cold storage (4°C and 80% relative humidity) for 7 days. Controls were dipped in water at

room temperature for 30 min before keeping them with treated fruits in both storage conditions. Each treatment was replicated three times.

2.4. *Quality evaluation*

Quality parameters including weight loss, firmness, soluble solids, peel and pulp color, and titratable acidity were measured after 7 days at room and cold storage. Weight loss was expressed as percentage of fruit weight reduction from initial weight. Firmness was measured in Newton (N) by a Texture Analyzer (Model TA-XT2, Stable Micro Systems, YL, UK) using a cylindrical (7.9 mm diameter) hemispherical tip probe. The speed of the probe was set at 400 mm/min; the measurements were made at three equally spaced positions (120° apart) along the equatorial fruit surface. Prior to firmness measurement, fruits skins were peeled off at all three positions. Peel color was measured at three marked spots on each fruit by a tristimulus colorimeter (Model CM-2002, Minolta Corp., Ramsey, NJ) and expressed in L, a*, and b* scale. Pulp color was measured at two spots on each exposed fruit surface after cutting it into two halves. Hand-squeezed juice from six persimmons was used to measure sample titratable acidity (TA) after each treatment. Five ml juice sample was titrated against 0.1 N NaOH till final pH reached 8.2. The TA value was expressed in terms of equivalent anhydrous malic acid in g/100 ml of juice. Total soluble solids (°Brix) were measured using a hand held refractometer (Model N-1α, ATAGO Co. Ltd., Tokyo, Japan) and expressed as percentage soluble solids in juice. Visual observations for skin and calyx browning were also made after 7 days of room and cold storages (4 °C).

The measurement of individual quality attribute was subjected to an analysis of variance (ANOVA) and means were separated using Tukey's method (SAS Institute, 2002, Cary, NC) at a significance level of 0.05 ($P<0.05$).

3. Results and discussions

3.1. *Comparison of thermal imaging and thermocouple methods*

Table 2 shows core and surface temperatures of persimmon fruit measured by thermal imaging and thermocouple methods. Temperature data were compared after 5, 10, 15, 20, 25, and 30 min of preheating at 40 °C and hydro-cooling at 4 °C for 30 min. A good agreement was obtained between these two methods both for surface and core temperatures. The temperature difference between thermal imaging and thermocouple methods was below 1.4 °C (Table 2).

3.2. *Preheating time determination*

Average temperature (mean ± S.D.) of persimmon fruit cut surface measured by thermal imaging after initial RF treatments with different preheating times are shown in Table 3. In general, in order to obtain relatively uniform treatments, longer preheating times and shorter RF heating were needed for lower target temperatures. For example, preheating at 40°C for 20 min provided the average fruit temperature of 47.7±0.6°C, aimed to achieve 48°C, while 15 and 25 min preheating offered the average fruit temperatures of 44.8±0.5 °C and 50.8 ± 0.8 °C, respectively, after RF heating, which were not suitable for 48 °C treatment (Table 3). Similarly, preheating times of 30 and 10 min at 40 °C were found appropriate for 46 °C and 50 °C final treatment temperature, providing the uniform average fruit temperatures of 46.1 ± 0.3 and 49.9±0.4 °C after RF heating. Therefore, based on the achieved target temperature and heating uniformity, preheating times of 30, 20 and 10 min at 40°C were chosen for final treatment temperature of 46, 48 and 50°C, respectively. The selected preheating times in 40°C water bath and subsequent RF heating times required for the fruit to reach three different final temperatures (namely 46, 48 and 50°C) as measured at the core and subsurface are summarized

in *Fig. 1*. It took about 70, 120, and 140 s of RF heating for fruit core to reach 46, 48, and 50°C, respectively, after preheating described above (*Fig. 1*).

3.3. *Temperature time profile of persimmon*

Figure 2 shows the temperature time history of persimmon fruit at different stages - preheating in 40 °C water for 20 min, RF heating to raise the fruit temperature up to 48 °C, holding at 48 °C for 6 min, and cooling at 4 °C for 30 min in 48 °C + 6 min heat treatment. The core and surface temperature of persimmon fruit were 35.4 °C and 40 °C, respectively, after 20 min preheating (*Fig. 3a*). Slow heat transfer from the surface to the core of fruit resulted relatively in lower core temperature. Core temperature of fruit during RF heating rose from 35.4 °C to 48.4 °C whereas surface temperature rose from 40 °C to 47.8 °C (*Fig. 3b*), showing preferential core heating by RF treatments. It is obvious that pretreatment surface heating prior to RF treatment compensated core RF heating of fruit and assured uniform fruit temperature (mean ± S.D., 47.7 ± 0.6 °C). Holding fruit in 48 °C water for 6 min further improved the heating uniformity. The average temperature (mean ± S.D.) after holding was 47.9±0.2 °C (*Fig. 3c*). Cooling for 30 min at 4 °C water reduced fruit surface and core temperatures to 5.4 and 13.4 °C, respectively (*Fig. 3d)*. Cooling time can be further reduced based on the required fruit core temperature to reduce operational cost in industrial applications of this technology.

3.4. Quality

3.4.1. *Weight loss*

RF heat treatment itself had no significant effect on weight loss of treated fruits after 7 days at room temperature and in cold storage (4 °C)($P>0.05$) (Tables 4 and 5). In another study also, no significant difference on weight loss was observed between RF treated and control persimmons after 12 days at 20 °C storage (Monzon *et al*., 2007). Table 6 shows the results of

factorial ANOVA analysis performed on individual quality attributes. Regardless of the RF treatment, storage conditions significantly affected the weight loss ($P<0.05$). Fruits stored in cold storage had lower weight loss (~1.4-1.5%) compared to those stored at room temperature (6.9-8.4%) (Tables 4 and 5). The sharp reduction in weight loss for samples in cold storage might be attributed to lower level of dehydration and reduced physiological changes in fruit such as respiration, transpiration and ripening.

3.4.2. *Firmness*

No significant difference was detected in firmness between control and the treated samples after 7 day storage at room temperature , except for fruits that went through the 48 °C + 8 min holding treatment ($P<0.05$) (Table 4). The reduced firmness for this particular treatment might have been caused by prolonged heating, resulting increased rate of ripening in the treated fruit. Monzon *et al*. (2007) also reported a reduction in the firmness of persimmons, after 48 °C RF treatment with holding times 12 and 18 min. All treated persimmons in cold storage were significantly firmer than the untreated control (Table 5). The reason for the increased firmness of persimmons could be the inhibition of ethylene synthesis due to heat treatment, which subsequently delays the ripening (Lurie & Mitcham, 2007). Such an increase in the firmness of treated persimmons was not observed in room condition, but it was definitely evident in cold storage. Studies on apples (Lurie & Klein, 1992a; Lurie & Nussinovitch, 1996) and tomato (Lurie & Klein, 1992b) showed that heat treatment followed by reduced temperature storage either significantly increased the firmness or delayed the ripening of commodity. Kim *et al*. (1994) reported that heat treatment at 45 °C for 1.75 h followed by 2 °C storage for a week significantly increased firmness of '*Golden Delicious*' apples than those

stored at 10, 18 and 25 °C. This observation might be helpful in extending storage life of persimmons.

3.4.3. *Peel and pulp color*

There was no significant difference in peel color between the control and all treated fruits after 7 day storage at room temperature, except for the 48 °C + 8 min holding treatment. Peel color (hue) was significantly lower in the 48 °C + 8 min holding treatment ($P<0.05$) (Table 4), which was evident by the dark shade on treated fruits surface. Heat exposure for relatively longer time followed by room storage could have enhanced the rate of ripening, resulting in dark color for this particular treatment. However, no significant difference was observed in peel color between treated and control fruits in cold storage ($P>0.05$) (Table 5).

Treatments at 48 °C for 8 min holding also showed significant effects on pulp color of RF treated persimmons after storage at room temperature ($P<0.05$) (Table 4). Decreases in hue (dark shade) indicated over ripening of fruits. Firmness loss and peel color change supported the findings for this particular treatment. No significant difference in pulp color was detected between treated and control fruits after 7 days of cold storage (4 °C)($P>0.05$) (Table 5).

3.4.4. *Total soluble solids and titratable acidity*

RF treatment had no significant effect on soluble solids and titratable acidity of persimmons ($P>0.05$). Studies on RF treated apples (Wang *et al*., 2006) and oranges (Birla *et al*., 2005) also showed similar results. Storage conditions significantly affected TA and TSS of fruits ($P<0.05$) (Table 6). Slight decrease in TA and TSS was observed in cold stored fruits compared to those stored at room temperature (Tables 4 and 5). This could be attributed to lower metabolic activities of fruits in cold storage (Prasana *et al*., 2000), resulting in slow rate of maturity. Quantity of malic acid in immature persimmons was found less than in mature

ones (Senter *et al.*, 1991). The lower TSS in cold storage could be due to the reduced conversion rate of starch into sugars.

3.4.5. *Visual observations*

In all RF treatments, calyx was slightly browner than controls and the browning was more severe in the longest holding time in each of three target temperatures. No shrivel or skin browning was observed in treated fruits.

4. Conclusions

Water assisted RF heating was investigated as a quarantine treatment for Mexican fruit fly in 'Fuyu' persimmons at 46, 48 and 50 °C. Quality parameters, including weight loss, firmness, soluble solids and titratable acidity, peel and pulp color, were evaluated after 7 days of room and cold storage. All RF treatments except for 48 °C + 8 min holding either significantly improved or had no effect on the overall quality of persimmons. Increased firmness in cold stored treated fruits may be useful for extending storage life of persimmons. Based on results, RF treatments for 46 °C + 25 min holding, or 48 °C + 6 min holding, or 50 °C + 2 min holding have potential to provide 100 % mortality of Mexican fruit fly with acceptable fruit quality. Water assisted RF heating can overcome heating non-uniformity problem associated with RF treatments in fresh fruits. Large scale tests are needed to establish a quarantine protocol for persimmons using water assisted RF heating technique.

Acknowledgement

This research was supported by grants from USDA-CSREES (2004-51102-02204) and USDA-NRI (2005-35503-16223) and partially by Washington State University Agricultural Research Center.

Table 1

Experimental design of radio frequency heat treatment

Treatments	Treatment description
46 °C + 20 min 46 °C + 25 min 46 °C + 30 min	Preheating at 40 °C and RF heating to raise temperature up to 46 °C and holding at 46 °C for 20, 25 and 30 min
48 °C + 4 min 48 °C + 6 min 48 °C + 8 min	Preheating at 40 °C and RF heating to raise temperature up to 48 °C and holding at 48 °C for 4, 6 and 8 min
50 °C + 1 min 50 °C + 2 min 50 °C + 4 min	Preheating at 40 °C and RF heating to raise temperature up to 50 °C and holding at 50 °C for 1, 2 and 4 min
Control	No heat treatment

Table 2

Comparisons of measured surface and core temperatures of 'Fuyu' persimmon between thermal imaging (TI) and thermocouple (TC) methods during preheating and hydro-cooling

Treatments	Time, min	Surface temperature, °C		Core temperature, °C	
		TI	TC	TI	TC
Preheating in	5	38.5	39.5	25.4	25.9
40 °C water	10	38.5	39.9	28.8	29.8
	15	38.6	40.0	32.5	33.1
	20	38.8	40.0	34.7	35.4
	25	39.2	40.0	36.6	37.0
	30	39.6	40.0	37.4	38.0
Hydrocooling	30	5.6	5.4	12.8	13.4
in 4°C water					

Table 3

Preheating time determinations at 40°C water baths based on heating uniformity after RF treatment of 'Fuyu' persimmons (with three replicates) at three different target temperatures.

Target Temperature after RF treatment	*Preheating time in 40°C water bath, min*	*Average and standard deviation temperatures after RF treatment, °C*
	25	43.9±0.3
46°C	30	**46.1±0.4**
	35	48.2±0.7
	15	44.8±0.5
48°C	20	**47.7±0.6**
	25	50.8±0.8
	5	44.8±0.9
50°C	10	**49.9±0.4**
	15	51.0±0.3

Table 4

Quality parameters of control and RF treated 'Fuyu' persimmons (with three replicates) after 7 days storage at room temperature (22°C, 35% RH)

Treatment	Weight loss, %	Firmness, N	Total soluble solids, %	Acidity, g/100 ml	Peel color, Hue	Pulp color, Hue
Control	6.9a*	16.75a	14.6a	0.15a	56.4a	53.2a
46 °C + 20 min	6.4a	16.43a	14.0a	0.14a	54.7a,b	52.9a,b
46 °C + 25 min	8.4a	18.61a	13.2a	0.13a	55.6a	54.6a
46 °C + 30 min	6.1a	16.04a	14.1a	0.13a	54.4a,b	52.6a,b
48 °C + 4 min	6.0a	16.59a	14.5a	0.12a	56.1a	54.2a
48 °C + 6 min	8.1a	18.40a	14.0a	0.15a	55.8a	53.8a
48 °C + 8 min	7.6a	11.94b	13.9a	0.14a	53.2b	50.5b
50 °C + 1 min	7.3a	17.14a	14.5a	0.12a	55.3a,b	52,5a,b
50 °C + 2 min	8.3a	19.96a	14.6a	0.14a	56.2a	52.7a,b
50 °C + 4 min	8.1a	16.20a	14.6a	0.12a	54.8a,b	53.7a

* Different letters within a column indicate that means are significantly different ($P<0.05$)

Table 5

Quality parameters of control and RF treated ‘Fuyu’ persimmons (with three replicates) after 7 days at cold storage (4 °C, 80% RH)

Treatment	Weight loss, %	Firmness, N	Total soluble solids, %	Acidity, g /100 ml	Peel color, Hue	Pulp color, Hue
Control	1.4a*	18.0a	12a	0.09a	56.3a	52.3a
46 °C + 20 min	1.5a	35.3b	12a	0.12a	56.9a	53.1a
46 °C + 25 min	1.5a	28.5c	13a	0.12a	56.1a	53.9a
46 °C + 30 min	1.5a	25.0c,d	11a	0.09a	56.1a	52.9a
48 °C + 4 min	1.5a	25.9c,d	12a	0.08a	56.2a	52.7a
48 °C + 6 min	1.5a	29.4b,d	12a	0.10a	55.9a	52.4a
48 °C + 8 min	1.4a	21.5a,d	12a	0.09a	55.9a	53.3a
50 °C + 1 min	1.4a	21.1a,d	11a	0.10a	55.5a	52.9a
50 °C + 2 min	1.5a	23.7c,d	11a	0.10a	55.9a	53.3a
50 °C + 4 min	1.4a	24.9c,d	12a	0.11a	55.5a	52.1a

* Different letters within a column indicate that means are significantly different ($P<0.05$).

Table 6

ANOVA P values ($\alpha = 0.05$) for the effect of treatment, storage and treatment × storage interaction for persimmon quality parameters

	Wt loss	Firmness	Soluble solids	Acidity	Peel color	Pulp color
Treatment (T)	0.0729	<0.0001	0.7965	0.0628	<0.0001	0.0021
Storage (S)	<0.0001	<0.0001	<0.0001	<0.0001	<0.0001	0.4480
T × S	0.0263	<0.0001	0.0959	0.0158	<0.0001	0.0002

***** $P < 0.05$ indicate a significant effect at the 5 % level from the of treatment, storage and treatment × storage on quality parameters

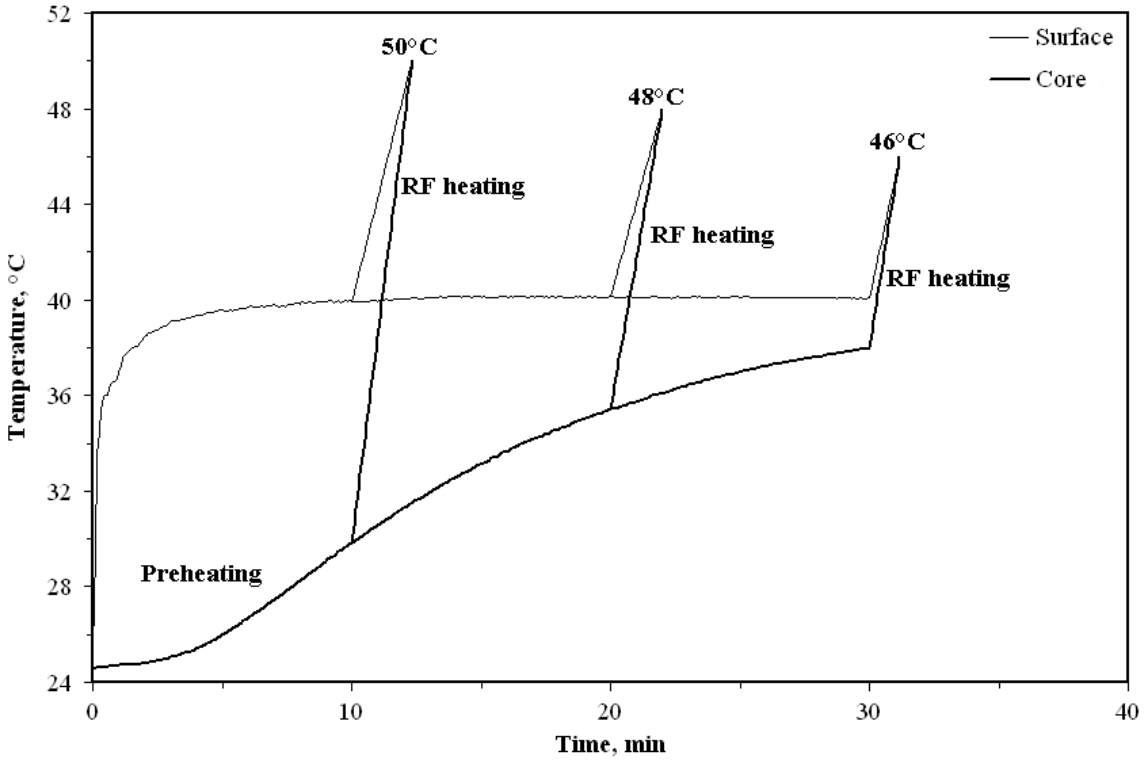

Fig. 1. Experimentally determined preheating and radio frequency (RF) heating times for the surface and core temperature of 'Fuyu' persimmon to each of the three selected target temperatures.

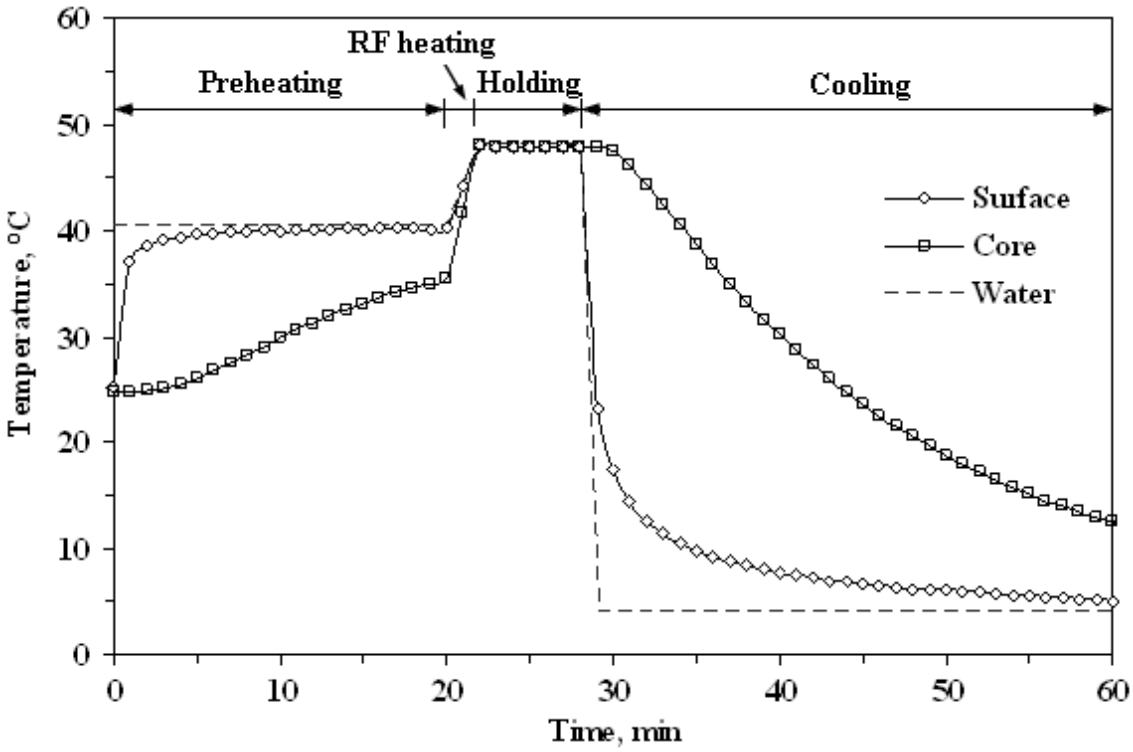

Fig. 2. Heating and cooling profiles for surface and core of 'Fuyu' persimmon (diameter of 7 cm), subjected to preheating in hot water at 40 °C followed by RF heating to raise temperature up to 48 °C, holding at 48 °C for 6 min and hydro-cooling for 30 min at 4 °C water.

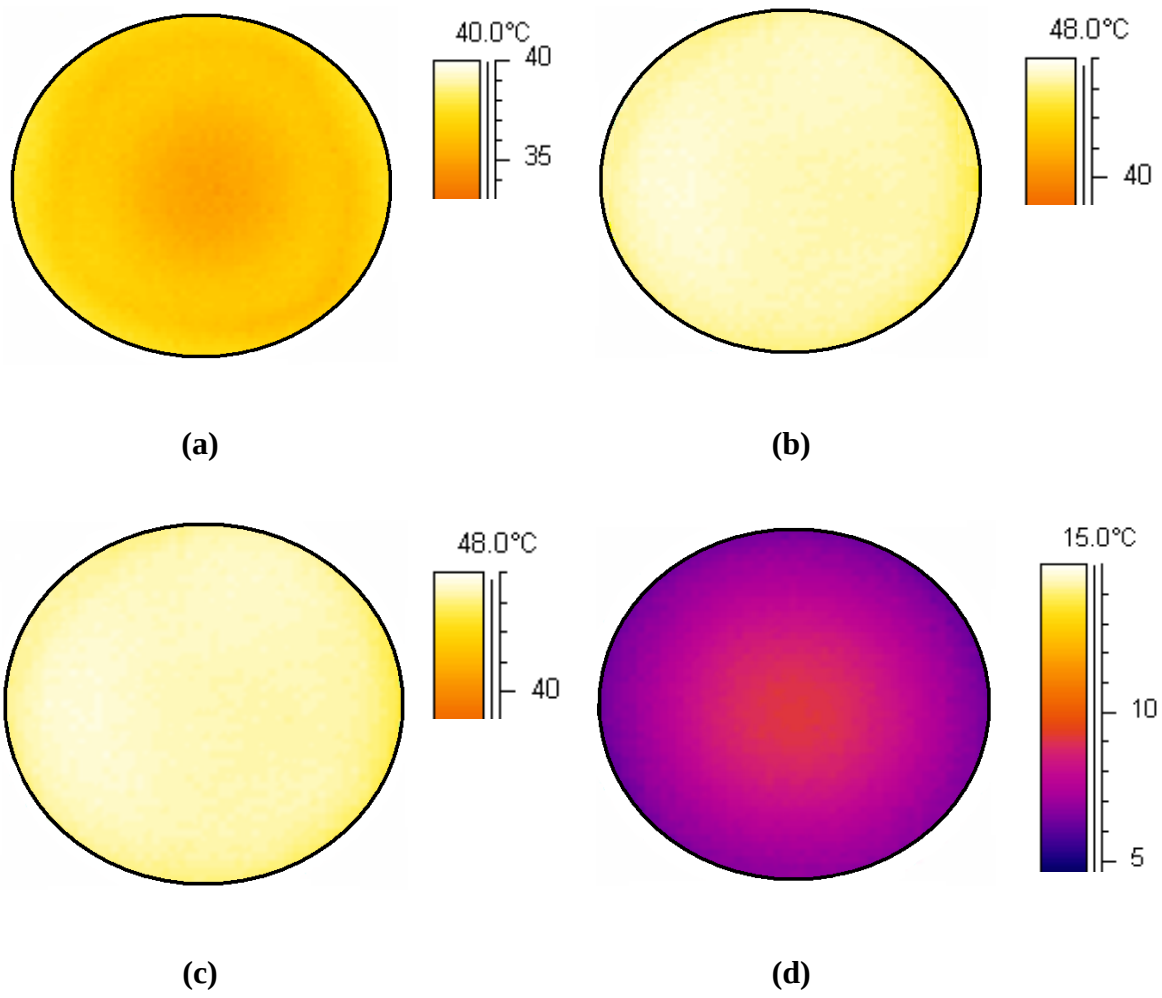

Fig. 3. Temperature distributions of persimmons obtained by thermal imaging after: (a) water preheating at 40 °C for 20 min, (b) RF heating from 40°C to 48°C, (c) holding in hot water at 48 °C for 6 min, and (d) cooling in cold water at 4 °C for 30 min.

References

Aegerter A F; Folwell R J (2000). Economic aspects of alternatives to methyl bromide in the postharvest and quarantine treatment of selected fresh fruits. *Crop Protection,* 19(3), 161–168

Birla S L; Wang S; Tang J; Fellman J K; Mattinson D S; Lurie S (2005). Quality of oranges as influenced by potential radio frequency heat treatments against Mediterranean fruit flies. *Postharvest Biology and Technology,* 38(1), 66–79

Birla S L; Wang S; Tang J; Hallman G (2004). Improving heating uniformity of fresh fruit in radio frequency treatments for pest control. *Postharvest Biology and Technology,* 33(2), 205–217

Clark C J; MacFall J S (2003). Quantitative magnetic resonance imaging of 'Fuyu' persimmon fruit during development and ripening. *Magnetic Resonance. Imaging,* 21(6), 679–685

Dentener P R; Alexander S M; Lester P J; Petry R J; Maindonald J H; McDonald R M (1996). Hot air treatment for disinfestation of lightbrown apple moth and longtailed mealy bug on persimmons. *Postharvest Biology and Technology,* 8(2), 143–152

Dentener P R; Bennett K V; Hoy L E; Lewthwaite S E; Lester P J; Miandonald J H; Connolly P G (1997). Postharvest disinfestation of lightbrown apple moth and longtailed mealy bug on persimmons using heat and cold. *Postharvest Biology and Technology,* 12 (3), 255–264

Feng X Q; Hansen J D; Biasi B; Tang J M; Mitcham E J (2004). Use of hot water treatment to control codling moths in harvested California 'Bing' sweet cherries. *Postharvest Biology and Technology,* 31(1), 41–49

Forbus W R; Payne J A; Senter S D (1991). Nondestructive evaluation of Japanese Persimmon maturity by delayed light-emission. *Journal of Food Science,* 56(4), 985–988

Hallman G J; Wang S; Tang J M (2005). Reaction orders for thermal mortality of third instar Mexican fruit fly (Diptera: Tephritidae). *Journal of Economic Entomology,* 98(6), 1905–1910

Hansen J D; Johnson J A (2007). Introduction. In: *Heat Treatments for Postharvest Pest Control: Theory and Practice* (Tang J; Mitcham E; Wang S; Lurie S, eds), pp 1–26. CABI, Oxon

Hansen J D; Sell C R; Moffit H R; Leesch J G; Hartsell P L (2000). Residues in apples and sweet cherries after methyl bromide fumigation. *Pest Management Science,* 56(6), 555–559

Homnava A; Payne J; Koehler P; Eitenmiller R (1991). Characterization of changes during ripening of oriental persimmon. *Journal of Food Quality,* 14(5), 425–434

Kim D M; Smith N L; Lee C Y (1994). Effect of heat-treatment on firmness of apples and apple slices. *Journal of Food Processing and Preservation* 18(1), 1–8

LayYee M; Ball S; Forbes S K; Woolf A B (1997). Hot-water treatment for insect disinfestation and reduction of chilling injury of 'Fuyu' persimmon. *Postharvest Biology and Technology.* 10(1), 81–87

Liu F W (1978). Modification of apple quality by high temperature. *Journal of American Society for Horticultural Science,* 103, 730–732

Lurie S; Klein J D (1992a). Calcium and heat-treatments to improve storability of Anna apples. *HortScience,* 27, 36–39

Lurie S; Klein J D (1992b). Ripening characteristics of tomatoes stored at 12-degrees-C and 2-degrees-C following a prestorage heat-treatment. *Scientia Horticulturae,* 51(1-2), 55–64

Lurie S; Mitcham E J (2007). Physiological responses of agricultural commodities to heat treatments. In: *Heat Treatments for Postharvest Pest Control: Theory and Practice* (Tang J; Mitcham E; Wang S; Lurie S, eds), pp 79–104. CABI, Oxon

Lurie S; Nussinovitch A (1996). Compression characteristics, firmness, and texture perception of heat treated and unheated apples. *International Journal of Food Science and Technology,* 31(1), 1–5

Monzon M E; Biasi B; Mitcham E J; Wang S; Tang J M; Hallman G J (2007). Effect of radiofrequency heating on the quality of 'Fuyu' persimmon fruit as a treatment for control of the Mexican fruit fly. *HortScience,* 42(1), 125–129

Monzon M E; Biasi B; Simpson T L; Johnson J; Feng X; Slaughter D C; Mitcham E J (2006). Effect of radio frequency heating as a potential quarantine treatment on the quality of 'Bing' sweet cherry fruit and mortality of codling moth larvae. *Postharvest Biology and Technology,* 40(2), 197–203

Prasanna K N V; Rao D V S; Krishnamurthy S (2000). Effect of storage temperature on ripening and quality of custard apple (Annona squamosa L.) fruits. *The Journal of Hortcultural Science and Biotechnology,* 75(5), 546–550

Senter S D; Chapman G W; Forbus W R; Payne J A (1991). Sugar and nonvolatile acid composition of persimmons during maturation, *Journal of Food Science,* 56(4), 989–991

Sharp J L; McGuire R G (1996). Control of Caribbean fruit fly (Diptera: Tephiritidae) in naval orange by forced hot air. *Journal of Economic Entomology,* 89(5), 1181–1185

Sharp J L; Ouye M T; Ingle S J; Hart W G (1989). Hot-water quarantine treatment for mangoes from Mexico infested with the Mexican fruit-fly and West-Indian-fruit-fly (Diptera, tephritidae). *Journal of Economic Entomology,* 82(6), 1657–1662

Smith K J; Lay-Yee M (2000). Response of 'Royal Gala' apples to hot water treatment for insect control. *Postharvest Biology and Technology,* 19(2), 111–122

Soriano J M; Pecchioli S; Romero C; Vilanova S; Llacer G; Giordani E; Badenes M L (2006). Development of microsatellite markers in polyploidy persimmon (Diospyros kaki Lf) from an enriched genomic library. *Molecular Ecology Notes,* 6(2), 368–370

Tang J; Ikediala J N; Wang S; Hansen J D; Cavalieri R P (2000). High-temperature-short-time thermal quarantine methods. Postharvest Biology and Technology, 21(1), 129–145

[USEPA] United States Environmental Protection Agency (1998). Reregistration Eligibility Decision. Aluminum and Magnesium Phosphide. Case s0025 and 0645. Office of Pesticide Programs, Special Review and Reregistration Division. Agricultural Statistics. Washington, DC

Wang S; Birla S L; Tang J; Hansen J D (2006). Postharvest treatment to control codling moth in fresh apples using water assisted radio frequency heating. *Postharvest Biology and Technology,* 40(1), 89–96

Wang S; Ikediala J N; Tang J; Hansen J D; Mitcham E; Mao R; Swanson B (2001). Radio frequency treatments to control codling moth in in-shell walnuts. *Postharvest Biology and Technology,* 22(1), 29–38

Wang S; Johnson J A; Tang J; Yin X (2005). Heating condition effects on thermal resistance of fifth-instar navel orangeworm (Lepidoptera: Pyralidae). *Journal of Stored Products Research,* 41(4), 469-478.

Wang S; Tang J; Cavalieri R P; Davies D C (2003). Differential heating of insects in dried nuts and fruits associated with radio frequency and microwave treatments. *Transactions of the ASAE,* 46(4), 1175–1182.

Wang S; Tang J; Johnson J A; Mitcham E; Hansen J D; Cavalieri R P; Bower J; Biasi B (2002). Process protocols based on radio frequency energy to control field and storage pests in in-shell walnuts. *Postharvest Biology and Technology,* 26(3), 265–273.

CHAPTER 3

COMPUTER SIMULATION OF RADIO FREQUENCY HEATING OF DRY FOOD MATERIALS, PART I: MODEL DEVELOPMENT AND VALIDATION

Manuscript prepared for Journal of Food Engineering

G. Tiwari[1], S. Wang[1], J. Tang[1*], S. L. Birla[2]

1 Department of Biological Systems Engineering,

Washington State University, Pullman, WA 99164-6120, USA.

Department of Biological Systems Engineering,

University of Nebraska, Lincoln, NE 68583, USA.

Corresponding author:

Juming Tang, 213 LJ Smith Hall, Pullman, WA 99164-6120, USA;

Phone: 509-335-2140; fax: 509-335-2722; e-mail: jtang@wsu.edu.

Abstract

Radio frequency (RF) heat treatment has been identified as a novel pasteurization and non-chemical quarantine method for dry food materials. But the major obstacle of this treatment is non-uniform heating in these food materials. The objectives of this study were to develop a computer simulation model for a 12 kW, 27.12 MHz RF system using a finite element based commercial software, FEMLAB. Hard red spring whole wheat flour as a uniform and representative material for dry food materials was selected. Dielectric properties of wheat flour were measured using an open-ended coaxial probe connected with impedance analyzer, and thermal properties were determined using a duel needle probe method. RF experiments with the pilot scale unit were conducted for 3 min using a fixed electrode gap of 155 mm. Simulated and experimented temperature profiles (° C) of wheat flour were compared in four different horizontal layers. Both, simulated and experimental results showed that temperature values were higher at the mid layers followed by top and bottom layer. Corners were more heated than centers in each layer. Simulation results showed that RF power density inside the wheat flour sample was higher at the edges and lower sections of the sample, causing higher temperature values in these sections. Sensitivity analysis showed that temperature uniformity in the sample was most affected by top electrode voltage and sample dielectric properties. The developed model can further be used to study the effect of some important parameters such as sample size, position, and shape and dielectric properties on RF heating of dry food materials.

Keywords: RF heat treatment, Computer simulation, Wheat flour, Dielectric properties, Heating uniformity

1. Introduction

Dry products such as grains (cereals, oil seeds and legumes), nuts, herbs, spices, bakery products and infant formulas are generally regarded as shelf stable foods and can be stored for long time due to their low moisture contents. Nevertheless, presence of pathogens and insect pests may cause considerable qualitative and quantitative losses in these products. For example, in lentils, if not stored properly, losses can be reached as high as 50 % due to insect damages (Ghosh et al., 2007). Wheat flour infested with *R. dominica* greatly affectes baking and rheological properties of bread made by the flour (Sanchez-Marinez et al., 1997). International trade of dry nuts such as walnuts and almonds may require complete elimination of targeted insect pests in these commodities in certain countries, such as Japan, South Korea and European countries (Wang et al., 2007a, b). Contamination of pathogens *Chronobacter sakazakii* and *Salmonella* spp in infant formulas (Breeuwer et al., 2003; Friedemann, 2007), and *Bacillus cereus* and *Clostridium perfrigens* in spices (Banerjee and Sarkar, 2003) may even pose a serious threat to consumer health.

Radio frequency (RF) heat treatment has been explored to investigate its potential in dry food products and to control targeted pathogens and insects in several dry products, such as disinfestations of navel orangeworm (*Amyelois transitella*), codling moth (*Cydia pomonella*), Indian meal moth (*Plodia interpunctella*) and red flour beetle (*Tribolium castaneum*) in in-shell walnuts (Wang et al., 2001a; 2002; 2007a, b), *grain borers* and *Angoumois grain moth* in rice (Lagunas-Solar et al., 2007), and *Salmonella* spp and *E. coli O157: H57* in fishmeal (Lagunas-Solar et al., 2005). But the major hurdle for RF heating technology to be commercially applicable is its non uniform heating. Non uniform temperature distribution may cause quality loss or insect/pathogen survival due to either over or under heating in different parts of a food

product. To make this technology commercially feasible, it is essential to understand the complex mechanism of RF heating.

Computer simulation has been effectively used to help understand the RF heating process in different food materials. Neophytou and Metaxas (1998, 1999) used finite element method to simulate electric field inside RF applicators by solving wave and Laplace equations. Yang et al. (2003) modeled RF heating of alfalfa and radish seeds packed inside rectangular polypropylene boxes in a 1 kW RF system using a commercial software TLM-FOOD HEATING based on transmission line and finite different time domain methods. Chan et al. (2004) solved wave equations to simulate electric field patterns in 1 % carboxymethyl cellulose (CMC) solution, placed in a 6 kW, 27.12 MHz RF system using finite element method. They compared simulated electric field patterns with the experimentally determined temperature patterns in CMC solutions using five load positions and container sizes. Marra et al. (2007) successfully simulated the temperature distribution and heating uniformity inside a cylindrical meat roll subjected to a 600 W RF heating using a commercially available finite element based software (FEMLAB). They reported differences in temperature uniformity inside the meat sample at different power levels. A computer simulation using FEMLAB was also successfully performed to study various factors causing heating non uniformity in fresh fruits, when subjected to RF heating inside a 12 kW, 27.12 MHz RF system (Birla et al., 2008a, b). Simulation results showed that dielectric properties, shape and position of fruit inside the RF applicator greatly affected heating uniformity of fresh fruits. Romano and Marra (2008) studied the effect of regular sample shapes (cube, cylinder and sphere) and their orientation on RF heating behavior in meat samples using a computer model and predicted that cubes should have better heating uniformity than cylinders and spheres. Wang et al. (2008) simulated and

validated a computer model to study the influence of dielectric properties of mashed potato and circulating water on the electric field distribution, heating rate and temperature distribution in a 6 kW RF system. Simulation results confirmed that increase in salt content (loss factor) did not guarantee the increase in RF power density.

Very few studies on the computer simulation of the RF heating of dry food products are reported in the literature. Yang et al. (2003) simulated the RF heating of alfalfa and radish seeds. This study was based on a small RF cavity and they reported discrepancies in temperature distributions between simulation and experimental results. Therefore, it is necessary to systematically study the RF heating characteristics in dry food materials and design parameters to improve the RF heating uniformity based on the validated computer simulation model.

The overall objective of this study was to investigate the behavior of RF heating in dry food materials with the use of a computer simulation model. Specific objectives were to (1) determine the dielectric and thermal properties of the wheat flour as a representative material of dry food products, (2) develop a computer simulation model for a 12 kW, 27.12 MHz RF system using commercial finite element software FEMLAB, and (3) validate the computer model by comparing with the transient experimental temperature profiles of wheat flour at four different layers after 3 min RF heating.

2. Materials and Methods

2.1. Material selection

Hard red spring whole wheat flour, *bronze chief*, was selected as a representative food material of the dry food products. The selection of wheat flour was based on compositional uniformity and particle size as compared to other dry food materials, such as food grains and

bakery products. The flour was procured from Wheat Montana farms, Three Forks, Montana, USA and stored at room temperature prior to RF experiments. The initial moisture content of wheat flour was 8.8% on wet basis.

2.2. Dielectric and thermal properties measurement

Dielectric properties (DPs) of wheat flour samples at a normal bulk density (without further compression) of 800 kg m^{-3} were measured with an open-ended coaxial-line probe (HP 85070B) connected to an impedance analyzer (HP 4291B, Hewlett Packard Corp., Santa Clara, CA, USA). This normal bulk density of wheat flour was similar to that (785 kg m^{-3}) reported by Rahman (1995). Sample temperatures were raised from 20 to 70 °C in every 10 °C interval in an oil bath by circulating 10% water and 90% ethylene glycol solution through the jacket of the test cell. The details of the measurement system and procedure can be found elsewhere (Wang et al., 2003; Guo et al., 2008). The selected temperature range should be practically applicable for the heat disinfestations of dry food materials without affecting their quality.

Thermal properties (thermal conductivity and specific heat) at a bulk density of 800 kg m^{-3} were measured by a dual needle probe method (KD2 Pro, Decagon Devices, Pullman, WA, USA) within the temperature range from 20 to 70 °C.

2.3. Development of computer model

2.3.1. Physical model

A 12 kW, 27.12 MHz parallel plate RF heating system (Strayfield Fastran with E-200, Strayfield International Limited, Wokingham, UK) was used for the study. The RF system included metallic enclosure, generator, and RF applicator with a pair of RF electrodes. A schematic diagram of the RF applicator was shown in Fig. 1. The bottom electrode was the integral part of metallic enclosure. Top electrode position could be changed with the help of

adjustable screw bars. RF power from the generator was fed in the middle of top electrode. A dielectric material (wheat flour) in a container was placed on the ground electrode.

2.3.2. Governing equations

Quasi static approximation for the RF electric field is a valid assumption inside the RF cavity due to its long wavelength (~ 11 m) compared to cavity size (1.8 × 1.4 × 1.0 m^3). Wave length of a wave in a non-magnetic homogeneous dielectric material (λ_m) can be expressed as:

$$\lambda_m = \lambda \Big/ \sqrt{\varepsilon_m'} \tag{1}$$

where ε_m' is the material dielectric constant and λ is the wavelength in air (Besser and Gilmore, 2003). Since, dry food materials have low dielectric constant values, assumption of quasi-static RF electric field inside dry food materials should also be valid.

Quasi-static electric field inside the RF cavity can be obtained by solving Laplace equation:

$$\nabla(\sigma + j2\pi f \varepsilon_o \varepsilon_m)\nabla V = 0 \tag{2}$$

where $j = \sqrt{-1}$, V is the voltage between the two electrodes (V) and related to the electric field ($\boldsymbol{E} = -\nabla V$), f is the frequency (Hz), ε_o is the permittivity of free space (8.86 × 10^{-12} F m^{-1}), σ and ε_m are the electrical conductivity (S m^{-1}) and the complex relative permittivity of the material, respectively. The complex relative permittivity ε_m can be expressed in terms of dielectric constant ε'_m and loss factor ε''_m of the material ($\varepsilon_m = \varepsilon'_m - j * \varepsilon''_m$). When a dielectric material is placed inside the RF applicator, RF power density (Q, W m^{-3}) in the material is given by:

$$Q = 2\pi f \varepsilon_o \varepsilon''_m \left|\boldsymbol{E}\right|^2 \tag{3}$$

The RF power density acts as a heat source and results in unsteady conductive heat transfer inside the material. The unsteady conductive heat transfer equation is given by:

$$\frac{\partial T}{\partial t} = \nabla \alpha \nabla T + \frac{Q}{\rho C_p} \tag{4}$$

where T is the local temperature (°C) inside the material, t is the time (s) of heating, ρ, α, and C_p are the density (kg m^{-3}), thermal diffusivity (m s^{-2}) and specific heat (J kg^{-1} $°C^{-1}$) of the food material, respectively.

2.3.3. Initial and boundary conditions

It was difficult to consider each and every details of RF systems in simulation as it required excessive computer resources. Only a quarter part of the RF machine, sample and container was modeled to avail advantages of system symmetry. Dimensions of the sample, container and RF system along with electrical and thermal boundary conditions are shown in Fig. 2. Electrical insulation ($\nabla E = 0$) was assigned to symmetrical planes of the RF applicator**,** coincided with the symmetrical planes of sample and container. In reality, voltage on top electrode varies all over the surface of top electrode. Voltage has its minimum value at the feed point and goes on increasing as we move away from the feed point. Barber (1983) reported if top electrode dimensions were less than 30% of the RF wave length, voltage can be assumed uniform in all parts of the top electrode. In the present RF system, top electrode dimensions (1.05×0.8 m^2) with feed point at its center (Fig. 1) were sufficiently small compared to 30% of RF wave length (~3.3 m), therefore, electric voltage on the top electrode was considered uniform in the simulation. Top electrode voltage was also assumed constant during the RF heat treatment, as voltage in typical industrial-scale RF systems varies only 7 % between standby to full load position (Metaxas, 1996). It was difficult to measure top electrode voltage in an

operating RF system, therefore, preliminary simulations were run by considering different values of top electrode voltage. Based on the comparison between preliminary simulation results and experimental results, value of top electrode voltage was considered as 13000 V for the final simulation. The similar approach for the evaluation of top electrode voltage has been reported (Marshall and Metaxas, 1998; Birla et al., 2008a). RF cavity walls along with bottom electrode were grounded, therefore voltage (V = 0 V) was set for these boundaries. Convective heat transfer (h = 20 W m^{-2} $°C^{-1}$) was assumed on the top exposed surface of the sample (Wang et al., 2001b). Other outer surfaces of the plastic container were considered as thermally insulated (∇T =0). Initial temperature was set at 23 °C based on the experimental room conditions.

2.3.4. Solution procedure

Commercially available software based on finite element method, FEMLAB (V3.4, COMSOL Multiphysics, Burlington, MA, USA) was used to solve coupled electromagnetic and heat transfer equations. Inbuilt FEMLAB modules (AC/DC quasi-static) and heat transfer by conduction with transient analysis were selected to solve partial differential equations. Modeling steps involved in simulation were shown in Fig. 3. The unstructured mesh consisting Lagrange- Quadratic element was generated in the entire domain of RF cavity. Relatively fine meshes were created near the sharp edges and corners of the sample and the container to increase the accuracy of solution. The final mesh consisted of 145781 domain elements (tetrahedral), 11192 boundary elements (triangular), 633 edge elements (linear) and 26 vertex elements. The direct linear system solver UMFPACK was used with a relative tolerance and an absolute tolerance of 0.01 and 0.001, respectively. Initial and maximum time steps were set as 0.001 and 1 s. Solution was considered convergent and grid independent when difference in

temperature values of sample in successive refining of grids was less than 0.1%. All computer simulations were performed for 24 hours in a Dell 670 workstation with two Dual Core, 2.80 GHz XEON processors and 12 GB RAM running on a Windows XP 64 bit operating system. Another set of simulations was run to analyze the sensitivity of influencing input parameters on the simulated temperature uniformity (STU , °C) by varying the model input parameters within their allowable limits. Selected input parameters were top electrode voltage, sample DPs and thermal conductivity and heat transfer coefficient of air. Top electrode voltage was varied between ± 5 percent from its nominal value of 13000 V. DPs of wheat flour (3.27- j 0.23) at 20 °C were varied ± 20 percent. Thermal conductivity of wheat flour was changed between 0.1 to 0.3 W m^{-1} $°C^{-1}$ with its nominal value of 0.2. Heat transfer coefficient under still air condition was varied between 0-20 W m^{-2} $°C^{-1}$. STU was defined as:

$$STU = \frac{1}{V_{vol}} \int_{V_{vol}} sqrt((T - T_{av})^2) dV_{vol} \quad (5)$$

where T and T_{av} are local and average temperatures (°C) inside the dielectric material over the volume (V_{vol} , m^{-3}), respectively. The subdomain integration scheme of FEMLAB was used to integrate Eq. (5). Results were expressed by ratio of percentage change in STU to the corresponding percent change in input parameters.

2.4. Model validation

2.4.1. Container material selection

Three trays of polypropylene (each having inner dimension 300 × 220 × 20 mm^3) stacked one above another were used as the container. This was designed to facilitate temperature mapping at multiple layers. The bottoms of the top two trays were made of polypropylene mesh (thickness 2 mm with mesh opening of 6 mm). The purpose of using mesh

as a bottom was to minimize the air gap between two adjacent trays when staked one above another. The lower tray bottom and sides of the container were made of 7 mm thin polypropylene sheet.

2.4.2. Experimental procedure

About one kg wheat flour was filled in each tray to maintain bulk density of 800 kg m^{-3} in experiments, as used in simulation. A very thin polypropylene film was placed on the perforated bottom of each tray prior to loading flour into trays. This was done to stop flour flow from one tray to another tray. The container (stacked trays) was put at the center of the bottom electrode. The wheat sample was subjected to 3 min RF heating with an electrode gap of 155 mm. The container was immediately removed from the RF system after treatments. The surface temperatures of all three trays were recorded using an infra-red image camera (ThermaCAM™ Researcher 2001, FL-IR Systems, Portland, OR, USA) with an accuracy ± 2 ° C, starting from the top to the bottom tray. Finally, wheat flour of the third (bottom) tray was carefully overturned on another polypropylene sheet to record the bottom surface temperature of the sample. All the four thermal imaging measurements were completed within 30 s. A fiber-optic sensor (UMI, FISO Technologies Inc., Quebec, Canada) was also inserted 40 mm from the bottom of the container to measure the temperature profile at the center of the second tray during 3-min RF heating. Experimental and simulated surface temperature distributions were compared at four different heights (0, 20, 40, and 60 mm) from the bottom of the container.

3. Results and discussion

3.1. Dielectric and thermal properties of wheat flour

Table 1 shows the temperature dependent dielectric and thermal properties of wheat flour at 27.12 MHz. Both, dielectric constant and loss factor increased slightly with an increase

in temperature. Nelson and Trabelsi (2006) also reported slight increase in dielectric properties of hard red winter flour at moisture content of 11 % d.b. within the temperature range from 5 to 55 °C. Thermal conductivity and specific heat of wheat flour also increased with increasing temperature. Increase in thermal conductivity and specific heat with temperature were reported in literature for many other dry products, such as rice flour and milk powder (Muramatsu et al., 2006), wheat flour (Rahman, 1995), lentils (Tang et al., 1991), and gram (Dutta et al., 1998). For use of these properties in simulation model, data were subjected to linear regression analysis. The regression equations are listed in Table 2. Since the increase in loss factor of wheat flour with temperature was trivial; therefore, an average loss factor value of 0.33 was used in the simulation. Dielectric and thermal properties of polypropylene container and air were adapted from Birla et al. (2008a).

3.2. Simulated temperature profiles of wheat flour

Fig. 4 shows simulated temperature profiles of one quadrant of a wheat flour sample in four different horizontal and vertical layers. Horizontally, temperature values were highest at the lower sections of the wheat flour except at the bottom layer, which was in contact with the bottom electrode. Vertically, temperature increased from the symmetrical (central) layer to outer layers of the wheat sample, except at the outer most layer, which was in contact with the container side walls. The temperature non uniformity in the sample could be attributed to electric field behavior. Though, the electric field was normal to the central parts of top sample, but it was deflected by the sample corners and edges (Fig. 5a). As a result, net electric field increased at the corners, edges and lower sections of the sample. Since RF power density at any location is proportional to the square of electric field, it also increased, (Fig 5b), resulting in higher temperature values at these parts. These findings were supported by the simulation of

cylindrical meat batters where higher temperatures at the edges and lower sections of the meat were observed after RF heating (Marra et al., 2007). Computer simulation of RF heating of model fruit, placed on the bottom electrode also showed higher heating at the lower part of the fruit (Birla et al., 2008a). Similar heating patterns were observed in seven polyurethane foam sheets, subjected to an industrial-scale RF heating (Wang et al., 2007a, b).

3.3. Comparison of simulated and experimental thermal profiles of wheat flour

Figs. 6 and 7 show a comparison between experimental and simulated surface temperature distribution of wheat flour in all four layers. Temperature profiles along the center line LL' (Figs. 6c and 7c) of each layer were also compared. The results demonstrate that simulated and experimental temperature distribution patterns for all layers are in good agreement. The values of experimentally determined temperature and the simulated temperature were matched well except for the corners of the sample where the simulated temperatures values were found higher than the experimental values. Along the line LL', simulated and experimented values were also in good agreement. The difference in simulated and experimentally determined temperature values, large at the corners and edges, could be due to either simplification of RF system or ignored moisture migration form outer hot sections to inners cold sections of the wheat flour during 3 min RF heating in simulation. Simulated and experimental temperature profiles measured at the center of first mid layer (40 mm form the container bottom) were also in good agreement (Fig. 8). Table 4 compared simulated and experimented average temperature values of all four layers after 3 min RF heating. It is clear that experimented average temperatures matched well with the simulated ones. But the values of simulated standard deviation were comparatively higher than those determined by

experiments. As corners and edges were more heated in simulation shown in Figs. 6 and 7, this increased the simulated standard deviation in each layer.

3.4. Sensitivity analysis

Results showed that STU was most sensitive to the top electrode voltage as change in STU value to the corresponding change in electrode voltage was highest (Table 3). Sample DPs and thermal conductivity of wheat flour also affected STU. Simulation results showed that heat transfer coefficient of air within the range of 0-20 W m^{-2} C^{-1} had negligible effect on simulated temperature uniformity.

4. Conclusions

A computer model for the RF heating of the dry products was developed for a 27.12 MHz RF system using a finite element based commercial software, FEMLAB using whole wheat flour as a model food. Dielectric and thermal properties of wheat flour were measured and used in the simulation model. Simulated results showed that temperature values at the mid layers were highest, followed by those of top and bottom layers. Corners were heated more than centers at each layer. Simulation results confirmed that non uniform distribution of RF power density resulted in temperature non uniformity in the sample. Therefore, analysis of RF power distribution inside food materials can be a starting step to understand the complex RF heating process and to predict the temperature distribution in dry food materials.

Table 1

Dielectric and thermal properties of hard red spring wheat flour at a bulk density of 800 kg m^{-3} and moisture content of 8.8 % w.b. The data represent the mean of two replicates.

Temperature (T, °C)	Dielectric constant (ε'_m)	Loss factor (ε''_m)	Thermal conductivity (k, W m^{-1} °C^{-1})	Specific heat (C_p, J kg^{-1} °C^{-1})
20	3.27 ± 0.03	0.29 ± 0.01	0.12 ± 0.003	1229.37 ± 36.23
30	3.34 ± 0.03	0.31 ± 0.00	0.14 ± 0.005	1644.38 ± 38.00
40	3.49 ± 0.02	0.31 ± 0.02	0.15 ± 0.003	1661.25 ± 35.23
50	3.73 ± 0.06	0.31 ± 0.01	0.17 ± 0.006	1823.75 ± 60.10
60	4.09 ± 0.01	0.34 ± 0.01	0.20 ± 0.007	1950.64 ± 13.25
70	4.77 ± 0.10	0.42 ± 0.01	0.27 ± 0.004	2188.75 ± 21.21

Table 2

Dielectric and thermo-physical properties of wheat flour, polypropylene and air used in computer simulation as a function of temperature (T, °C)

	Wheat flour	Polypropylene	Air
Dielectric constant (ε'_m)	3.72-0.0345T +0.0007T^2	2	1
Loss factor (ε''_m)	0.33	0.0023	0
Specific heat, (C_p, J kg^{-1} °C^{-1})	23T + 757	1800	_
Thermal conductivity (k, W m^{-1} °C^{-1})	1.36×10^{-4}T^2 0.0094T+0.2819	0.2	_
Density (ρ, kg m^{-3})	800	900	_

Table 3

Relative sensitivity of simulated temperature uniformity (*STU*) of wheat sample with respect to model input parameters

Input parameters	Nominal value	Percentage change in input	Change in *STU* / Corresponding change in input parameters
Electrical voltage (V)	13000	±4	1.34
DPs	3.27- j 0.23	±20	0.49
Thermal conductivity (W m^{-1} °C^{-1})	0.2	±50	0.12
Heat transfer coefficient of air (W m^{-2} °C^{-1})	10	±100	0.03

Table 4
Experimental and simulated average temperature ± standard deviation (° C) at four different horizontal layers of wheat flour in a plastic container (300 × 220 × 60 mm^3) after 3 min RF heating with an electrode gap of 155 mm and initial temperature of 23 ° C

Position of layer (thickness from the bottom of container)	Experiment (° C)	Simulation (° C)
Top layer (60 mm)	55.8 ± 2.3	54.5 ± 4.3
First mid layer (40 mm)	67.9 ± 3.0	68.2 ± 5.7
Second mid layer (20 mm)	70.9 ± 2.9	70.9 ± 5.5
Bottom layer (0 mm)	48.4 ± 1.6	49.7 ± 3.6

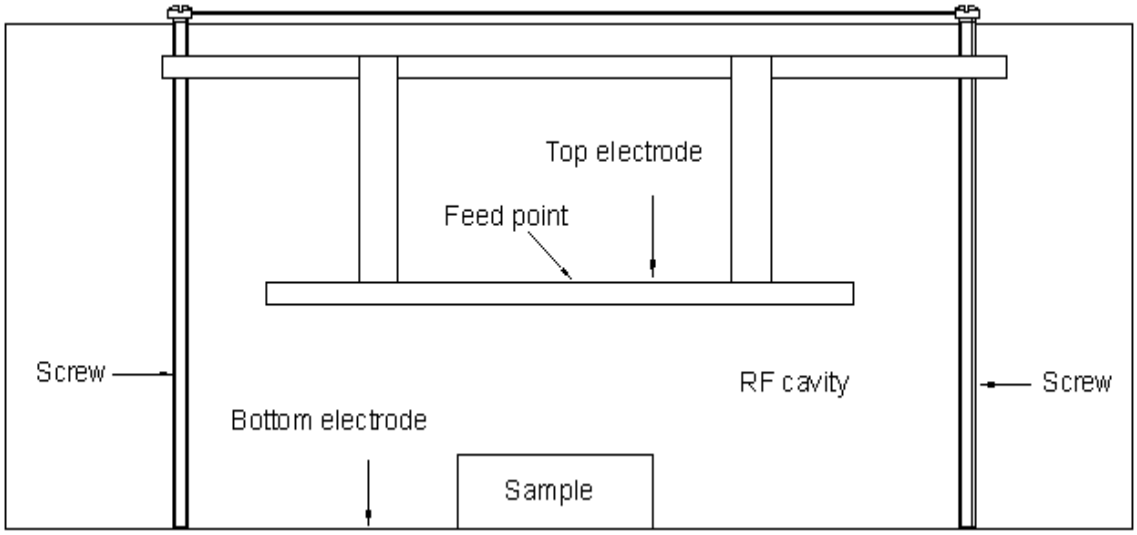

Fig.1. Schematic diagram of a 12 kW, 27.12 MHz radio frequency system

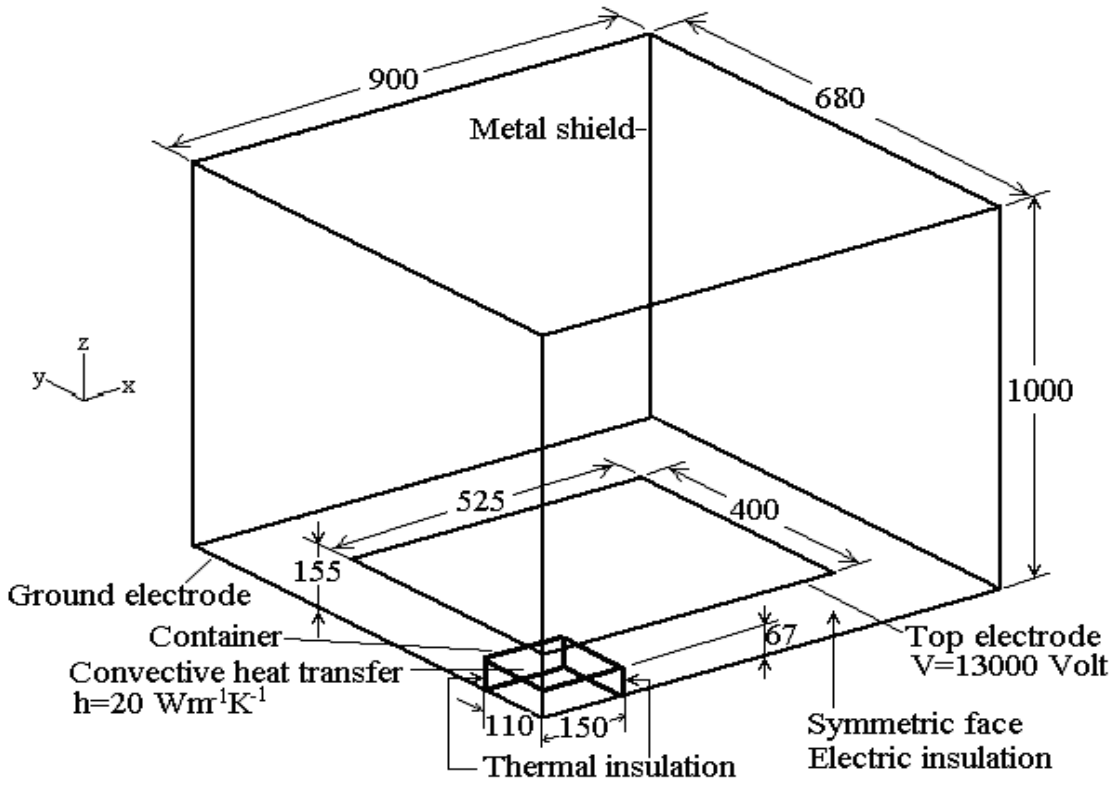

Fig. 2. Geometry and boundary conditions of one quadrant of 12 kW, 27.12 MHz radio frequency systems used in simulation (dimensions are in mm).

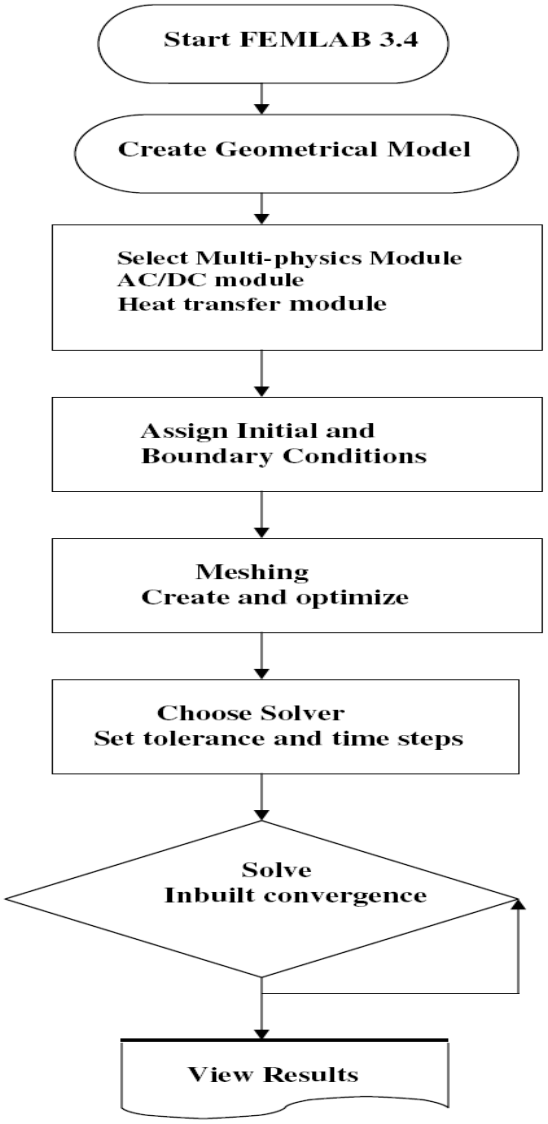

Fig. 3. Flow chart of modeling using FEMLAB 3.4

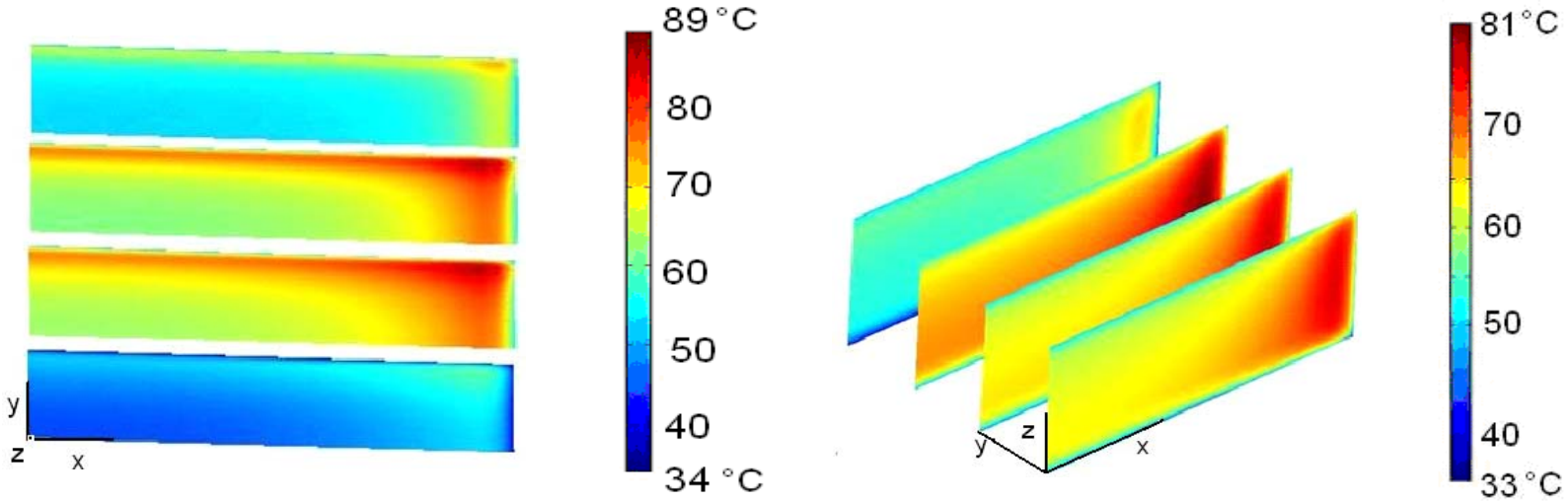

(a) Four horizontal layers, from bottom plane

(b) Four vertical layers, from central line plane

Fig. 4. Simulated temperature (°C) profiles of one quadrant wheat flour sample (150 × 110 × 60 mm^3) at (a) four different horizontal layers (0, 20, 40, and 60 mm) from the bottom (b) four different vertical layers (0, 36, 72, and 110 mm) from the vertical center plane of sample after 3 min RF heating with an electrode gap 155 mm and initial temperature of 23 °C.

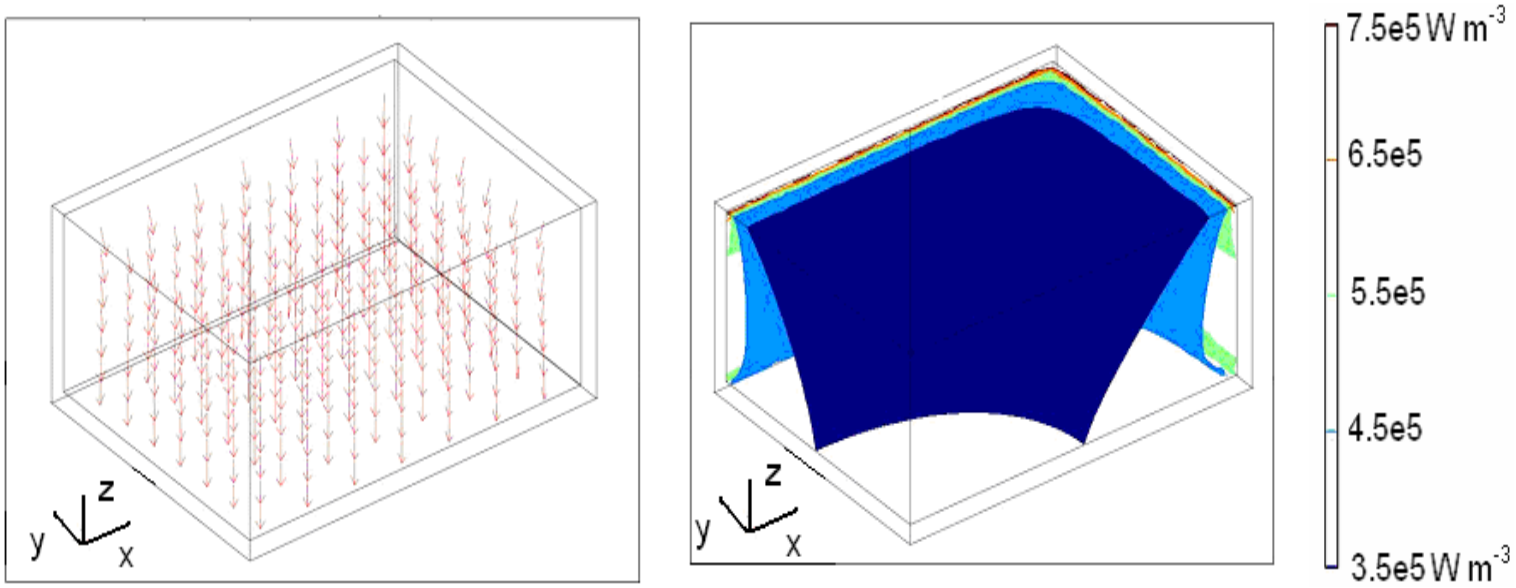

(a) Electric field distribution (b) RF power density

Fig. 5. Simulated electric field distribution (a) and RF power density distribution (W m^{-3}) of one quadrant wheat flour sample (150× 110 × 60 mm^3) after 3 min RF heating with an electrode gap of 155 mm.

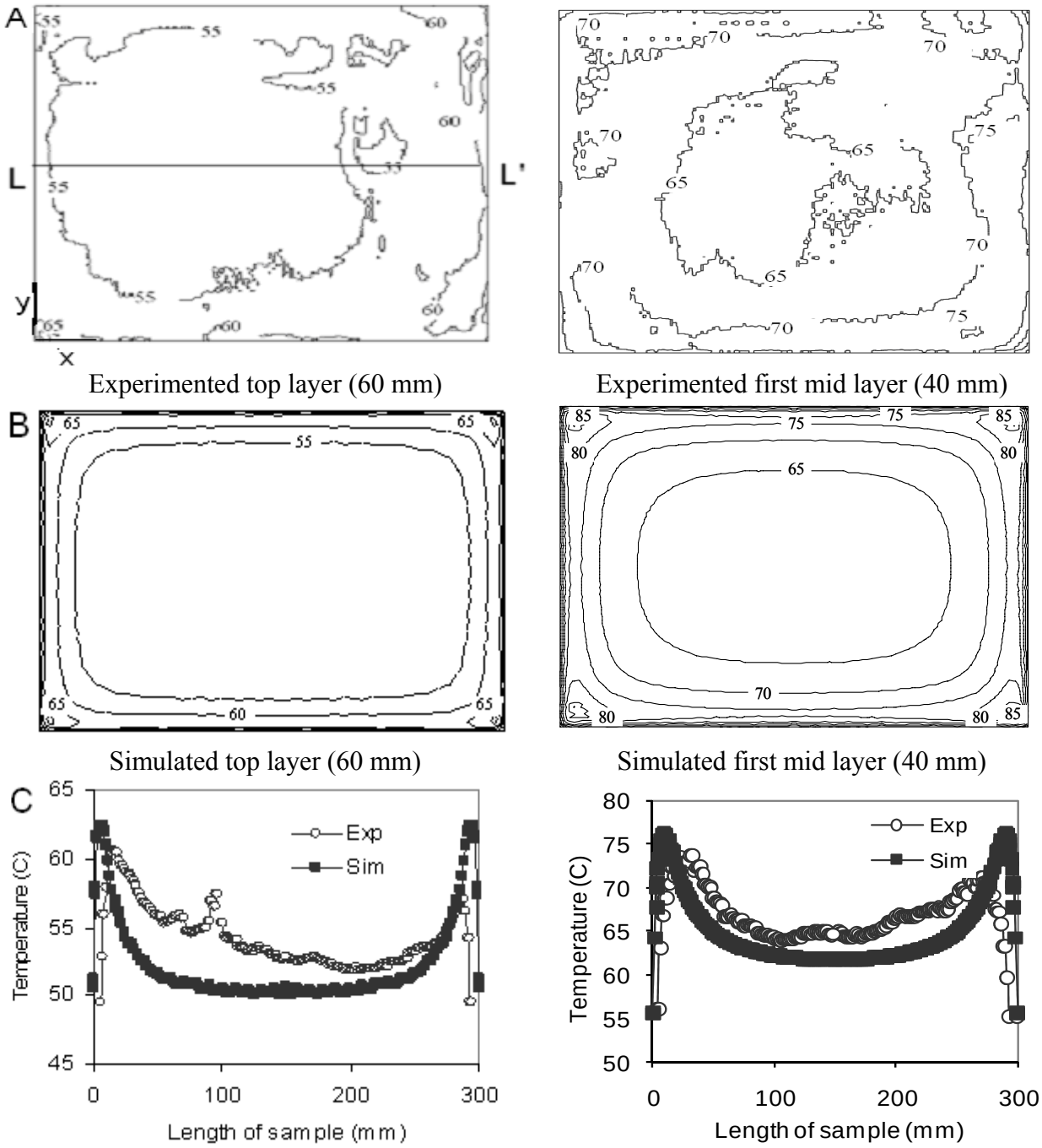

Fig. 6. Experimental (a) and simulated (b) temperature distributions (°C) of hard red spring wheat flour in top and first mid layers (60 and 40 mm from the bottom of sample) placed in a polypropylene container (300×220×60 mm^3) on the top of the bottom electrode with the comparison of the temperature profiles (c) along the line LL', after 3 min RF heating with an initial temperature of 23 °C and a fixed electrode gap of 155 mm.

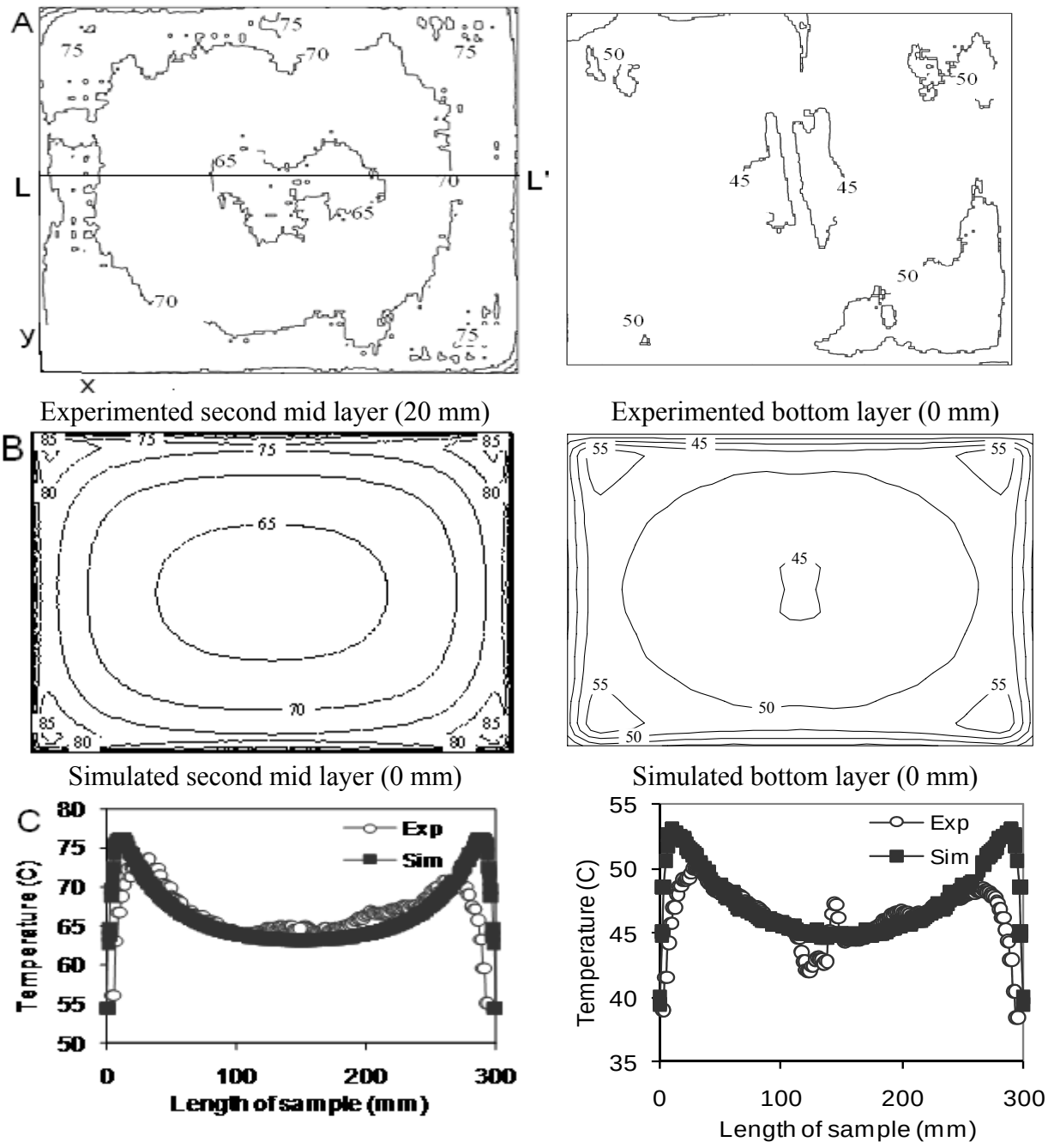

Fig. 7. Experimental (a) and simulated (b) temperature distributions (° C) of hard red spring wheat flour in second mid and bottom layers (20 and 0 mm from the bottom of sample) placed in a polypropylene container (300×220×60 mm^3) on the bottom electrode with the comparison of the temperature profiles (c) along the line LL' after 3 min RF heating with an initial temperature of 23 °C and a fixed electrode gap of 155 mm.

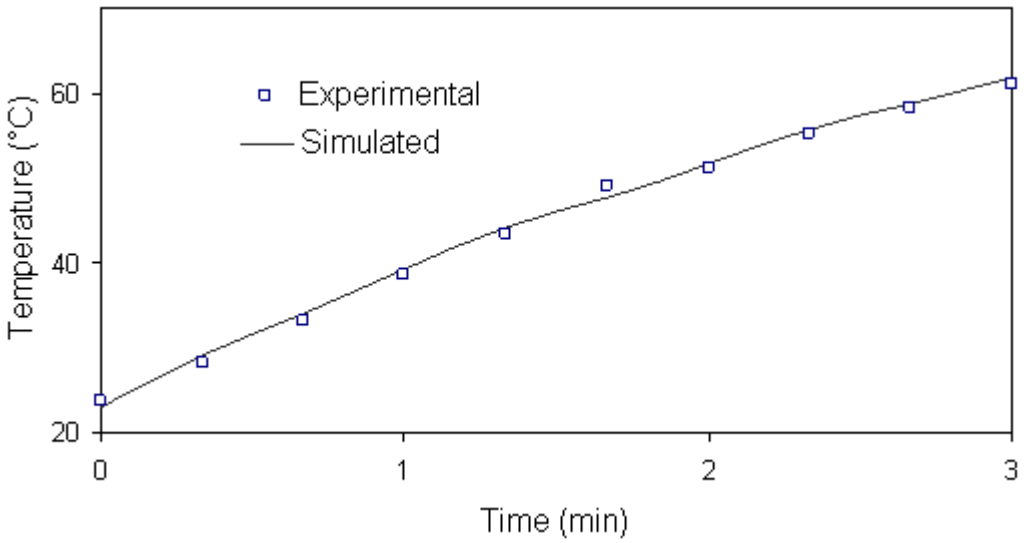

Fig. 8. Experimental and simulated temperature-time histories of hard red spring wheat flour at the center of first mid layer (40 mm) from the bottom of sample (300×220×60 mm^3), placed in a polypropylene container on the top of grounded electrode during 3 min RF heating with an electrode gap of 155 mm.

References

Banerjee, M., & Sarkar, P.K. (2003). Inhibitory effect of garlic on bacterial pathogens from spices. *World Journal of Microbiology and Biotechnology,* 19 (6), 565-569.

Barber, H. (1983). *Electroheat*. 1st ed. Granada Publishing Limited, London

Birla, S.L., Wang. S., & Tang, J. (2008a). Computer simulation of radio frequency heating of model fruit immersed in water. *Journal of Food Engineering,* 84(2), 270–280.

Birla S.L., Wang, S., Tang, J., & Tiwari, G. (2008b). Characterization of radio frequency heating of fresh fruits influenced by dielectric properties. *Journal of Food Engineering*, 89(4), 390–398.

Besser, L., & Gilmore, R. (2003). *Practical RF circuit design for modern wireless systems: Passive circuits and systems,* Norwood: Artech House Publishers.

Breeuwer, P., Lardeau, A., Peterz, M., & Joosten, H.M. (2003). Desiccation and heat tolerance of Enterobacter sakazakii. *Journal of Applied Microbiology*, 95(5), 967–973.

Chan, T.V.C.T., Tang, J., & Younce, F. (2004). 3 Dimensional numerical modeling of an industrial radio frequency heating systems using finite elements. *Journal of Microwave Power and Electromagnetic Energy,* 39(2), 87–105.

Dutta, S.K., Nema,V.K., & Bhardwaj, R.K. (1998). Thermal properties of gram. *Journal of Agricultural Engineering Research,* 39 (4), 269–275.

Friedemann, M. (2007). Enterobacter sakazakii in food and beverages (other than infant formula and milk powder). *International Journal of Food Microbiology,* 116(1), 1–10.

Ghosh, P.K., Jayas, D.S., Srivastava, C., & Jha, A.N. (2007). Drying and storing lentils: engineering and entomological aspects In *Lentil: an ancient crop for modern times* (pp 385-414). Netherlands: Springer.

Guo, W., Tiwari, G., Tang, J., & Wang, S. (2008). Frequency, moisture and temperature-dependent dielectric properties of chickpea flour. *Biosystems Engineering*, 101(2), 217-224.

Lagunas-Solar, M.C., Pan, Z., Zeng, N.X., Truong, T.D., Khir, R., & Amaratunga, K.S.P. (2007). Application of radiofrequency power for non-chemical disinfestation of rough rice with full retention of quality attributes. *Applied Engineering in Agriculture,* 23(5), 647–654.

Lagunas-Solar, M.C., Zeng, N.X., Essert, T.X., Truong, T.D., Pina, C., Cullor, J.S., Smith, W.L., & Larrain, R. (2005) Disinfection of fishmeal with radiofrequency heating for improved quality and energy efficiency. *Journal of the Science of Food and Agriculture*, 85, 2273–2280.

Marra, F., Lyng, J., Romano, V., & McKenna, B. (2007). Radiofrequency heating of foodstuff: Solution and validation of a mathematical model. *Journal of Food Engineering,* 79(3), 998–1006.

Marshall, M.G., & Metaxas, A.C. (1998). Modeling of the radio frequency electric field strength developed during the RF assisted heat pump drying of particulates. *Journal of Microwave Power and Electromagnetic Energy*, 33(3), 167-177.

Metaxas, A. C. (1996). *Foundations of electroheat – A unified approach*. Ist ed. John Wiley & Sons. New York:

Muramatsu, Y., Tagawa, A., & Kasai, T. (2006). Effective thermal conductivity of rice flour and whole and skim milk powder. Journal of Food Science 70(4), 279–287.

Nelson, S.O., Trabelsi, S. (2006). Dielectric spectroscopy of wheat from 10 MHz to 1.8 GHz. Measurement Science and Technology 17(8), 2294–2298.

Neophytu, R. I., & Metaxas, A.C. (1998). Combined 3D FE and circuit modeling of radio frequency heating systems. *Journal of Microwave Power and Electromagnetic Energy*, 33 (4), 243–262.

Neophytu, R.I., & Metaxas, A.C. (1999). Combined tank and applicator design of radio frequency heating systems. *IEE Proceedings-Microwaves Antennas and Propagation* 146(5), 311–318.

Rahman, S. (1995). *Food properties handbook*. CRC Press. Florida:

Romano, V., & Marra, F. (2008). A numerical analysis of radio frequency heating of regular shaped foodstuff. *Journal of Food Engineering*, 84(3), 449–457.

Sánchez-Mariñez, R.I., Cortez-Rocha, M.O., Ortega-Dorame, F., Morales-Valdes, M., & Silveira, M.I. (1997). End-use quality of flour from *Rhyzopertha Dominica* infested wheat. *Cereal Chemistry*, 74(4), 481–483.

Tang, J., Sokhansanj, S., Yannacopoulos, S., & Kasap, S.O. (1991). Specific heat capacity of lentil seeds by differential scanning calorimetry. *Transactions of the ASAE*, 34(2), 517–522.

Wang, J., Olsen, R. G., Tang, J., & Tang, Z. (2008). Influence of mashed potato dielectric properties and circulating water electric conductivity on radio frequency at 27 MHz. *Journal of Microwave Power and Electromagnetic Energy*, 42(2), 31–46.

Wang, S., Ikediala, J.N., Tang, J., Hansen, J.D., Mitcham, E., Mao, R., & Swanson, B. (2001a). Radio frequency treatments to control codling moth in in-shell walnuts. *Postharvest Biology and Technology*, 22(1), 29–38.

Wang, S., Monzon, M., Johnson, J.A., Mitcham, E. J., & Tang, J. (2007a). Industrial-scale radio frequency treatments for insect control in walnuts: I. Heating uniformity and energy efficiency. *Postharvest Biology and Technology*, 45(2), 240–246.

Wang, S., Monzon, M., Johnson, J.A., Mitcham, E.J.,& Tang, J. (2007b). Industrial-scale radio frequency treatments for insect control in walnuts: II: Insect mortality and product quality. *Postharvest Biology and Technology,* 45(2), 247–253.

Wang, S., Tang, J., & Cavalieri, R.P. (2001b). Modeling fruit internal heating rates for hot air and hot water treatments. *Postharvest Biology and Technology,* 22(3), 257–270.

Wang, S., Tang, J., Cavalieri, R.P., & Davies, D.C. (2003). Differential heating of insects in dried nuts and fruits associated with radio frequency and microwave treatments. *Transactions of the ASAE,* 46(4), 1175-1182.

Wang, S., Tang, J., Johnson, J.A., Mitcham, E., Hansen, J.D., Cavalieri, R., Bower, J., & Biasi, B. (2002). Process protocols based on radio frequency energy to control field and storage pests in in-shell walnuts. *Postharvest Biology and Technology,* 26(3), 265-273.

Yang, J., Zhao, Y., & Wells, J.H. (2003). Computer simulation of capacitive radio frequency (RF) dielectric heating on vegetable sprout seeds. *Journal of Food Process Engineering,* 26(3), 239–263.

CHAPTER 4

COMPUTER SIMULATION OF RADIO FREQUENCY HEATING OF DRY FOOD MATERIALS, PART II: MODEL PREDICTIONS

G. Tiwari[1], S. Wang[1], J. Tang[1*], S. L. Birla[2]

Prepared manuscript for Journal of Food Engineering

1 Department of Biological Systems Engineering,

Washington State University, Pullman, WA 99164-6120, USA.

2 Department of Biological Systems Engineering,

University of Nebraska, Lincoln, NE 68583, USA.

Corresponding author:

Juming Tang, 213 LJ Smith Hall, Pullman, WA 99164-6120, USA;

Phone: 509-335-2140; fax: 509-335-2722; e-mail: jtang@wsu.edu.

Abstract

The objectives of this research were to investigate the influence of various factors on radio frequency (RF) power distribution in dry food materials, placed in a 12 kW, 27.12 MHz parallel plate RF system, using a finite element computer model after validation with wheat flour. The factors investigated were sample size, shape, relative position between RF electrodes, and dielectric properties (DPs) of the sample and the surrounding medium. Effects of electrode gap and top electrode configuration on RF power distribution behavior of the sample were also studied. RF power uniformity of the samples was compared using power uniformity index (PUI). Simulated results showed that RF power uniformity in cuboid shaped samples, placed on the bottom electrode, first decreased and then increased with the increase in sample size. Sample shape and its vertical position between the fixed gap parallel plate electrodes also affected RF power distribution and uniformity. A cuboid sample had higher RF power densities at the edges while an ellipsoid had higher power densities in the center parts. Simulated results showed that smaller values of DPs resulted in better RF power uniformities in the samples. Reducing the electrode gap improved RF power uniformity of the sample. While studying the influence of top electrode configuration on the RF power distribution and uniformity, the results showed that optimum RF power uniformity in a particular sample size could be achieved with a particular top electrode bending position and angle. The results are useful in understanding complex RF heating, designing and scaling up efficient RF systems.

Keywords: Radio frequency, Computer simulation, Dielectric properties, Power uniformity index

1. Introduction

Radio frequency (RF) technology has been explored in various food processing operations such as pasteurization and sterilization (Bengtsson et al., 1970; Houben et al., 1991; Brunkhorst et al. 2000; Luechapattanaporn et al., 2005; Lagunas-Solar et al. 2005, 2007; Byrne et al. 2010) and insect disinfestations in various agricultural commodities such as fresh fruits (Birla et al., 2004, 2005; Wang et al 2006, ; Tiwari et al., 2008) and dry nuts (Wang et al., 2001, 2002, 2003, 2005, 2008b). A major obstacle of RF technology to be commercially applicable is its potential non uniform heating. Different factors such as sample dielectric properties (DPs), size, shape, its position between the RF electrodes, and electrode configuration may affect temperature uniformity in a RF treated food product. Barber (1983) reported that temperature uniformity could be improved if electrodes are shaped to fit the surface of the material. Wang et al. (2005) observed temperature non uniformity in in-shell walnuts, placed at different locations inside a 12 kW, 27.12 MHz RF system after 3 min heating. Effect of three sample shapes (cube, cylinder and sphere) on temperature uniformity of meat has been simulated by Romano and Marra (2008). They reported that cubes should have better temperature uniformity compared to cylinders and spheres. Birla et al. (2008a) reported difference in temperature profiles of a model fruit when it was placed at different vertical and horizontal positions between the fixed gap RF electrodes. Simulation on RF heating of mashed potato, conducted by Wang et al. (2008a) showed that DPs of meshed potato and surrounding water affected heating rate and temperature distribution. Birla et al. (2008b) showed that DPs of different constitutional parts (peel and pulp) of a fruit influenced its final temperature distribution after RF heating. Petrescu and Ferariu (2008) reported the effect of vertical gap between RF electrodes, and the horizontal distance between the successive pair of electrodes on

the heating uniformity of a dielectric material kept inside a staggered RF applicator. Wang et al. (2010) used three different electrode gaps to select the most suitable heating time for the RF heat treatment of lentils. Keeping the complexity of RF heating behavior in mind, a complete investigation on RF heating behavior is essential to optimize temperature distributions in treated food products.

Experimental methods are time consuming, costly, and often provide limited variability. Computer simulation can be used as a fast, cheap, flexible and effective tool to virtually analyze and provide an insight of RF heating mechanism in food materials. Computer simulation has previously been used to study RF heating uniformity in various food materials such as fresh fruits (Birla et al., 2008a, b), meat (Marra et al., 2007; Rayner, 2007; Romano and Marra, 2008), grain seeds (Yang et al., 2003), mashed potato (Wang et al., 2008a), and carboxy methyl cellulose solution (Chan et al., 2004). Recently, Tiwari et al. (2010) developed and validated a finite element based computer model for RF heating of dry food products using wheat flour as a representative material. Simulation results in that study demonstrated that non uniform distribution of RF power density (which acted as a heat source) was responsible for temperature non uniformity in wheat flour. Therefore, as a starting step, it was important to access and study the behavior of RF power density inside a dry product, influenced by important factors such as sample size, shape, position, DPs, electrode gap and top electrode configuration.

In the past, different criteria and index have been used to study, evaluate and compare RF power and temperature uniformity in food samples. Neophytou and Metaxas (1998) used normalized RF power density to compare RF power uniformities in rapeseeds and raw potatoes. Temperature uniformity of walnuts, soybeans, wheat and lentils has been experimentally

assessed and compared by using a heating uniformity index, defined as the ratio of difference in standard deviation rises to average sample temperature rises during RF treatments (Wang et al., 2005). Romano and Marra (2008) compared the simulated average, maximum and minimum temperatures of meat samples in three different shapes (cube, cylinder and sphere). In the present work, RF power densities in dry food samples are assessed and compared under different conditions, using a simulated power uniformity index (PUI). The overall objective of the study was to help design and scale up efficient RF systems for industrial applications. Specific objectives of this study were to investigate the effect of (1) sample size, shape and its relative vertical position between the electrodes, (2) sample and surrounding material, and (3) electrode gap and top electrode configuration on sample RF power density distribution.

2. Material and methods

2.1. Governing equations

2.1.1. RF power density and Laplace equations

When a dielectric material is placed between two plate RF electrodes, the local RF power density (Q, W m^{-3}) in the material is defined as:

$$Q = 2\pi f \varepsilon_o \varepsilon''_m \left|\boldsymbol{E}\right|^2 \quad (1)$$

where f is the frequency (Hz), ε_o and ε''_m are the permittivity of the free space (8.86 × 10^{-12} F m^{-1}), and the loss factor of the material, respectively. $\left|\boldsymbol{E}\right|$ is the modulus of electric field (V). Electric field ($\boldsymbol{E}$) inside the RF applicator is defined as the negative gradient of the electric voltage ($\boldsymbol{E} = -\nabla V$).

Quasi-static electric field approximation of Maxwell equation is used in the modeling of RF heating of dry food materials (Tiwari et al., 2010). Maxwell equation with quasi static electric field approximation is given by:

$$\nabla(\sigma + j*2\pi f \varepsilon_o \varepsilon_m)\nabla V = 0 \quad (2)$$

where $j = \sqrt{-1}$, σ and ε_m are electrical conductivity (S m^{-1}) and complex relative permittivity of the material, respectively. The complex relative permittivity ε_m of the material is related to dielectric constant ε'_m and loss factor ε''_m ($\varepsilon_m = \varepsilon'_m - j*\varepsilon''_m$).

2.1.2. Average RF power density and RF power uniformity index (PUI) of the sample

Average RF power density (Q_{av}, W m^{-3}) in a dielectric material is defined as volume integral of RF power density (Q, W m^{-3}) divided by material volume (V_{vol}, m^3):

$$Q_{av} = \frac{1}{V_{vol}} \int_{V_{vol}} Q dV_{vol} \quad (3)$$

RF power uniformity index (PUI) in a dielectric material is defined as:

$$PUI = \frac{\frac{1}{V_{vol}} \int_{V_{vol}} sqrt((Q - Q_{av})^2) dV_{vol}}{Q_{av}} \quad (4)$$

It is clear from Eq. (4) that PUI should be smaller for better RF power uniformity in the dielectric material. The minimum possible value of PUI is zero, which indicates uniform RF power in dielectric material. A well designed RF system should have low PUI.

2.2. Physical and simulation model

A 12 kW, 27.12 MHz RF system (Strayfield Fastran with E-200, Strayfield International Limited, Wokingham, UK) was used as a physical model. The description of the RF system can be found elsewhere (Birla et al., 2008; Tiwari et al., 2010). It was not feasible to include each and every single detail of the RF system in simulations due to excessive time and computer resource requirements. Therefore, only a quarter part of the symmetric RF system

was simulated. Fig. 1 showed the RF cavity geometry, boundary conditions and coordinate system used in simulation.

2.3. DPs of sample and surrounding medium

Tiwari et al. (2010) measured the DPs of wheat flour within the temperature range of 20 to 70 °C. Average DPs (3.78- j *0.33) of wheat flour were used in all simulations, except for the cases in which effect of sample DPs on RF power uniformity were investigated. Similarly, air (1- j *0) was used as surrounding material in all simulations, except for the cases in which effect of surrounding material dielectric constants on RF power uniformity were investigated.

2.4. Boundary conditions

Constant electrical voltage (13000 V) was applied on top electrode (Tiwari et al., 2010). Since, bottom electrode was grounded and attached to the metallic casings of the RF cavity, voltage (0 V) was assigned to all metallic casings and bottom electrode. Electrical insulation ($\nabla E = 0$) was considered to the symmetrical faces of RF applicator and sample.

2.5. Simulation methodology

Commercially available finite element based software FEMLAB (V3.4, COMSOL Multiphysics, Burlington, MA, USA) was used for simulations. An Inbuilt AC/DC module with quasi-static analysis was selected to solve Maxwell equation. In each simulation, model geometry was first constructed and meshed. A relatively fine mesh was generated at the interface of sample and the surrounding medium. Linear system solver (UMFPACK) was used to solve the partial differential equation. For each case, simulation was repeated by refining the mesh size. Average RF power density (Q_{av}) and PUI of the sample were calculated in each repetition using FEMLAB inbuilt integration scheme. Solution was considered mesh independent when sample PUI in successive repetitions did not change till three decimal points.

Solution time for each simulation varied between 20-60 min, depending on sample and mesh size. All simulations were performed on a Dell 670 workstation with two Dual-Core, 2.80 GHz XEON processors and 12 GB RAM running a Windows XP 64-bit operating system.

2.6. Simulation sequence

2.6.1. Simulation with varying sample size, position and shape

Wheat flour samples shaped in cuboids, were placed on the ground electrode. A series of simulations were run by changing lengths and widths of samples progressively at regular intervals between 50-600 mm, while the height was fixed as 60 mm. Another set of simulations were performed by varying sample heights ranging between 10 and 100 mm with lengths and widths fixed as 150 mm. The electrode gap in each simulation was set at 155 mm. Trends of RF power density distribution and PUIs of flour in each simulation were determined.

Based on previous simulation results, three cuboids (50×50×60 mm^3, 150×150×60 mm^3, 300×300×60 mm^3) were selected to study the effect of sample vertical position between the fixed gap RF electrodes. Dimensions represented lengths, widths and heights of cuboids along x, y and z axis. Coordinate system is shown in Fig. 1. Cuboids were placed at seven vertical positions (z = 0, 17.5, 37.5, 47.5, 57.5, 77.5 and 95 mm) from the bottom electrode. Positions (z = 0, 47.5 and 95 mm) are the vertical elevations when samples were placed on the bottom electrode, exactly in the middle of RF electrodes and in touch with the top electrode. Positions (z = 17.5, 37.5, 57.5 and 77.5) are the vertical elevations in which samples were placed at equal distances (-30, -10, +10 and +30 mm) from the central position. Trends of RF power density distribution with PUIs were determined in each simulation.

A cuboid, an ellipsoid and a cylinder were chosen to study the effect of container shape. Dimensions of shapes were considered as 150×150×60 mm^3, which represented length, width

and height in the cuboid, equatorial radiuses and height in the ellipsoid and two mutually perpendicular radiuses and height in the cylinder along x, y and z directions, respectively. Samples were placed at three different vertical positions: on the ground electrode, in the middle of electrodes and in contact with the top electrode. RF power density contours and PUIs of samples were determined in each simulation.

2.6.2. Simulation with varying DPs of the sample and surrounding medium

To study the effect of DPs on sample PUI, simulations were run by changing the dielectric constant of the sample from 1 to 100, for various loss factors ranging between 0.5 and 100. A cuboid sample (150×150×60 mm^3) was placed on the ground electrode with an electrode gap of 155 mm. Another set of simulations was performed in five different size cuboids with narrowed range of dielectric constant (6 – 14) for a set loss factor of 10. Surrounding material dielectric constant was also varied between 1 and 30 with a set sample DPs (8- j *10) to study the effect of surrounding material dielectric constant on PUI. Sample DPs were selected, based on previous simulation results.

2.6.3 Simulation with varying electrode gap and top electrode configuration

Simulations were run by changing top electrode position between 65 mm and 155 mm, while a cuboid sample (150×150×60 mm^3) was kept on the ground electrode. Electrode gap was changed by varying the position of top electrode. Tiwari et al. (2010) accounted that edge heating in wheat flour sample placed inside a rectangular container was mainly due to increased electric field concentration at the corners and edges. Therefore, it was hypothesized that bending the top electrode upward should reduce the electric field strength in these parts and improve the heating uniformity of the sample. A schematic diagram of RF cavity with top electrode bending at different positions and angles was shown in Fig. 2. Top electrode was bent

upwards from it both ends at different lengths and angles. Firstly, simulations were run for different bending positions (0, 100, 200, 300, 400, 500 mm) measured from the center of the electrode. Bending angles in all these simulations were set as 15°. Secondly, angles were varied between 0-90°, with the bending position fixed as 200 mm. In all simulations, a cuboid sample (300×210×60 mm^3) was placed on the ground electrode.

3. Results and discussions

3.1. Distribution of RF power density in different sample sizes

Fig. 3 shows the general trends of RF power density distribution of wheat flour in three different cuboids, placed on the ground electrode. The cuboids were selected in such a way that two cuboids (150×300×60 mm^3, 300×300×60 mm^3) were completely and the other cuboid (600×300×60 mm^3) was partially between the RF electrodes, as the top electrode size was 525×400 mm^2. It was clear from the Fig. 3 that RF power densities increased from inner to outer sections of first two cuboids. Higher RF power densities occurred at the edges compared to other parts, indicated edge heating in these samples. It was also noticeable that relative sample volumes containing same RF power density contours were more in 300×300×60 mm^3 than 150×300×60 mm^3, which indicated that sample size affected RF power uniformity, which will be explained in detail in section 3.3. RF power density distribution was different for the third sample where density contours first increased and then decreased from inner to outer sections of the sample. Lowest RF power densities of this sample were at the outer most section.

Difference in RF power density patterns in the different sample sizes can be explained by electric field behavior. When samples were put completely between the RF electrodes, electric field, deflected by the edges and corners increased the net electric field at the outer

sections compared to inner sections of the samples (Marra et al., 2007; Birla et al., 2008a; Tiwari et al., 2010). Since RF power density is proportional to the square of electric field, it also increased from inner to outer sections of the samples. In case of third sample, net electric field was comparatively smaller at the outer-most sections of the sample as sample was larger than the electrode size. That is why, RF power density increased and then decreased from inner to outer sections of third sample.

3.2. Distribution of RF power density in different sample shapes, placed in different positions between the RF electrodes

It was also desirable to investigate the effect of sample shapes (a cuboid, a cylinder and an ellipsoid) on the RF power density distribution as most of the agricultural materials are kept either in boxes, cans or in pouches. Fig. 4 showed the general trends of RF power density distribution in the cuboid, ellipsoid, and cylinder, kept at three different positions. It was clear that cuboid and cylinder had higher RF power densities at the outer sections, while ellipsoid had higher densities at its inner sections. In cuboid and cylinder, electric field is deflected by the sample edges, resulted in increase of net electric field concentration at the outer sections of the samples; while in ellipsoid, the electric field was deflected by every point located on its curved surface. As a result, net electric field concentration at the inner sections was higher compared to outer sections of the sample.

RF power density patterns in samples also changed with their placement positions. Sample in contact with either of the electrodes had higher RF power densities near the contact surfaces due to increased electric field concentration at the contact surfaces. Samples placed in the middle of RF electrodes showed higher RF power densities at their central sections as

electric field deflected by both (top and bottom) edges, increased net electric field concentration at the central parts of the sample.

3.3. Effect of sample size on PUI

Figs. 5 and 6 summarized the effect of sample size on PUI of wheat flour. Simulated results demonstrated (Fig. 5) that increase in sample length and width caused an initial increase and then reduction of PUI. Values of PUI were highest when sample lengths and widths lied between 150 and 200 mm, 35-50% of the top electrode size (525×400 mm^2). Since patterns of PUI change were similar with respect to lengths and widths, only lengths were varied in later simulations. PUI was the lowest when sample length was equal to electrode length (525 mm). Increase in sample length beyond electrode length increased PUI. Similarly, when sample height was increased, PUI decreased after showing initial increase (Fig. 5). It was clear form the Figs. 5 and 6 that RF power uniformity should be better for sample sizes, either approaching to zero or approaching to maximum possible size that can be kept completely between the RF electrodes.

When sizes approached to zero, major part of electric field directly passed through the ground electrode without entering in samples. Because of that, RF power was more uniform in small samples, as indicated by low PUIs. With increase in sizes, more electric field started entering into the samples. At first, most of electric field entered obliquely as sizes were comparatively smaller than top electrode size. Oblique electric field increased RF power non uniformities in samples. With further increase in sample size, electric field started entering normally (except a little part, which was getting deflected by sample edges and corners) in the sample. This caused increase in RF power uniformity again.

3.4. Effect of sample vertical position on PUI

Fig. 7 shows the effect of sample vertical position on PUI. Three sample sizes were selected based on results explained in Fig. 5. These sizes could be considered as small, medium and big compared to the top electrode size. It was clear from Fig. 7 that trends of PUI change depended on sample sizes as well as their relative vertical positions between the RF electrodes. For samples of size 50×50×60 mm^3, PUI increased and then decreased when a sample was moved up from bottom to top electrode. PUI change was symmetrical around the central (z = 47.5 mm) position, with its highest value at this position. In sample size (150×150×60 mm^3) unlike size (50×50×60 mm^3), PUIs were highest when samples were placed on the bottom electrode (z = 0 mm) or in touch with the top electrode (z = 95 mm). PUI change was symmetrical around central (z = 47.5 mm) position. For the sample size (300×300×60 mm^3), PUI change was not symmetric around the central position. After initial decrease of PUI when moved from z = 0 to 17.5 mm, sample PUI continued to increase when it was moved towards top electrode. Ideally, PUI change should be symmetrically distributed around the central position, but simulated results showed that it was not true in case of large samples. The reason could be attributed to the unequal sizes of top and bottom electrodes. The bottom (grounded) electrode was the integral part of RF cavity with no open edges where as the top electrode had open edges. Electric field distribution near the open edges of the top electrode must have affected RF power uniformity of big sample sizes, when they were moved closer to the top electrode. Based on the results, it could be concluded that RF power should be more uniform in small samples if they are placed either in contact with top or bottom electrode but for middle and large size samples, better RF power uniformity can be achieved in carefully selected positions between the RF electrodes.

Table 1 compared the simulated PUIs of cuboid, ellipsoid and cylinder, placed at three different vertical elevations. PUIs were lowest in ellipsoid, followed by the cylinder and cuboid for all three positions. Ellipsoid placed in the center of RF electrodes had lowest PUI among all selected positions.

3.5. Effect of DPs of sample and surrounding medium on sample PUI

Fig. 8 shows the effect of sample DPs on PUIs. Results indicate that smaller DPs resulted in better RF power uniformities in samples. Dry products should provide better uniform RF heating as they possess smaller DPs. It was also observed if loss factor was ≤ 1, PUI continued to increase with the increase in dielectric constant. But for a loss factor >1, PUIs first decreased and then increased with increase in dielectric constant. It was interesting to notice that PUIs had their minimum values whenever dielectric constants were about the same as loss factors, though this was more discernable for smaller DPs. Results in Fig. 9 show that trends of PUI change were independent of sample sizes. PUI first decreased and then increased between dielectric constant 6 and 14, showing its minimum at a dielectric constant value of 8 when the loss factor was 10. Fig. 10 shows the effect of surrounding material dielectric constant on PUI. Sample DPs were set as (8- j *10), based on the previous simulations. PUI first decreased and then increased with increase in surrounding material dielectric constant. PUI was lowest when surrounding material dielectric constant was between 10 and 15. From the results, it is clear that RF uniformity can be achieved when surrounding material dielectric constant is in comparable range of sample DPs.

3.4. Effect of electrode gap on PUI

PUI of wheat flour decreased as electrode gap was reduced from 155 to 65 mm, as shown in Fig. 11. As explained earlier, proportion of oblique electric field, which caused RF power non uniformity decreased when electrode gap was reduced.

3.5. Effect of top electrode bending/configuration

Fig. 12A shows the effect of top electrode bending position on sample PUI. Results demonstrated that top electrode bending position greatly affected sample PUI. When top electrode was bent at 200 mm, PUI was lower compared to when it was bent at other five positions. Similarly, Fig 12B showed the effect of top electrode bending angle on PUI of wheat flour sample. Increase in bent angle, first decreased and then increased PUI. Sample PUI was lowest at bent angle 20°. RF power density distribution in wheat flour in two different positions and angles were shown in Fig 13. It was clear from the fig. 13 that top electrode configuration affected the RF power uniformity in the sample as magnitudes of electric fields and their distributions inside wheat flour sample changed with top electrode bending positions and angles. Optimum RF power uniformity in a particular sample size could be achieved with a particular top electrode bending position and angle.

Conclusions

Effects of various factors such as sample size, shape, its relative position between the RF electrodes, top electrode configuration and DPs of sample and surrounding medium on the RF heating of a low loss food material placed inside a 27.12 MHz RF system were studied using a developed finite element computer model in FEMLAB 3.4. Simulated results showed that RF heating uniformity could be improved using larger sample sizes placed in the air between RF electrodes. Cubes and cylinders showed edge heating while ellipsoids showed center heating. Simulated results also showed that smaller DPs provided better RF power

uniformities in the material. Top electrode bending (bent position and angle) affected RF heating uniformity in the sample. The study helped understand the RF heating process, influenced by various parameters. The developed model can further be used to optimize RF heating process parameters in order to get uniform heating after they have been experimentally validated.

Table 1

Simulated PUIs of wheat flour sample in three different shapes (a cuboid, an ellipsoid and a cylinder), placed at three different vertical positions between RF electrodes with a fixed gap of 155 mm

Sample shape	Relative position of sample	Simulated PUI
A cuboid (150×150×60 mm^3)	Touching bottom electrode	0.23
	In the center of RF electrodes	0.22
	Touching top electrode	0.23
An ellipsoid (150×150×60 mm^3)	Touching bottom electrode	0.16
	In the center of RF electrodes	0.06
	Touching top electrode	0.16
A cylinder (150×60 mm^3)	Touching bottom electrode	0.22
	In the center of RF electrodes	0.22
	Touching top electrode	0.22

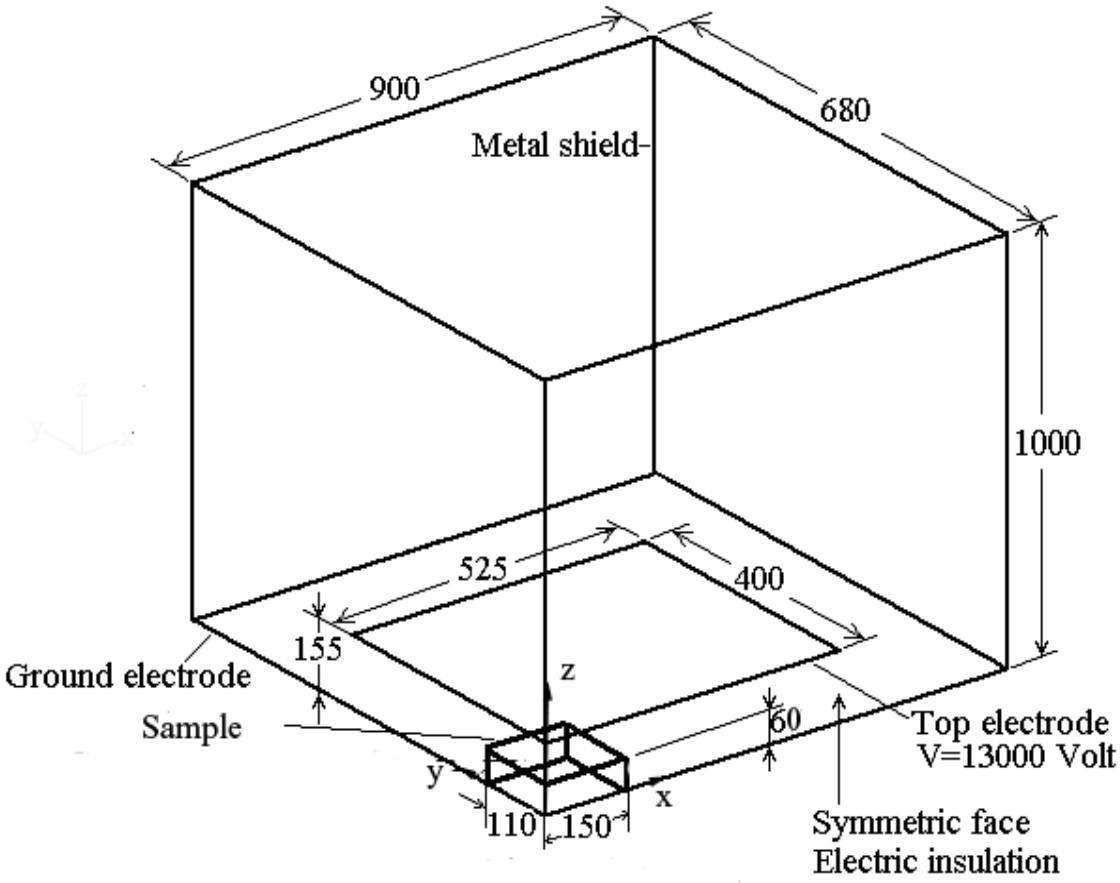

Fig. 1. Geometrical and boundary conditions of one quadrant of 12 kW, 27.12 MHz radio frequency (RF) system (dimensions are in mm)

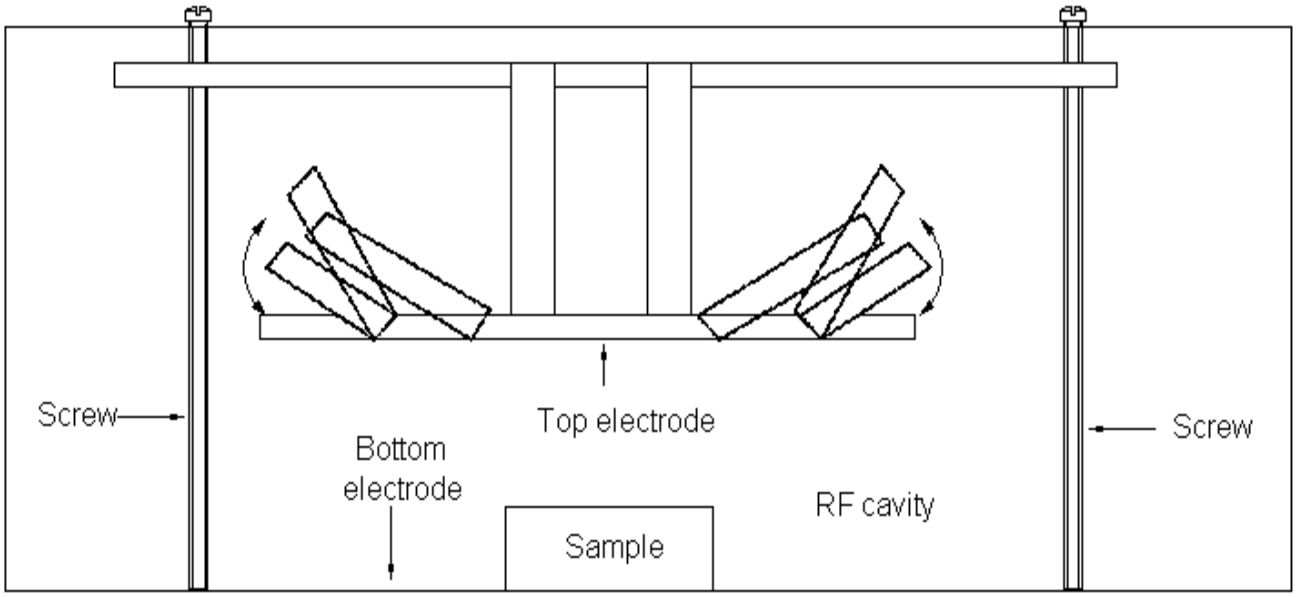

Fig. 2. Schematic diagram of radio frequency cavity showing change in top electrode configuration by bending it upward from its both ends at different lengths and angles.

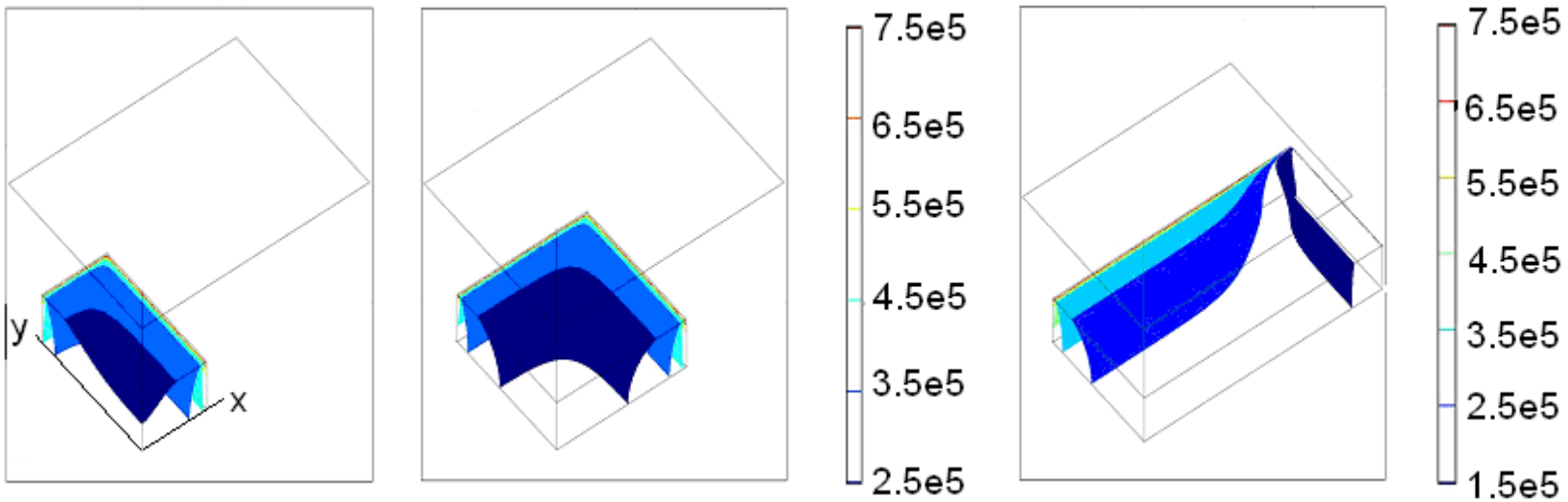

Size (150×300×60 mm^3) Size (300×300×60 mm^3) Size (600×300×60 mm^3)

Fig. 3. Simulated RF power density contours (W m^{-3}) of wheat flour sample in three different sizes, placed on the bottom electrode with a fixed electrode gap of 155 mm. Top electrode size was 525 × 400 mm^2.

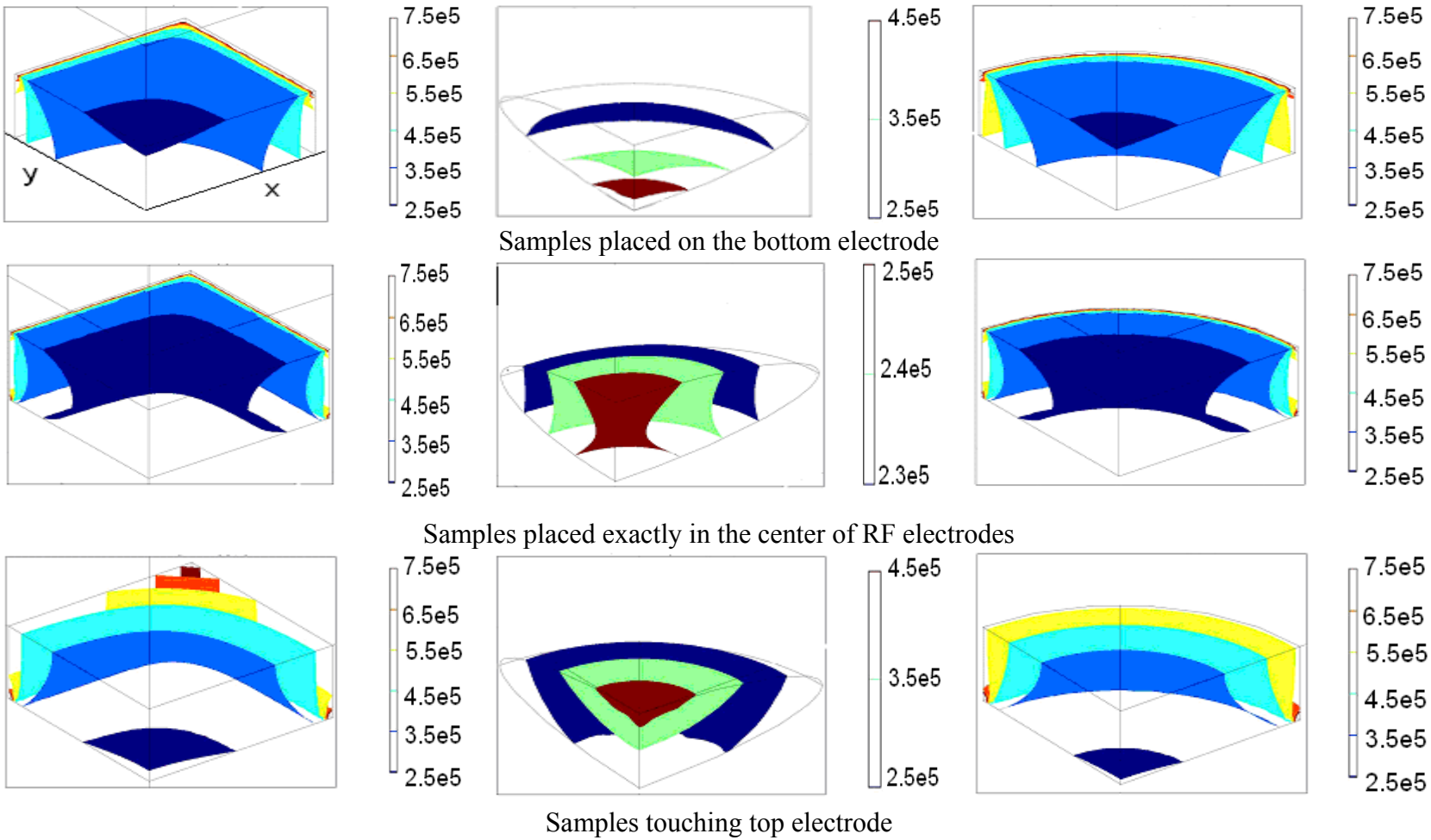

Fig. 4. Simulated RF power density contours (W m^{-3}) of wheat flour sample in three different shapes (a cuboid, an ellipsoid and a cylinder) placed at three different vertical positions between the RF electrodes of fixed gap of 155 mm.

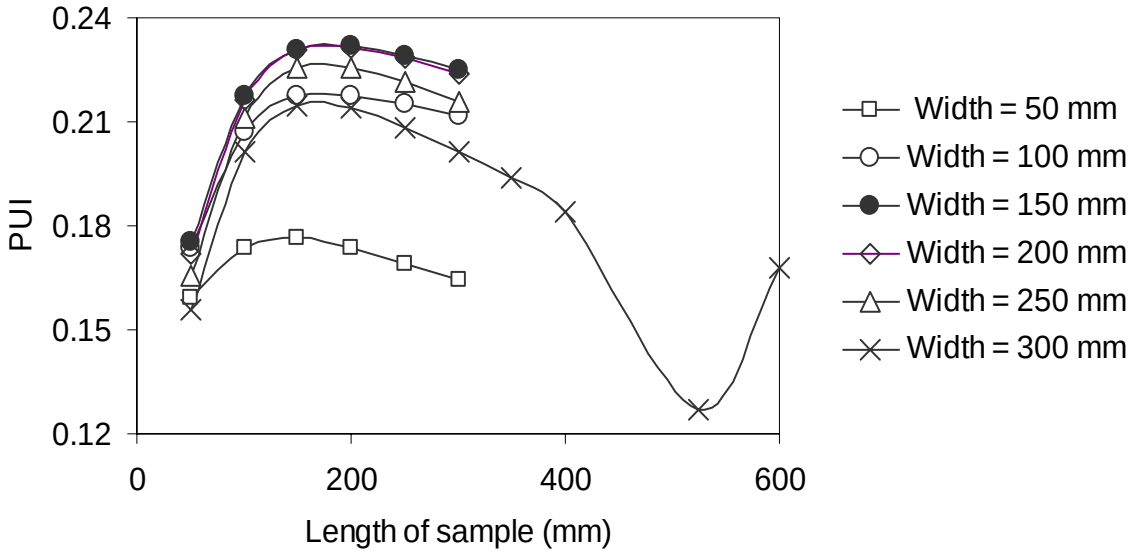

Fig. 5. Simulated RF power uniformity indexes (PUIs) of cuboid shaped wheat flour mass with varying sample lengths and widths. Cuboids were placed on the bottom electrode with top electrode size (525 × 400 mm^2) and a fixed electrode gap of 155 mm. Sample heights were set as 60 mm.

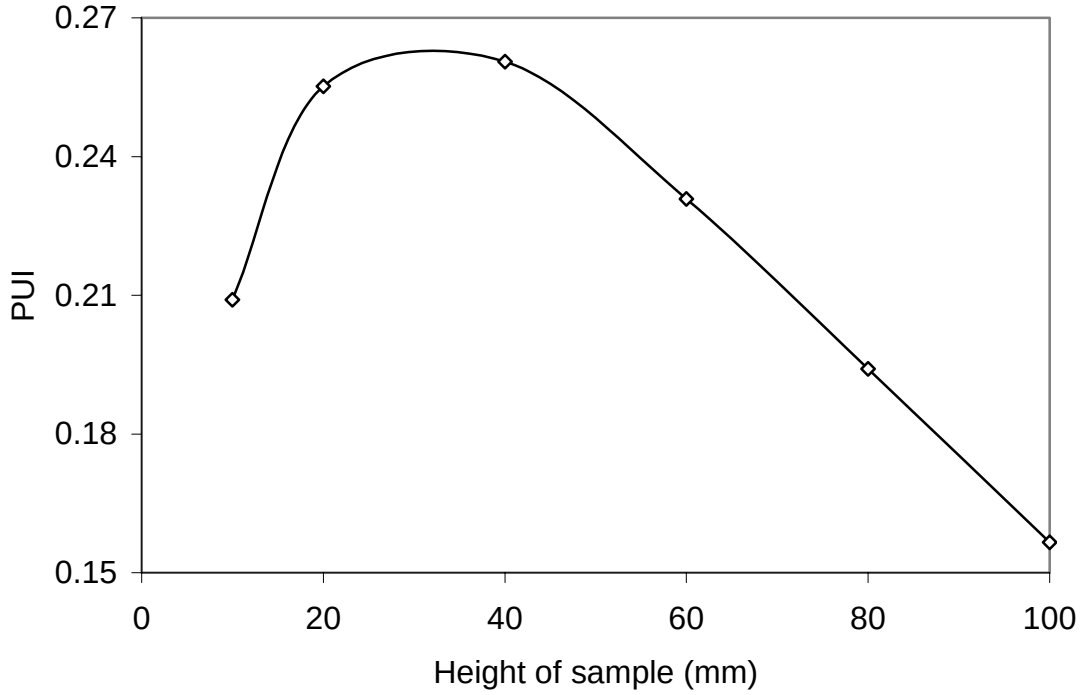

Fig. 6. Simulated RF power uniformity indexes (PUIs) of cuboid shaped wheat flour with varying sample heights. Samples were kept on the bottom electrode with a fixed electrode gap of 155 mm. Top electrode size was 525 × 400 mm^2 and samples length and width both were set as 150 mm.

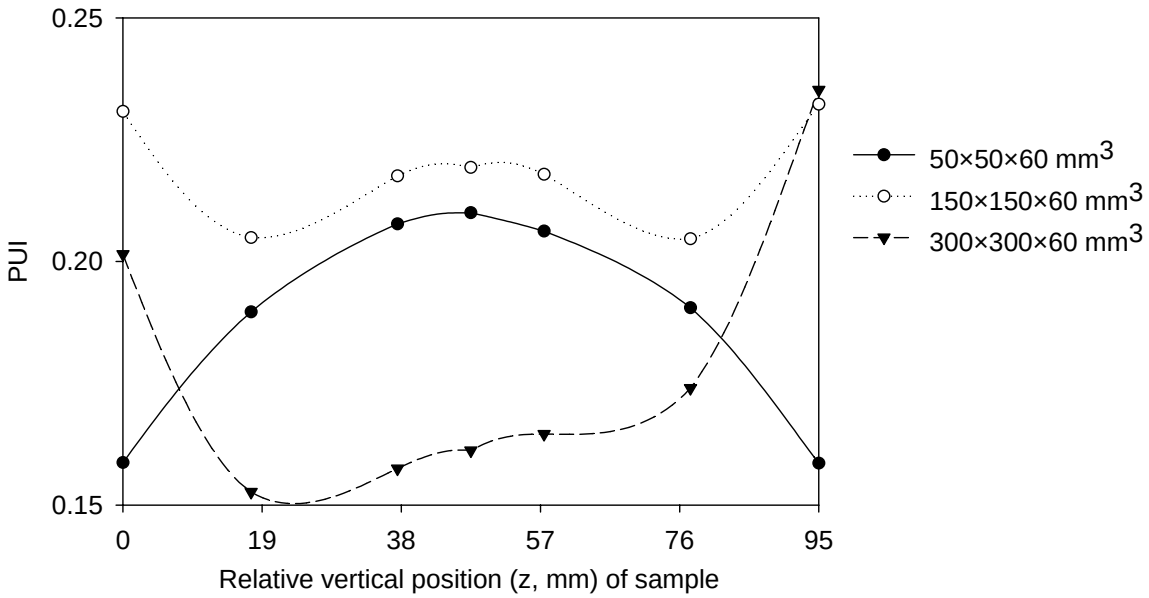

Fig. 7. Simulated power uniformity indexes (PUIs) of cuboid shaped wheat flour in three different sizes, kept at seven different vertical positions (along z axis) under the fixed electrode gap of 155 mm. Coordinate system was shown in Fig.1.

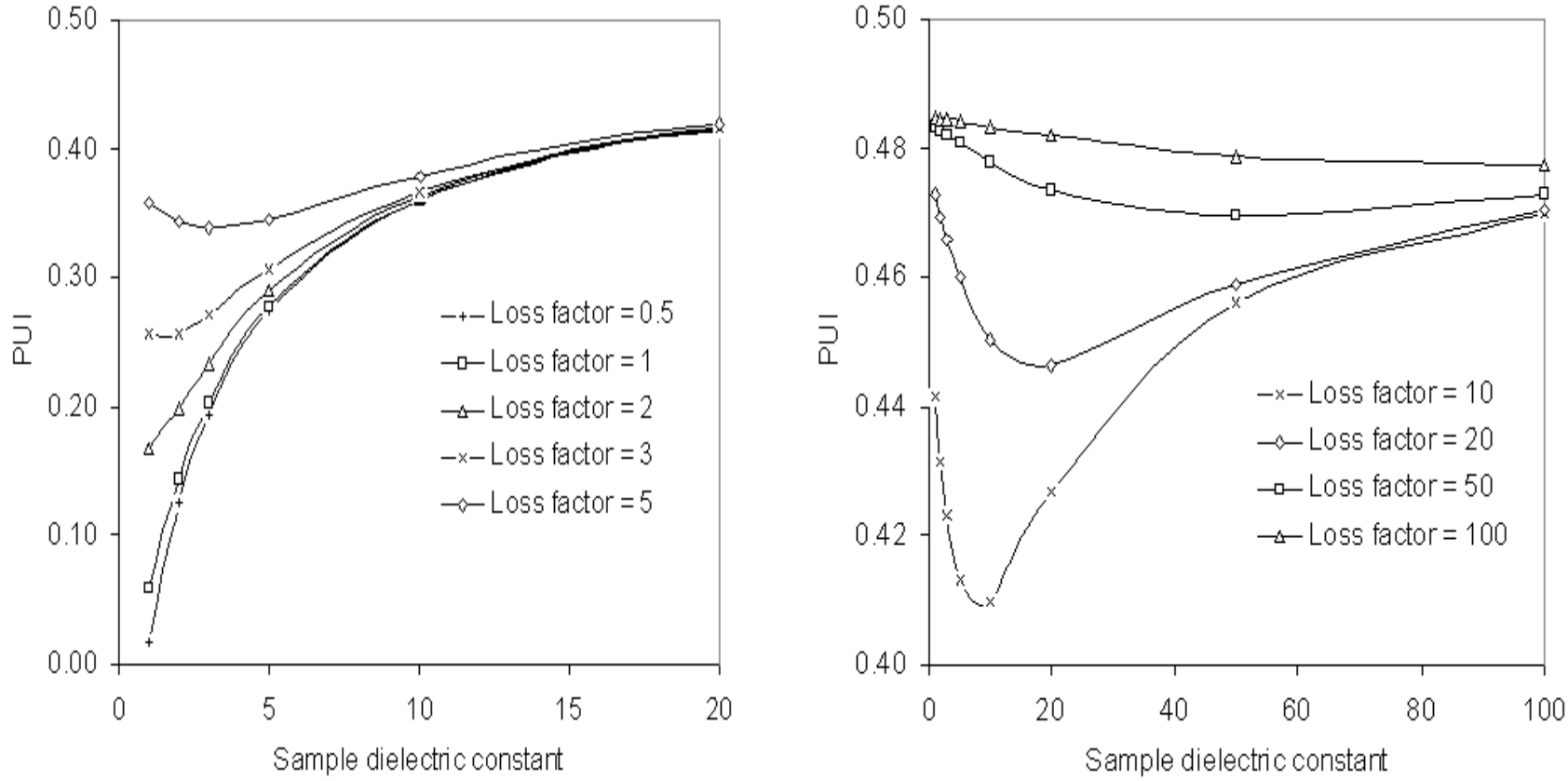

Fig. 8. Simulated power uniformity indexes (PUIs) in cuboid shaped sample (150×150×60 mm^3) with varying DPs. Samples were placed on the bottom electrode with an electrode gap of 155 mm.

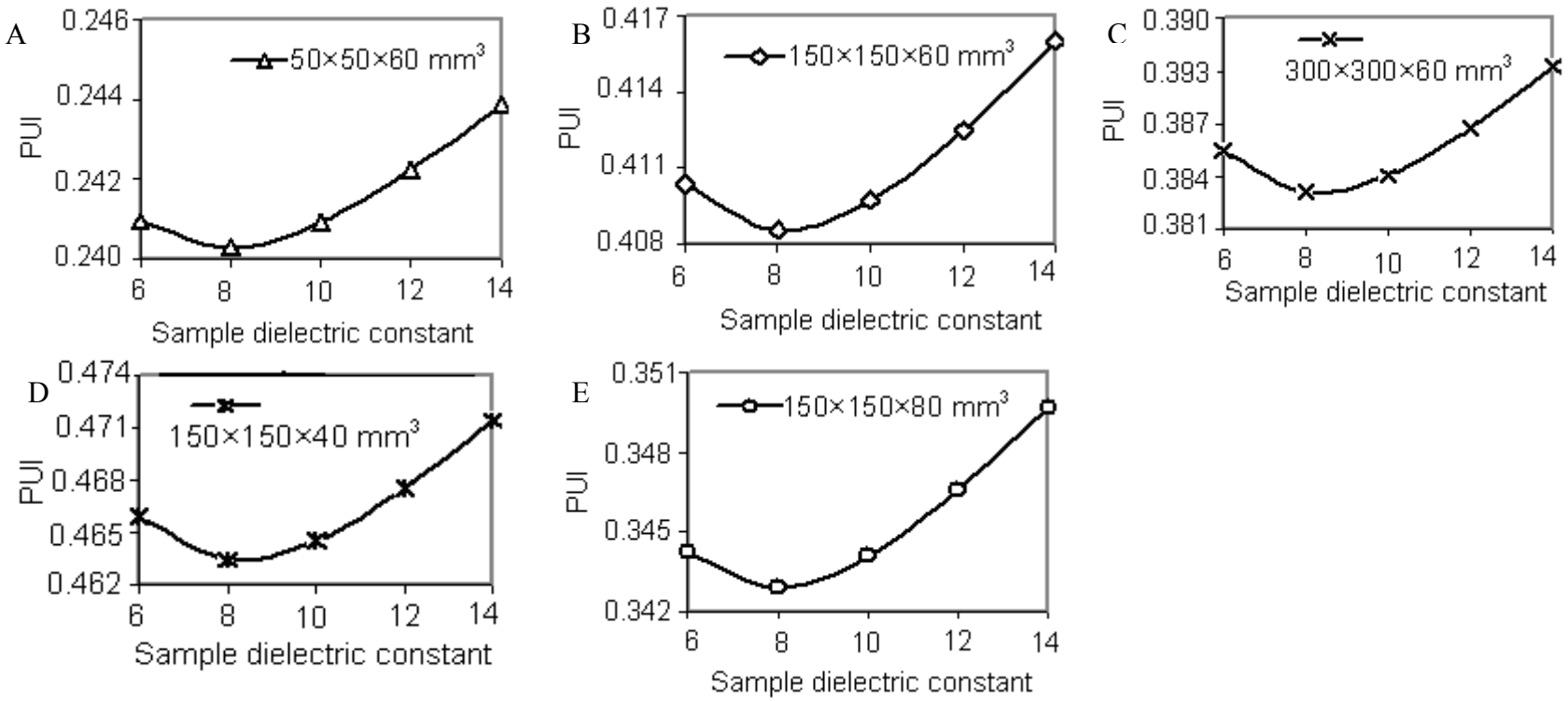

Fig. 9. Trends of simulated power uniformity indexes (PUIs) of samples with varying dielectric constants in five different sizes. Loss factor value was fixed as 10.

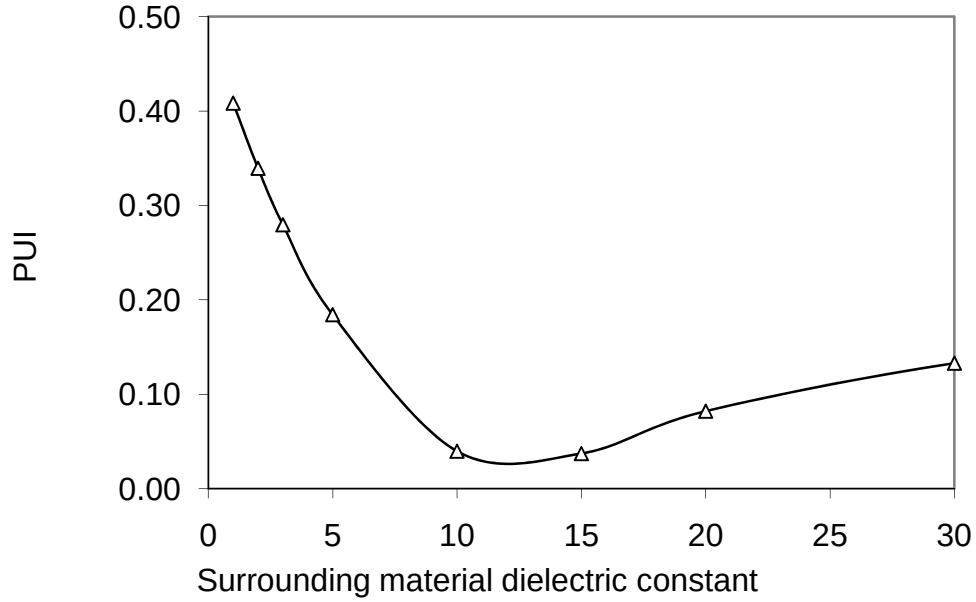

Fig. 10. Simulated power uniformity indexes (PUIs) in sample ($150\times150\times60$ mm^3) in different surrounding medium dielectric constant. Sample DPs was fixed as $(8-10*j)$ and it was kept on the bottom electrode with an electrode gap of 155 mm.

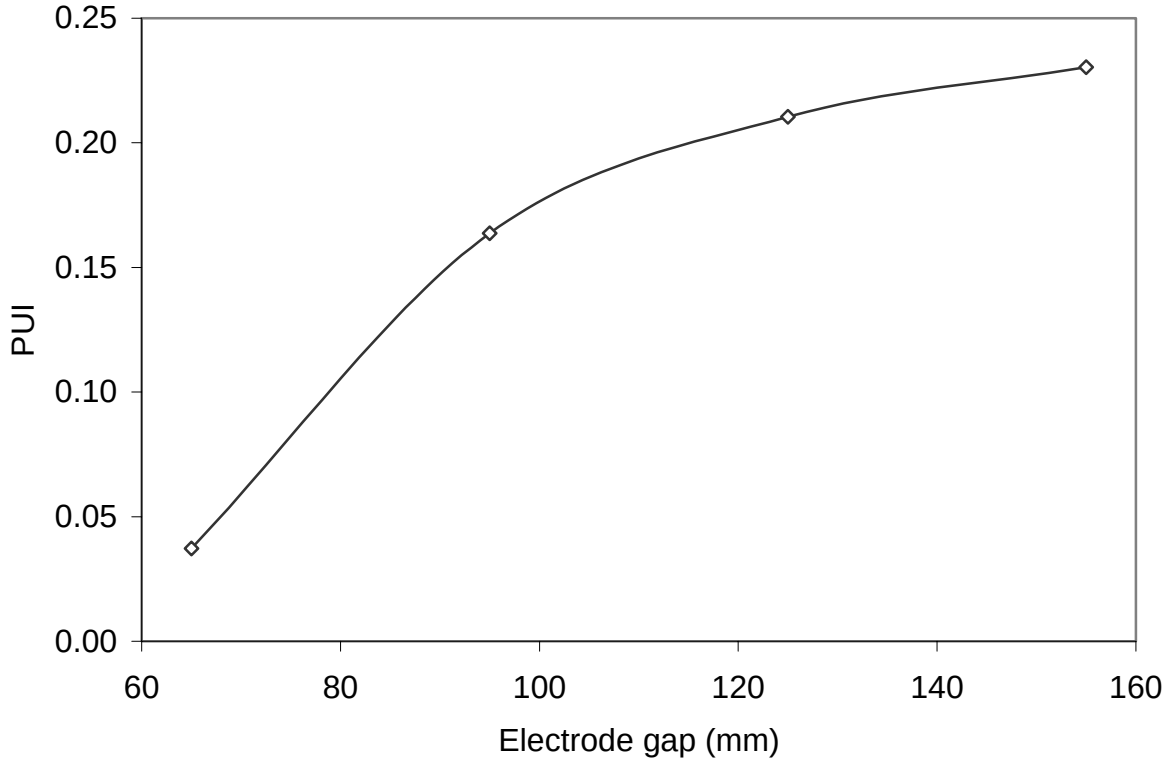

Fig. 11. Simulated power uniformity indexes (PUIs) of cuboid shaped wheat flour ($150\times150\times60$ mm^3) with varying electrode gaps. Sample was kept on the bottom electrode with an electrode gap of 155 mm.

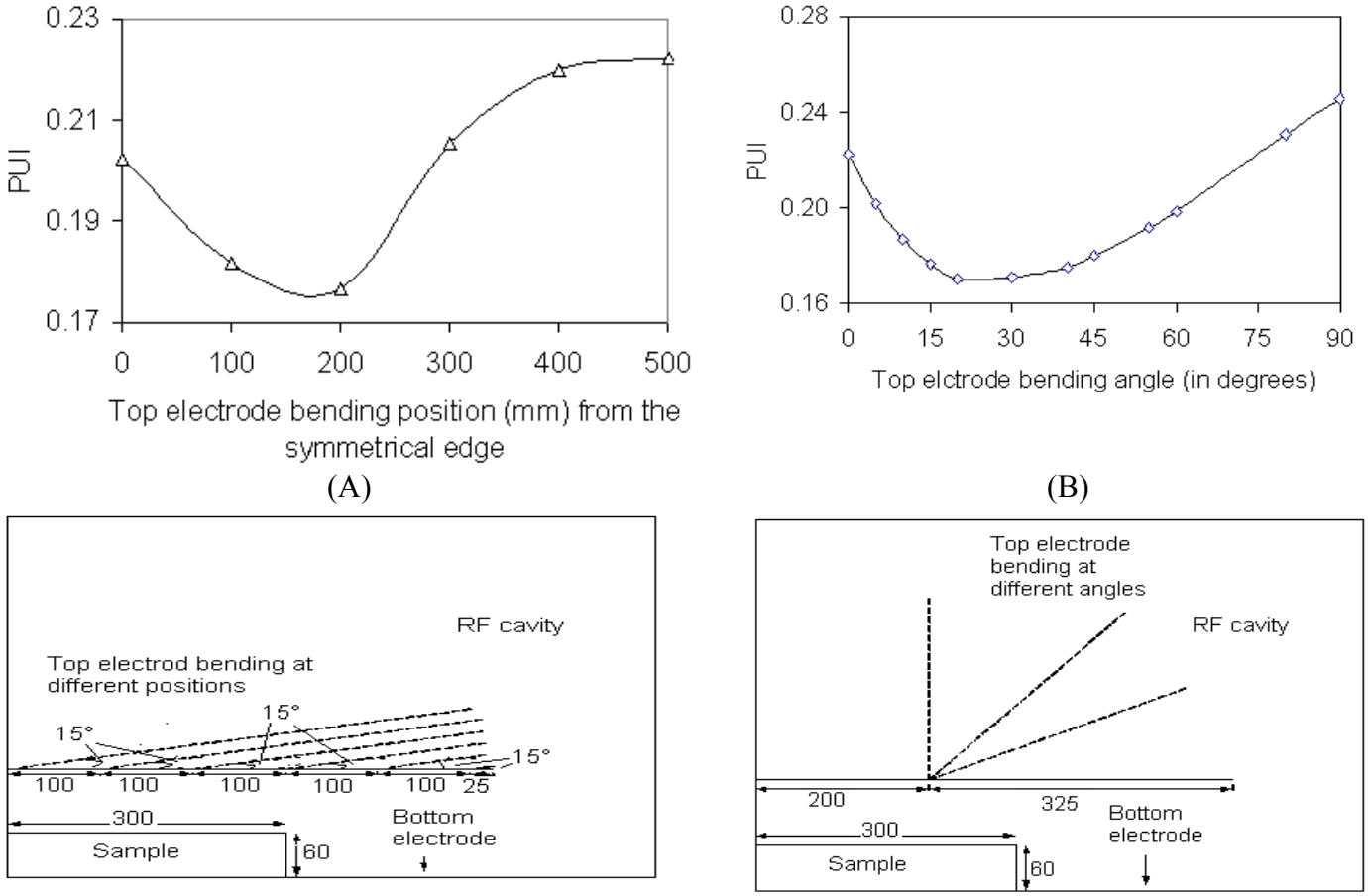

Fig. 12. Simulated power uniformity indexes (PUIs) in a cuboid shaped wheat flour (300 ×210 × 60 mm^3) sample, placed on the bottom electrode when top electrode (525×400 mm^2) was bent (A) at six different positions (0, 100, 200, 300, 400 and 500 mm) along the length of electrode, keeping bending angle fixed as 15° (B) at different angles (in degrees), keeping bending position fixed as 200 mm.

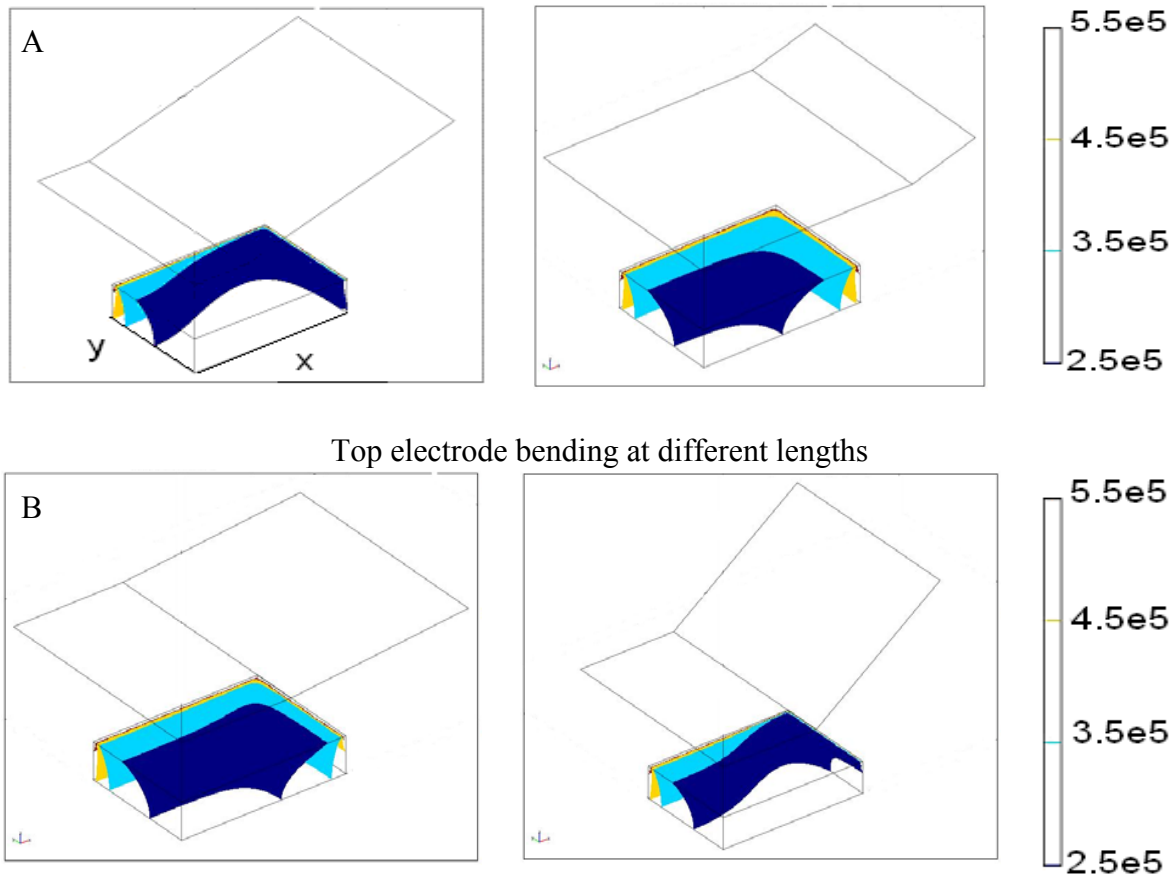

Fig. 13. Simulated power density contours (W m^{-3}) in a cuboid shaped wheat flour sample (300 ×210 × 60 mm^2) placed on the bottom electrode when top electrode (525×400 mm^2) was (A) bent 100 and 300 mm along the length of electrode, keeping bending angle fixed as 15° (B) bent upwards 5° and 45°, keeping bending position fixed as 200 mm.

References

Barber, H. (1983). Electroheat. *1st ed.* London: Granada Publishing Limited.

Bengtsson, N.E., Green, W., & Valle, F.R.D. (1970). Radio frequency pasteurization of cured hams. *Journal of Food Science,* 35(5), 682-687.

Birla, S.L., Wang, S., & Tang, J. (2008a). Computer simulation of radio frequency heating of model fruit immersed in water. *Journal of Food Engineering*, 84(2), 270-280.

Birla, S.L., Wang, S., Tang, J., Fellman, J.K., Mattinson, D.S., & Lurie, S. (2005). Quality of oranges as influenced by potential radio frequency heat treatments against Mediterranean fruit flies. *Postharvest Biology and Technology,* 38(1), 66-79.

Birla, S.L., Wang, S., Tang, J., & Hallman, G. (2004). Improving heating uniformity of fresh fruit in radio frequency treatments for pest control. *Postharvest Biology and Technology,* 33(2), 205-217.

Birla, S.L., Wang, S., Tang, J., & Tiwari, G. (2008b). Characterization of radio frequency heating of fresh fruits influenced by dielectric properties. *Journal of Food Engineering,* 89(4), 390-398.

Brunkhorst, C., Ciotti, D., Fredd, E., Wilson, J.R., Geveke, D.J., & Kozempel, M. (2000). Development of process equipment to separate nonthermal and thermal effects of RF energy on microorganisms. *Journal of Microwave Power and Electromagnetic Energy,* 35(1), 44-50.

Byrne, B., Lyng, J.G., Dunne, G., & Bolton, D.J. (2010). Radio frequency heating of comminuted meats - considerations in relation to microbial challenge studies. *Food Control*, 21(2), 125-131.

Chan, T. V. C. T., Tang, J., & Younce, F. (2004). 3-dimensional numerical modeling of an industrial radio frequency heating system using finite elements. *Journal of Microwave Power and Electromagnetic Energy,* 39(2), 87-105.

Houben, J., Schoenmakers, L., Vanputten, E., Vanroon, P., & Krol, B. (1991). Radiofrequency Pasteurization of Sausage Emulsions as a Continuous Process. *Journal of Microwave Power and Electromagnetic Energy,* 26(4), 202-205.

Lagunas-Solar, M.C., Pan, Z., Zeng, N.X., Truong, T.D., Khir, R., & Amaratunga, K.S.P. (2007). Application of radio frequency power for non-chemical disinfestation of rough rice with full retention of quality attributes. *Applied Engineering in Agriculture*, 23(5), 647-654.

Lagunas-Solar, M.C., Zeng, N.X., Essert, T.K., Truong, T.D., Pina, C., Cullor, J.S., Smith, W.L., & Larrain, R. (2005). Disinfection of fishmeal with radiofrequency heating for improved quality and energy efficiency. *Journal of the Science of Food and Agriculture,* 85(13), 2273-2280.

Luechapattanaporn, K., Wang, Y.F., Wang, J., Tang, J.M., Hallberg, L.M., & Dunne, C.P. (2005). Sterilization of scrambled eggs in military polymeric trays by radio frequency energy. *Journal of Food Science,* 70(4), E288-E294.

Marra, F., Lyng, J., Romano, V., & McKenna, B. (2007). Radio-frequency heating of foodstuff: solution and validation of a mathematical model. J*ournal of Food Engineering*, 79(3), 998-1006.

Neophytou, R.I., & Metaxas, A.C. (1998). Combined 3D FE and circuit modeling of radio frequency heating systems. *Journal of Microwave Power and Electromagnetic Energy,* 33(4), 243-262.

Petrescu, C., & Ferariu, L. (2008). Modeling of dielectric heating in radio-frequency applicator optimized for uniform temperature by means of genetic algorithms. *World Academy of Scienece, Engineering and Technology,* 47, 129-134.

Rayner, M. (2007). Multi Physics modeling of radio frequency cooking. *Excerpt from the proceedings of the COMSOL users conference*, Grenoble France.

Romano, V., & Marra, F. (2008). A numerical analysis of radio frequency heating of regular shaped foodstuff. *Journal of Food Engineering*, 84(3), 449-457.

Tiwari, G., Wang, S., Birla, S.L., & Tang, J. (2008). Effect of water-assisted radio frequency heat treatment on the quality of 'Fuyu' persimmons. *Biosystems Engineering*, 100(2), 227-234.

Tiwari, G., Wang, S., Tang, J., & Birla, S.L. (2010). Computer simulation of radio frequency heating of dry food materials, Part I: model development and validation. *Journal of Food Engineering* Submitted for publication.

Wang, J., Olsen, R.G., Tang, J., & Tang, Z. (2008a). Influence of mashed potato dielectric properties and circulating water electric conductivity on radio frequency heating at 27 MHz. *Journal of Microwave Power and Electromagnetic Energy,* 42(2), 31-46.

Wang, S., Birla, S.L., Tang, J., & Hansen, J.D. (2006). Postharvest treatment to control codling moth in fresh apples using water assisted radio frequency heating. *Postharvest Biology and Technology,* 40(1), 89-96.

Wang, S., Ikediala, J.N., Tang, J., Hansen, J.D., Mitcham, E., Mao, R., & Swanson, B. (2001). Radio frequency treatments to control codling moth in in-shell walnuts. *Postharvest Biology and Technology,* 22(1), 29-38.

Wang, S., Tang, J., Cavalieri, R.P., & Davies, D.C. (2003). Differential heating of insects in dried nuts and fruits associated with radio frequency and microwave treatments. *Transactions of the ASAE,* 46(4), 1175-1182.

Wang, S., Tang, J., Johnson, J.A., Mitcham, E., Hansen, J.D., Cavalieri, R.P., Bower, J., & Biasi, B. (2002). Process protocols based on radio frequency energy to control field and storage pests in in-shell walnuts. *Postharvest Biology and Technology,* 26(3), 265-273.

Wang, S., Tiwari, G., Jiao, S., Johnson, J.A., & Tang, J. (2010). Developing postharvest disinfestation treatments for legumes using radio frequency energy. *Biosystems Engineering*, 105(3), 341-349.

Wang, S., Yue, J., Chen, B., & Tang, J. (2008b). Treatment design of radio frequency heating based on insect control and product quality. *Postharvest Biology and Technology,* 49(3), 417-423.

Wang, S., Yue, J., Tang, J., & Chen, B. (2005). Mathematical modelling of heating uniformity for in-shell walnuts subjected to radio frequency treatments with intermittent stirrings. *Postharvest Biology and Technology,* 35(1), 97-107.

Yang, J., Zhao, Y., & Wells, J. H. (2003). Computer simulation of capacitive radio frequency (RF) dielectric heating on vegetable sprout seeds. *Journal of Food Process Engineering*, 26(3), 239-263.

CONCLUSIONS AND RECOMMENDATIONS

This research was an effort to understand the behavior of radio frequency (RF) heating, especially in dry agricultural commodities using computer simulation. Also, this research evaluated the potential of water assisted RF heating in a *Fuyu'* persimmon as an alternative quarantine treatment method. Major results along with recommendations are summarized for future studies:

1 Simulated and experimented results showed that RF treated wheat flour had higher temperature values at the corners and lower sections of the sample.

2. Simulation results confirmed that non uniform distribution of RF power density caused temperature non uniformity in the sample.

3. Sensitivity analysis of the simulated results showed that temperature uniformity in RF treated wheat flour sample was most sensitive to the top electrode voltage among other parameters such as sample DPs, thermal conductivity of wheat flour and heat transfer coefficient air. Thermal conductivity of wheat flour and heat transfer coefficient of air had negligible effect on the temperature uniformity of the sample.

4. Simulated results showed that RF heating uniformity could be improved using larger sample sizes placed in the air between RF electrodes.

5. Cubes and cylinders showed edge heating while ellipsoids showed center heating.

6. Smaller DPs provided better RF power uniformities in food materials.

7. Simulated results also showed that top electrode bending (bent position and angle) affected RF heating uniformity in the sample. Optimum RF power uniformity in a particular sample size could be achieved with a particular top electrode bending position and angle.

8. The developed model can further be used to optimize RF heating process parameters in order to get uniform heating.

The following areas need further research to address the issues related to non-uniform RF heating

1 The developed RF model used the assumption that RF waves inside the RF applicator behaved like a quasi-static electric field because of its longer wave length compared to RF applicator size. Very few studies have been performed considering wave nature of RF waves. A comparative study between quasi-static and wave approaches should be very useful to help understand the mechanism of RF heating in different food materials.

2. The developed computer model predicted that sample size, shape, its vertical position between the RF electrodes and top electrode configuration affected RF heating. Experimental validation for these findings is recommended.

3. In the past, some experimental studies showed that mixing or moving the food samples between the RF electrodes could improve the temperature uniformity in the treated sample. These findings should be theoretically validated by computer simulation.